Cours/Lecture Series

pt. 1

1995–1996 ACADEMIC TRAINING PROGRAMME

LECTURE SERIES FOR POSTGRADUATE STUDENTS

SPEAKER : A. H. WALENTA /Univ. of Siegen, Germany
TITLE : Introduction to Detectors
TIME : 6, 7, 8, 9 & 10 November, 11.00 to 12.00 hrs
PLACE : Auditorium

ABSTRACT

The lecture will cover the most popular detector principles, gas detectors (ion chambers, MPWC's and MSGC's), semiconductor detectors, scintillators and cryogenic detectors. The basic detector physics as interaction of radiation with matter, information transport via free charges, photons and phonons and the signal formation will be presented in some depth with emphasis on the influence on specific parameters for the detector performance. In particular the resolution for position, time, energy and intensity measurement and the efficiency will be discussed. Concepts for momentum measurements, particle identification and energy measurements (calorimeters) as well for imaging applications in medicine, biology and industry (non destructive testing) will be put into relation to the specific detection principles. Signal extraction, electronic signal processing and principles of information capture will close the logic circle to the input : the radiation properties.

The lecture will provide some sources for data tables and small demonstration computer programs for ionisation (dE/dx), gas gain, pulse shaping, dead time losses etc.

1995/DSU/CP-MP
Distr. int. & ext.
SIS/H/346

Introduction to Detectors

A.H. Walenta, Univ. of Siegen, Germany

1) Introduction

Survay of detector applications and properties

2) Gas (filled) detectors

- Energy loss of charged particles
- x-ray absorption
- energy resolution, gas amplification
- multi channel detectors and position resolution: MWPC, DC, IDC, TPC, MSGC...
- ion chambers and imaging: DQE, MTF...
- single photon counting and imaging

3) Semiconductor detectors

- p-n junctions, detector properties
- analogue electronics, noise, filters
- spectroscopy

4) Scintillators

- light detection (PM-tubes)
- scintillating mechanism, efficiency and time resolution
- light guides, fibres

5) 2D-detectors

- diffraction measurements with x-rays
- standard imaging devices: film, image plates, screen & image intensifier
- counting pixel detectors,

Becquerel

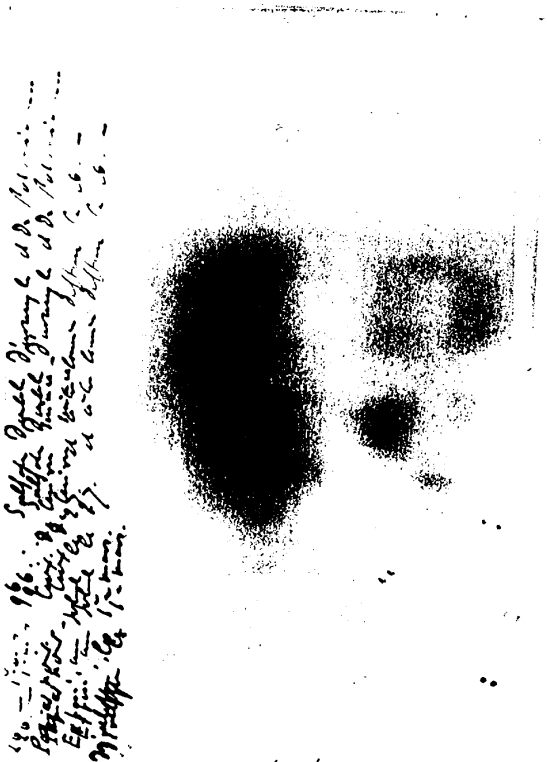

o detection of radiation

Geiger & Bothe

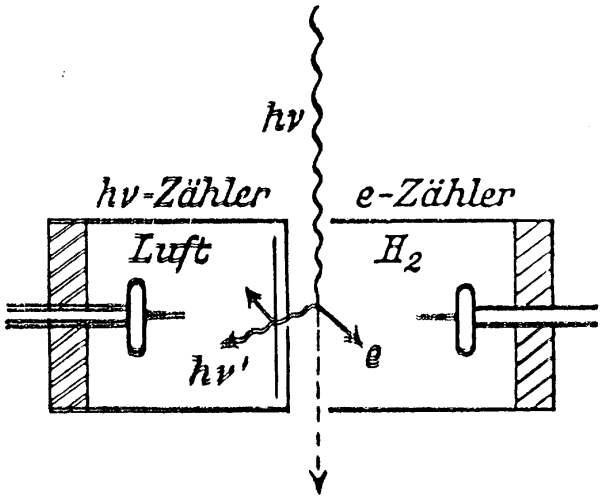

- o coincidence method
- o particle aspect
- o high sensitivity (single electron)

C. D. Anderson

23 MeV

HR = 7.5·10^4 Gauss cm

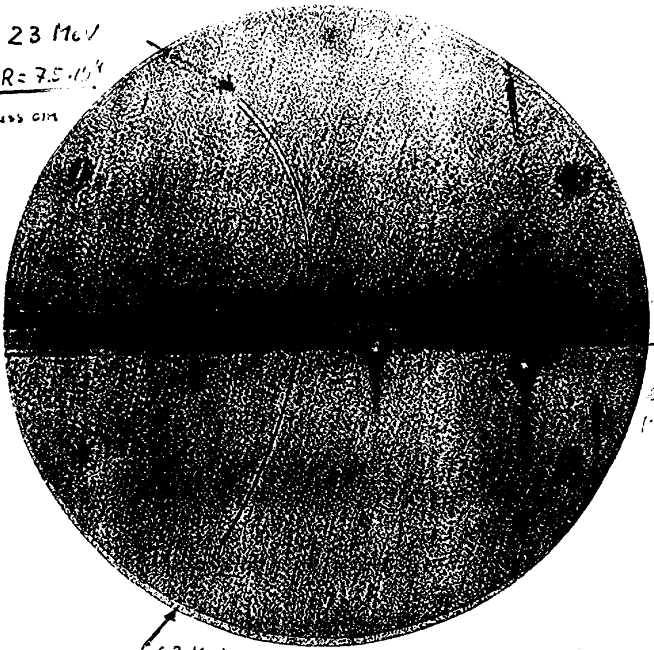

lead plate

63 MeV, pos.

HR = 2.1 10^4 Gauss cm

- imaging detector
- momentum measurement (B-field)

$$R = \frac{p}{0.3\,qB} \quad (m,\ \mathrm{GeV/c},\ \mathrm{tesla})$$

- [illegible] with large range ([illegible]) [illegible] with [illegible] HR

a) $x/x_0 = 1.0$ b) $x/x_0 = 0.01$

c) [illegible] 400 μm d) $\sigma = 100\,\mu m$ e) $\sigma = 25\,\mu m$

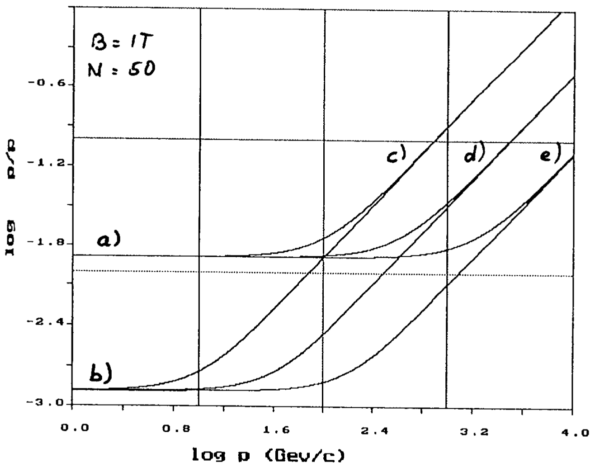

$$s = 0.3\,\frac{BL^2}{8P}$$ measure s with precision σ

$$\left(\frac{\Delta P}{P}\right)^N = \frac{\sigma P}{0.3BL^2}\sqrt{\frac{720}{N+4}} \oplus \frac{0.05}{BL}\sqrt{\frac{1.43\,L}{X_0}}$$

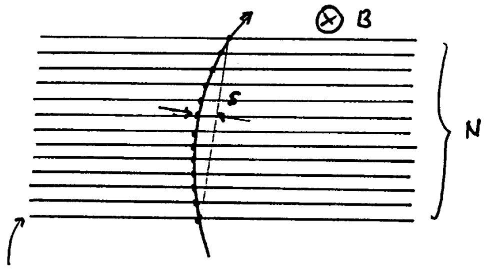

detector thickness causes scattering, radiation length x/x_0

Reines & Cowan

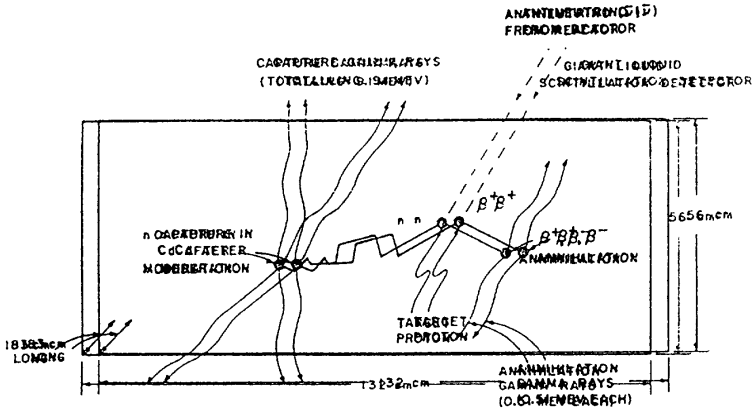

$\bar{\nu} + p \rightarrow n + \beta^+$

$\beta^+ + e^- \rightarrow 2\gamma$

→ capture, delayed γ-rays

- massive detector, time measurement
- specific information for particle identification (pulse height, timing)

UA1, CERN

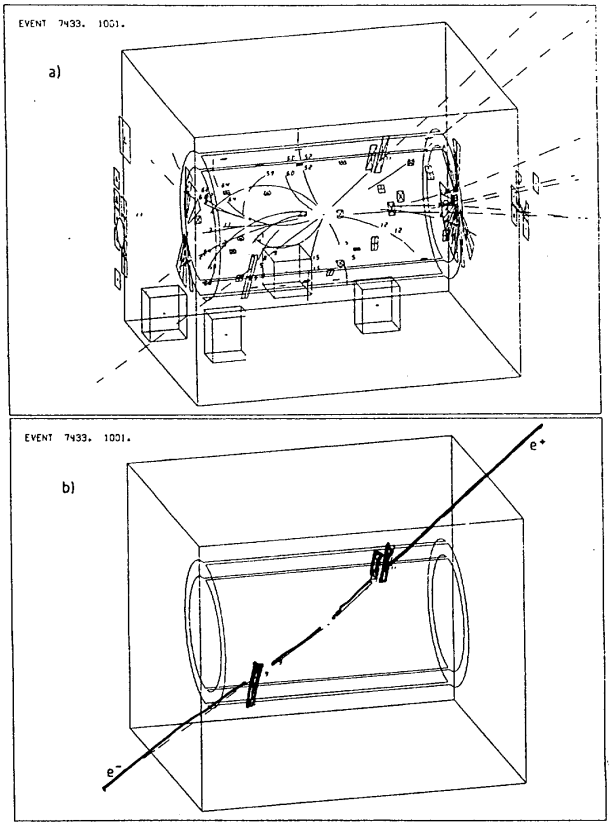

$Z^0 \rightarrow e^+ e^-$ — calorimeter hits
— tracks

- 4π -detectors
  event reconstruction

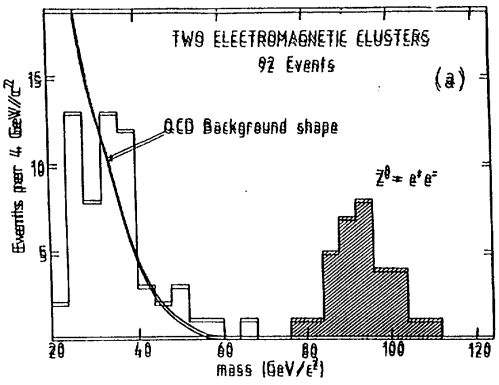

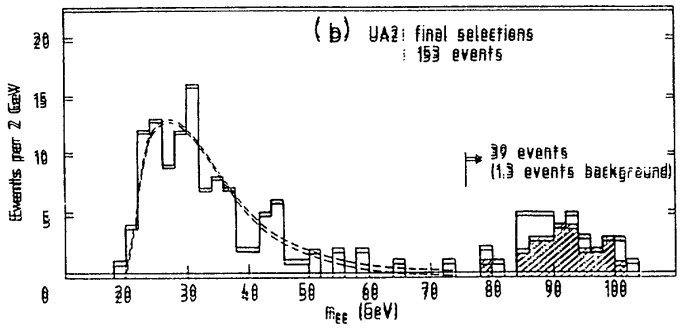

Schneider et al.

Compton scattering with bound electrons
⇝ momentum distribution

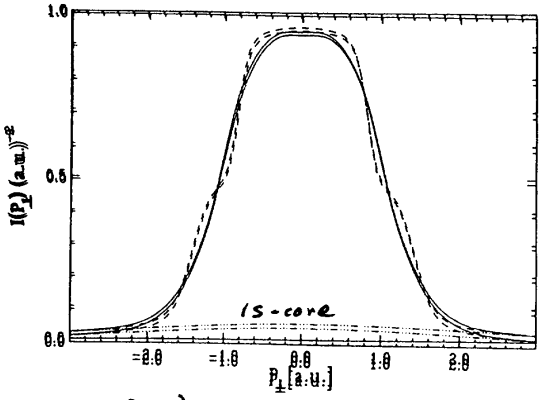

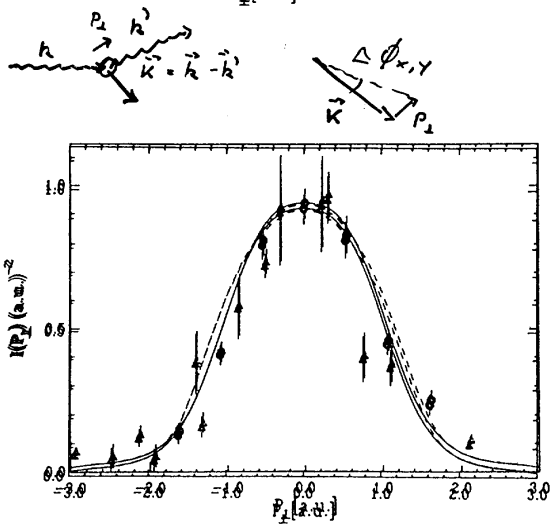

use position sensitive semiconductors

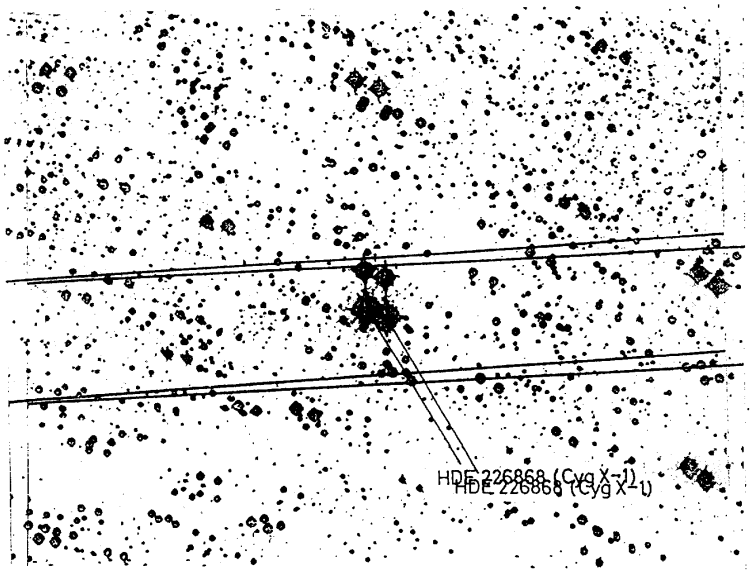

x-ray emitting Cygnus X-1
pulsating, candidate for black hole

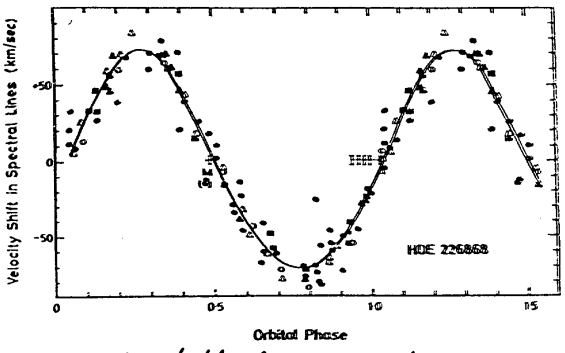

Doppler shift of companion

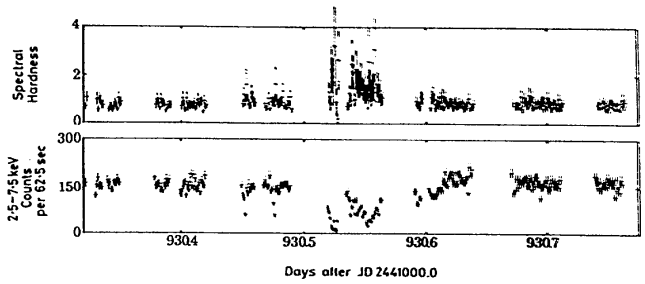

x-ray intensity, correlated

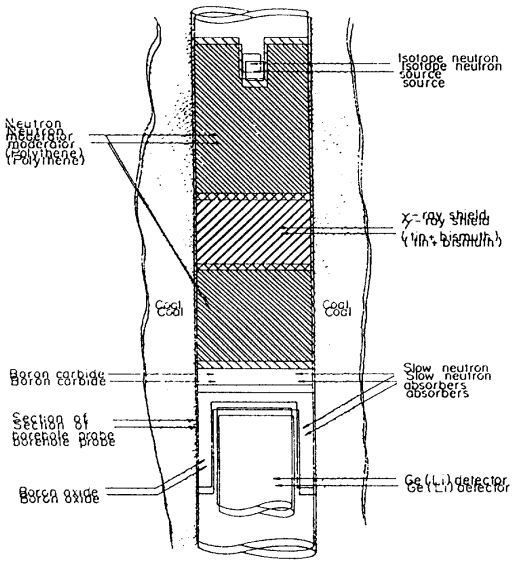

bore hole spectroscopy

determin. quality of coal

before exploiting (ash - contents)

Prompt γ-rays from thermal neutron capture

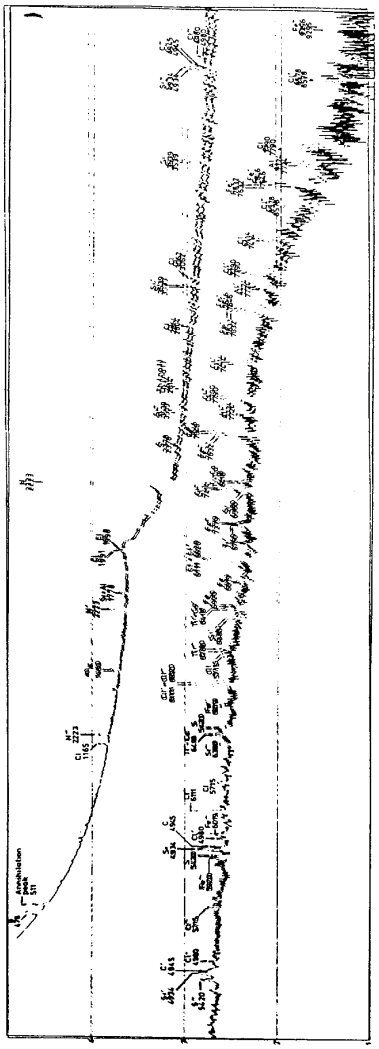

Fig. 3.7: γ-ray spectrum of the coal sample containing 30.6% ash

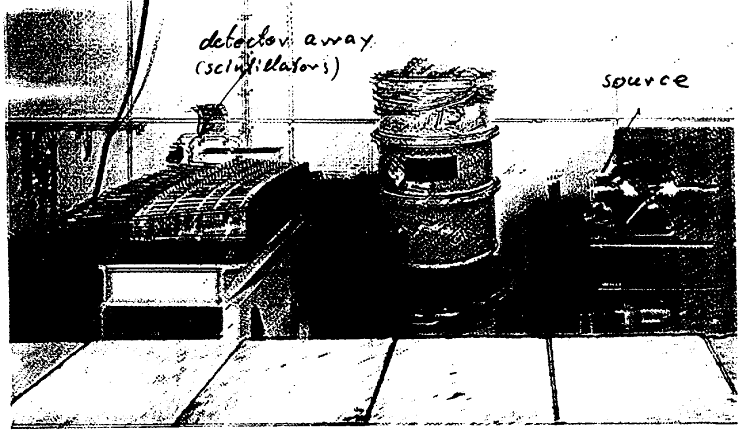

8, x-ray [illegible] nuclear waste
[illegible]

Nuclear medicine, scanner.

determines life process

Radio nucleides as tracers

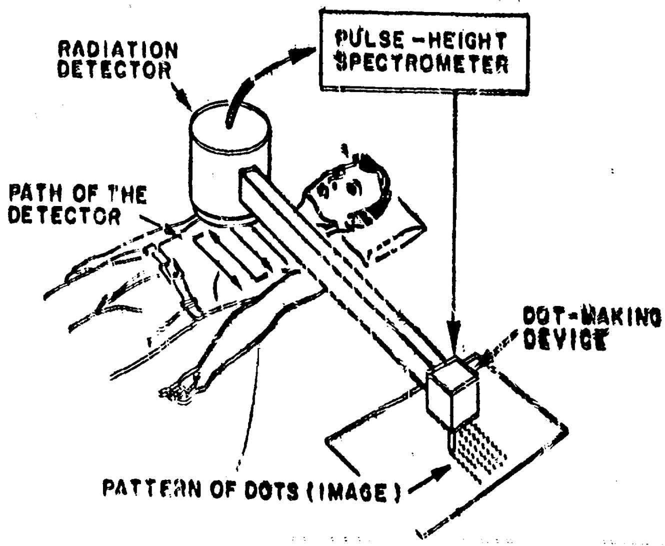

chest x-ray

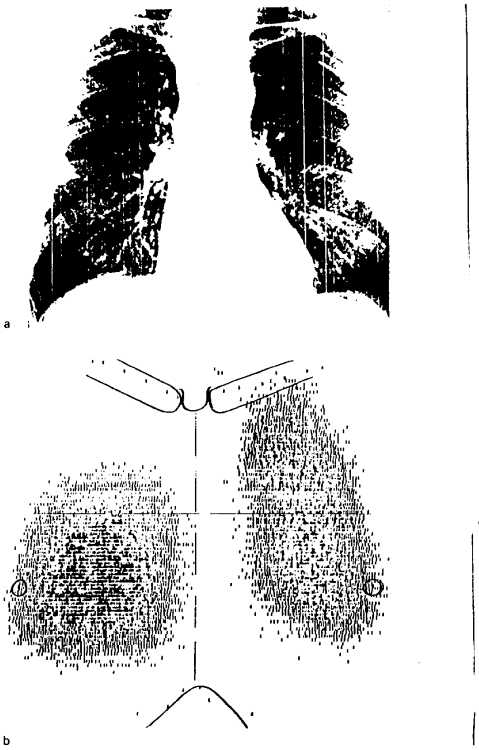

lung activity (Xe)

The Proportional Counter

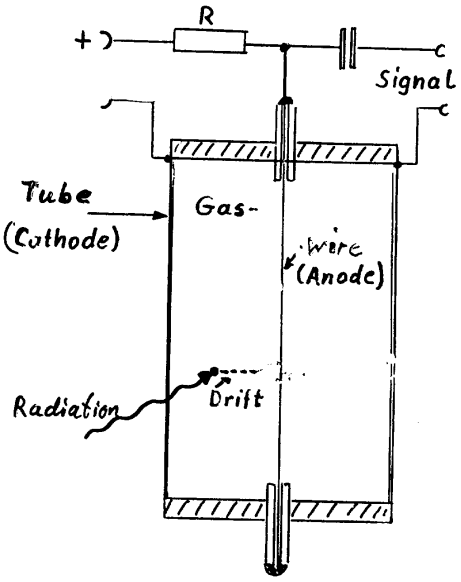

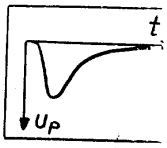

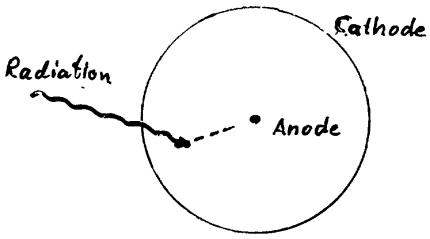

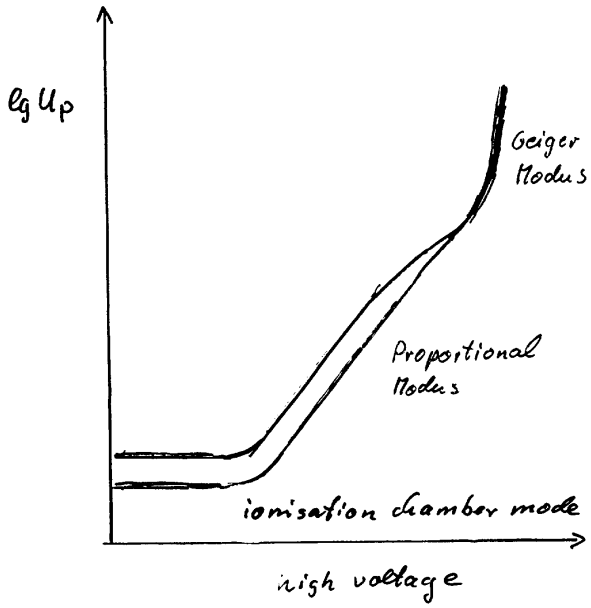

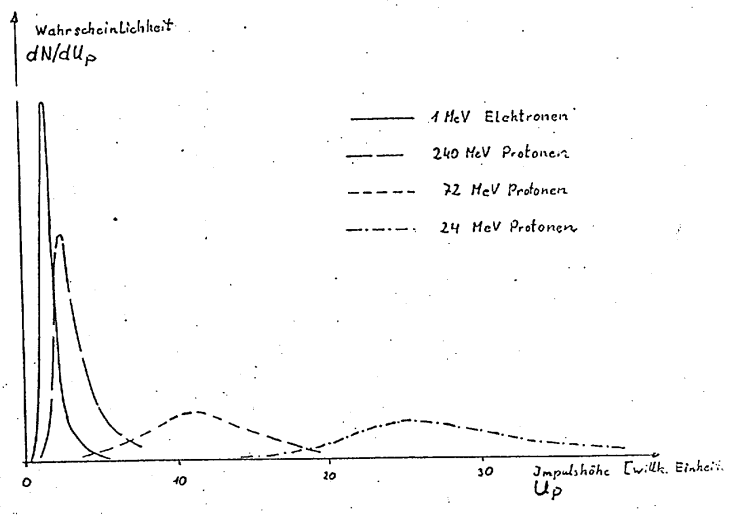

Energy loss spectra of protons

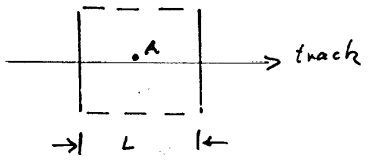

measure $\Delta E/L \sim U_p$

1 cm, 90% Ar + 10% CH_4

Energy loss of charged particles

electrons in atom $q_0 = Z e_0$

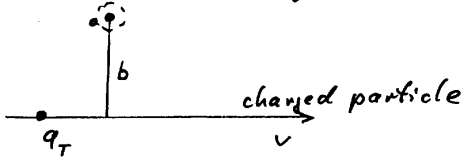

Momentum transfer:

$$p' = \int_0^\infty F(t)\,dt = \int q_0\,\mathcal{E}(t)\,dt \qquad \mathcal{E}: \text{electric field}$$

$$E' = \frac{p'^2}{2m} \qquad \text{for free electron}$$

$\phi(E', E)\,dE'\,dx$: probability for encounter in $E' .. E'+dE'$ in dx

$\Rightarrow$

1) number of encounters

$$\left\langle \frac{dN}{dx} \right\rangle = \int_{E'_{min}}^{E'_{max}} \phi(E', E)\,dE'$$

2) Energy loss

$$\left\langle \frac{dE}{dx} \right\rangle = \int_{E'_{min}}^{E'_{max}} E'\,\phi(E', E)\,dE'$$

calculation of $\phi(E', E)$

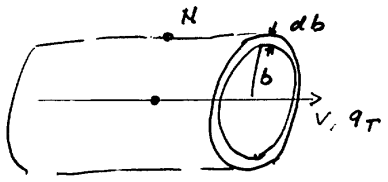

$$4\pi q_T = \int \mathcal{E}\,dF = \int \mathcal{E}\,2\pi b v\,dt = 2\pi b v \int \mathcal{E}\,dt$$

$\Rightarrow$

$$q_0 \int \mathcal{E}(t)\,dt = \frac{2 q_T q_0}{b v} = p' = \frac{2 Z e^2}{b \beta c}$$

$\Rightarrow$

$$E'(b) = \frac{p'^2}{2m} = \frac{4 Z^2 e^4}{2 m c^2 \beta^2 b^2} = \alpha \frac{1}{b^2}$$

$$\frac{dE'}{db} = -2\alpha \frac{1}{b^3} \qquad db = -\frac{b^3}{2\alpha}\,dE'$$

$$\phi(b)\,db = \frac{2\pi b}{F}\,db$$

$\rightsquigarrow$

$$\phi(E')\,dE' = \frac{2\pi Z^2 e^4}{F\,dx\,m c^2 \beta^2} \frac{1}{E'^2}\,dE'\,dx$$

$$\phi(E')\,dE' = \frac{N 2\pi Z^2 e^4}{m c^2 \beta^2} \frac{1}{E'^2}\,dE'\,dx$$

for N: electron density

$$\phi(E')dE' = \frac{\tilde{A}\varrho}{\beta^2}\,\frac{dE'}{E'^2}\,dx$$

$$\tilde{A} = 0.1536\,\frac{Z}{A}\ \text{MeV cm}^2/\text{g}$$

Energy loss:

$$\left\langle \frac{dE}{dx} \right\rangle = \int_{E'_{min}}^{E'_{max}} E'\phi(E')dE' = \frac{\tilde{A}\varrho}{\beta^2}\int \frac{dE'}{E'}$$

$$= \frac{\tilde{A}\varrho}{\beta^2}\,\ln\frac{E'_{max}}{E'_{min}}$$

1) b_{max}

$\Delta t \approx \frac{1}{\langle\nu\rangle}$ atomic frequency, adiabatic

$$\Delta t \approx b/v \le \frac{1}{\langle\nu\rangle}\,\frac{1}{\sqrt{1-\beta^2}}$$

$$\Rightarrow$$

$$b_{max} = \frac{\beta c}{\langle\nu\rangle(1-\beta^2)^{1/2}}$$

$$E'_{min} = \alpha\,\frac{\langle\nu\rangle^2(1-\beta^2)}{\beta^2 c^2}$$

2) $b_{min}\ (E'_{max})$

$$b_{min} > \frac{h}{p} = \frac{h}{m_e\beta\gamma c} = \frac{h(1-\beta^2)^{1/2}}{m_e\beta c}$$

$$E'_{max} = \alpha\,\frac{m_e^2c^2\beta^2}{h^2(1-\beta^2)}$$

$$\Rightarrow$$

$$\left\langle \frac{dE}{dx} \right\rangle = \frac{\tilde{A}\varrho}{\beta^2}\,\ln\frac{m_e^2c^4\beta^4}{h^2(1-\beta^2)^2\langle\nu\rangle^2\beta c}$$

$$= \frac{\tilde{A}\varrho}{\beta^2}\left[2\ln\frac{2m_ec^2}{\bar{I}} + 2\ln(\beta\gamma)^2 - \underbrace{2\beta^2 - 2\delta}\right]$$

Bethe; corrections rel., density

$\bar{I} = h\langle\nu\rangle$: mean ionisation potential

$$\ln\bar{I} = \frac{\sum Z_\nu n_\nu \ln I_\nu}{\sum Z_\nu n_\nu}$$

$$\overline{\tilde{A}\varrho} = \frac{\sum n_\nu \frac{Z_\nu}{A_\nu}\varrho_\nu}{\sum n_\nu}$$

mixtures ν

n_ν: atoms

Z_ν: electrons/atom

Range

$$R = \int_{E_0}^{0} \frac{dE}{\frac{dE}{dx}}$$

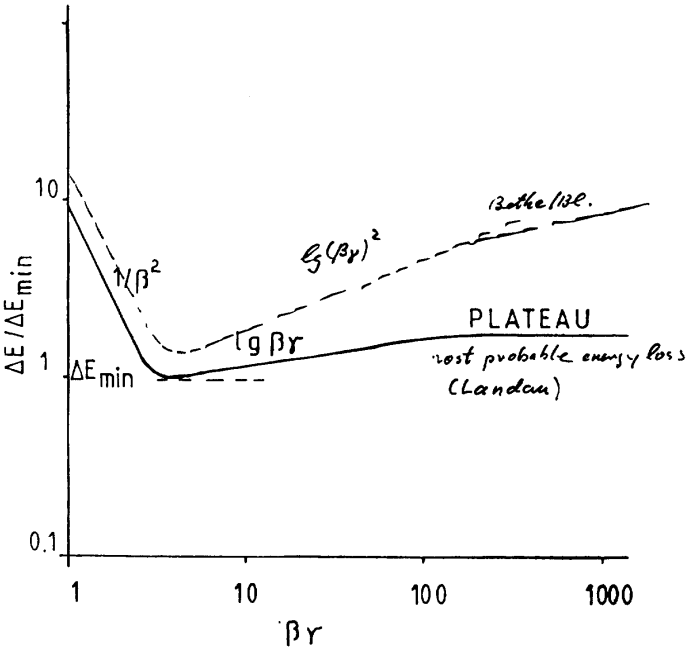

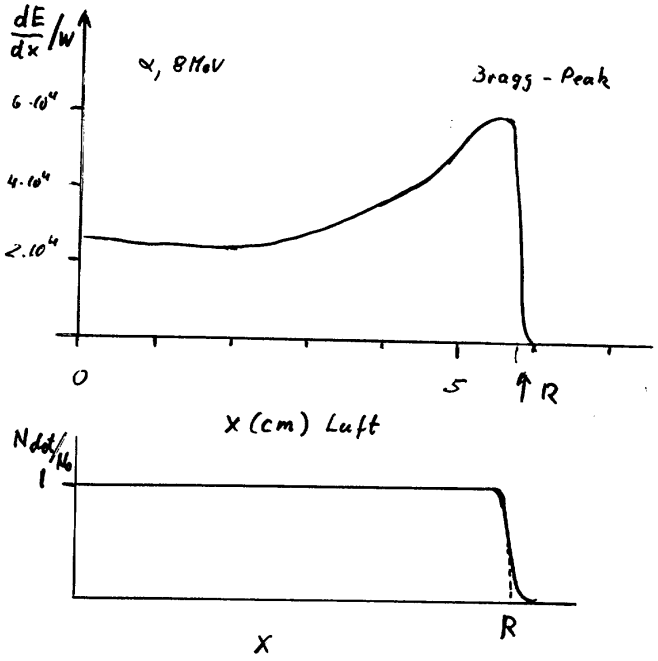

Longitudinal drift

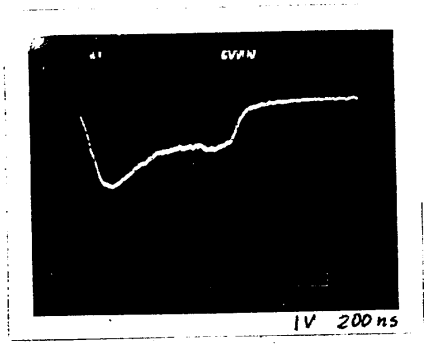

^{241}Am $U_K = 700\,V$ $U_D = 500\,V$

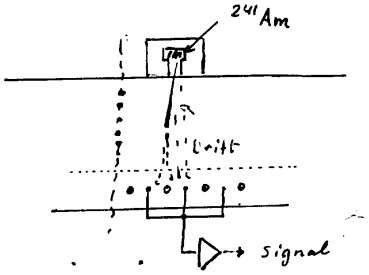

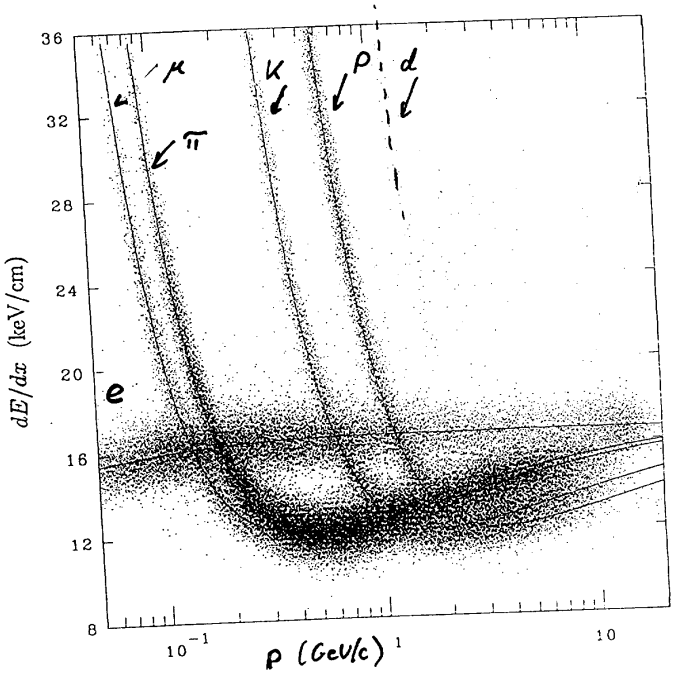

TPC data, $E_{tot} = 29\,GeV$

full lines: predicted values

(10c)

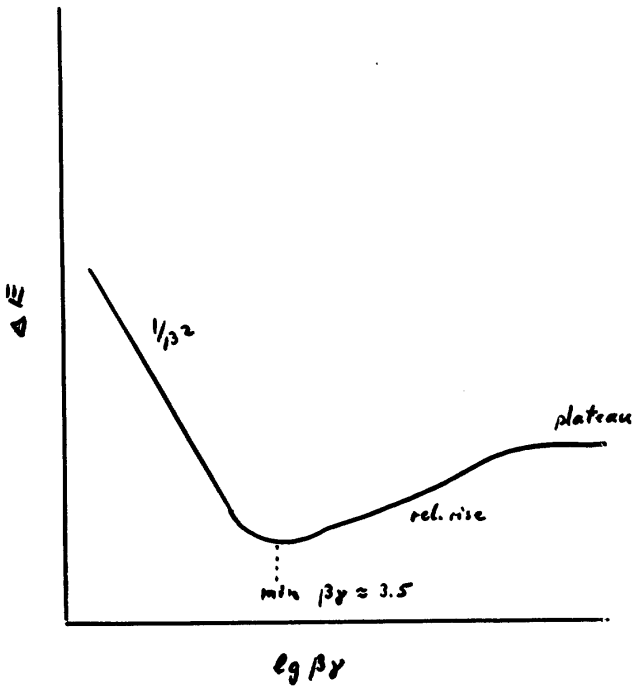
dE
1/β²
plateau
rel. rise
min βγ ≈ 3.5
lg βγ

(11a)

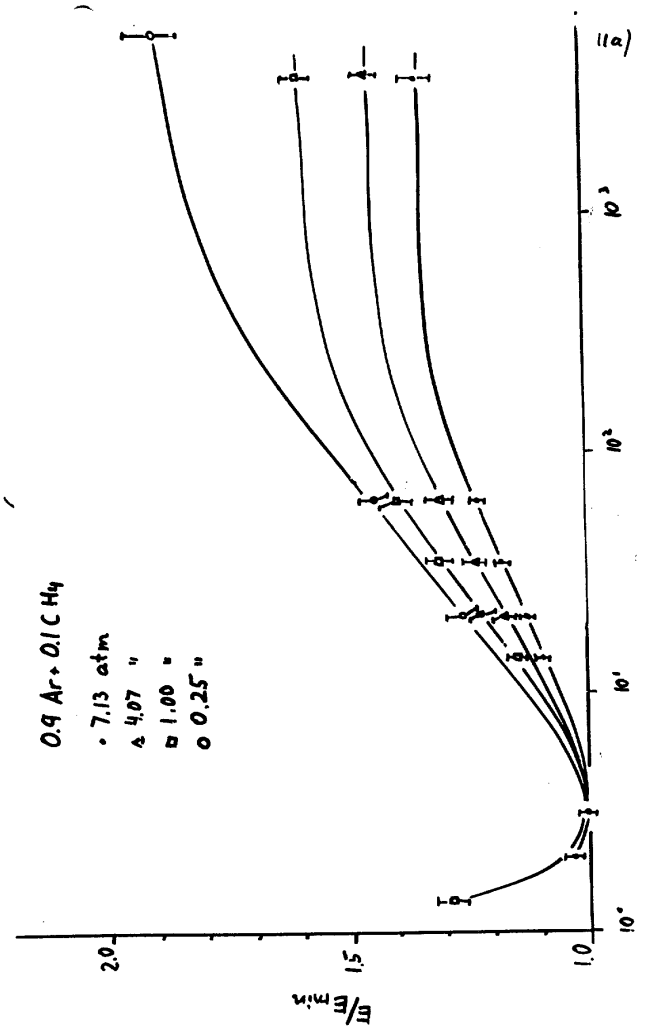
0.9 Ar + 0.1 C H4
• 7.13 atm
▲ 4.07 "
□ 1.00 "
○ 0.25 "
E/Emin
2.0
1.5
1.0
10³
10²
10¹
10⁰

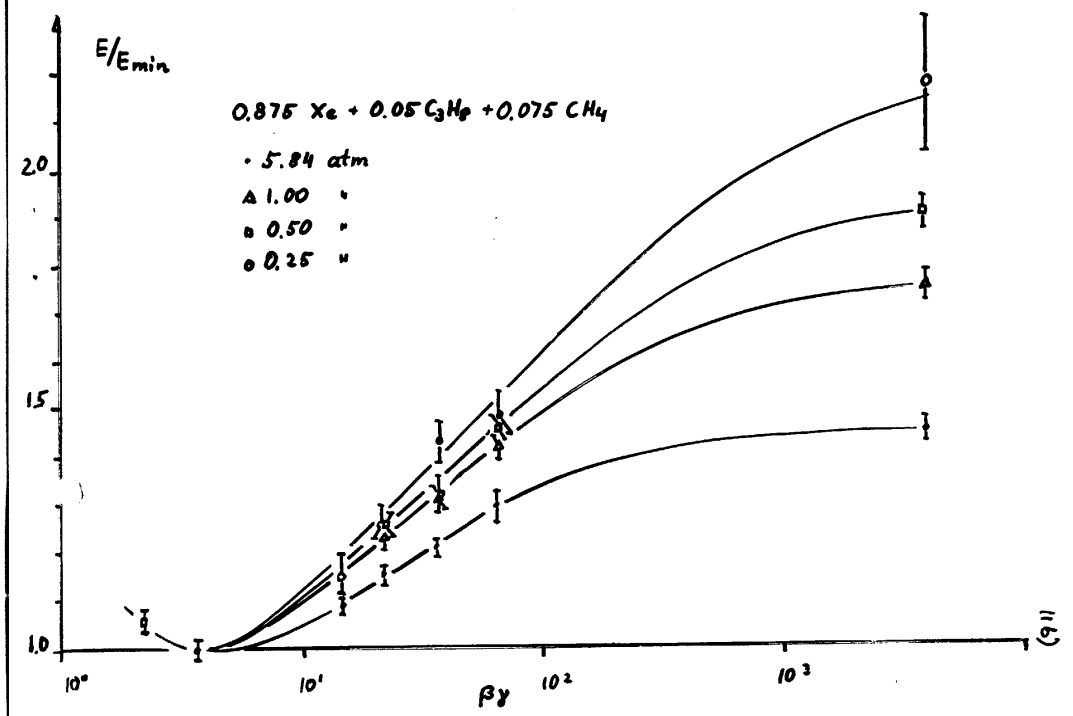
E/Emin
0.875 Xe + 0.05 C3H8 + 0.075 CH4
• 5.84 atm
▲ 1.00 "
□ 0.50 "
○ 0.25 "
2.0
1.5
1.0
10°
10¹
10²
10³
βγ
(9)

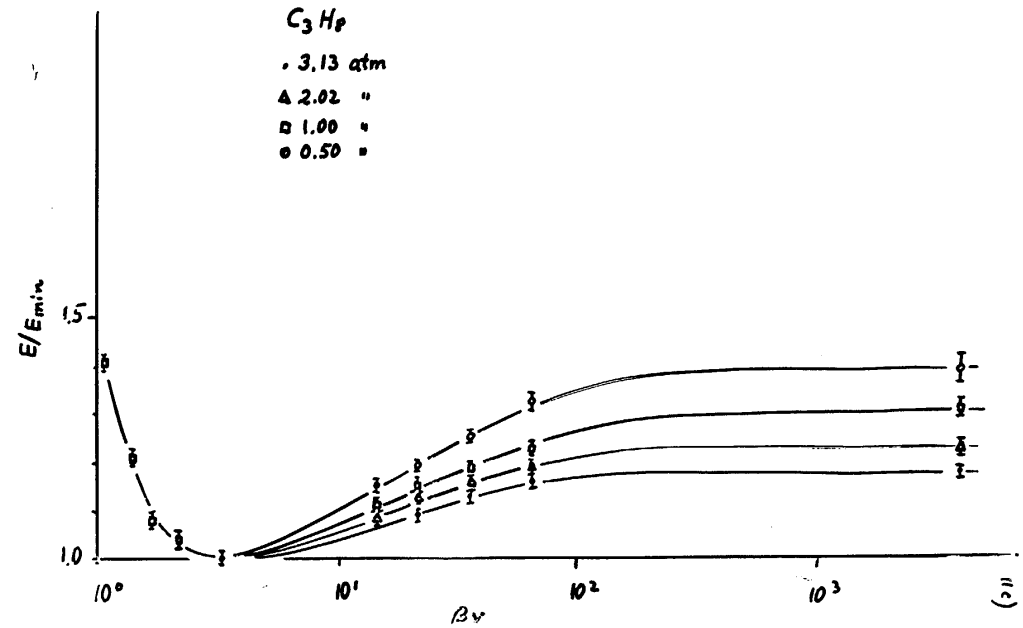
C3H8
• 3.13 atm
▲ 2.02 "
□ 1.00 "
○ 0.50 "
E/Emin
1.5
1.0
10°
10¹
10²
10³
βγ
(10)

ISIS, CERN, Oxford

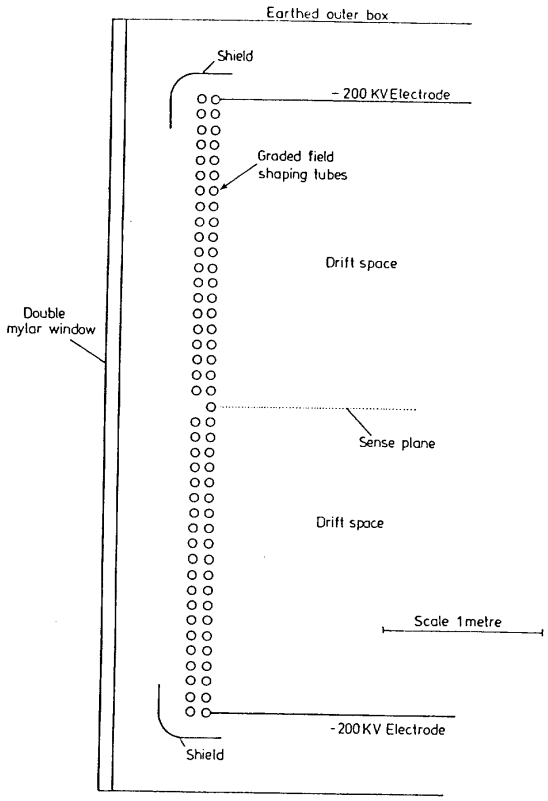

Fig. 2

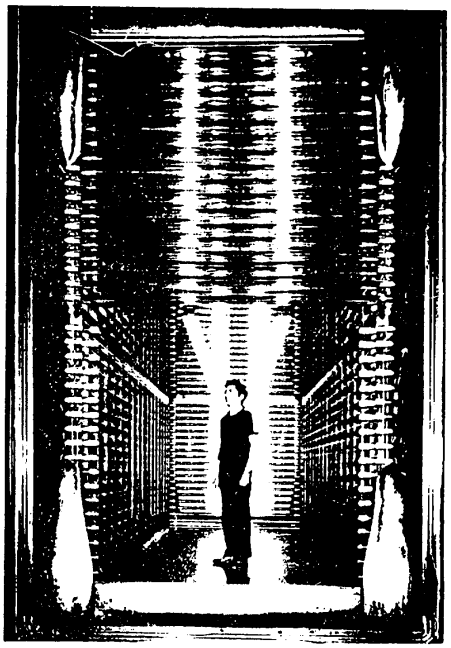

View of ISIS looking downstream during construction.

4m x 2m x 5.12 m

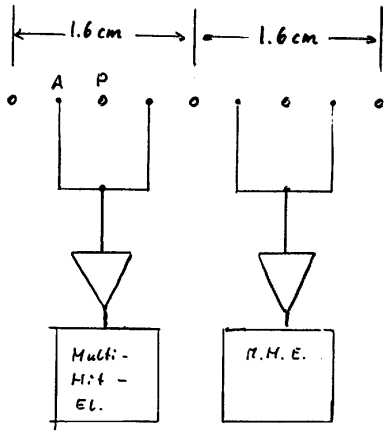

anodes 640

channels 320

E 500 V/cm

gas 80% Ar + 20% CO_2 (Oxisorb)

gain 10^4

gate 800 μs

Electrode arrangement of the ISIS-detector
A: anode, P: potential wire

tion.

single event in ISIS

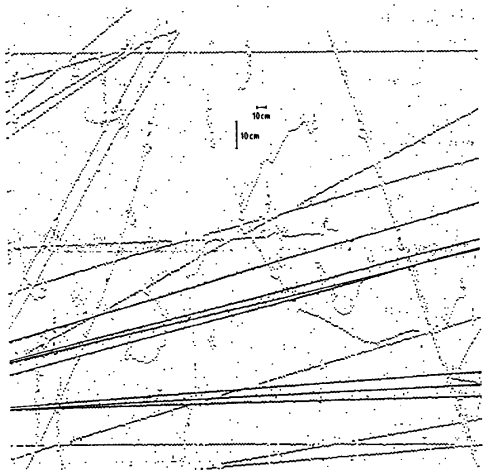

Fig.4. Display of track-hit data in ISIS2 for a single event. For some of the tracks the vectors seen in the other drift chambers of the spectrometer are seen superposed.

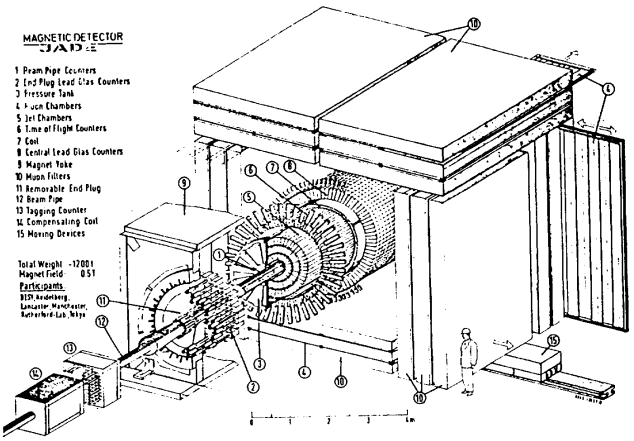

Fig. 1. JADE experimental apparatus

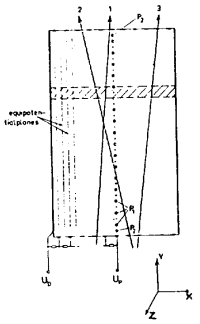

Fig. 2. Cross section of a jet chamber cell. 1, 2, 3: particle tracks; hatched area: drift space belonging to one anode wire.

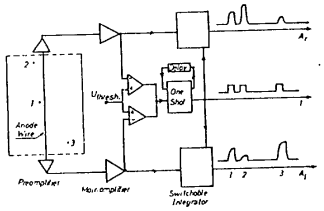

Fig. 3. Plan view of a drift space and associated electronics

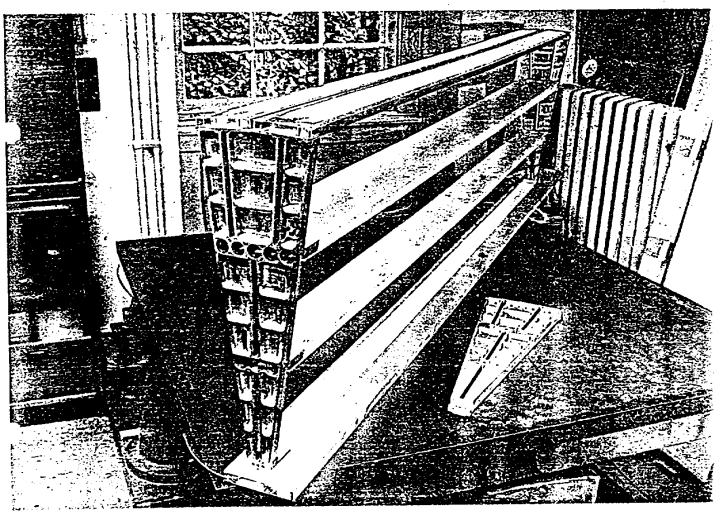

One segment of the JADE central detector at the Heidelberg institute.

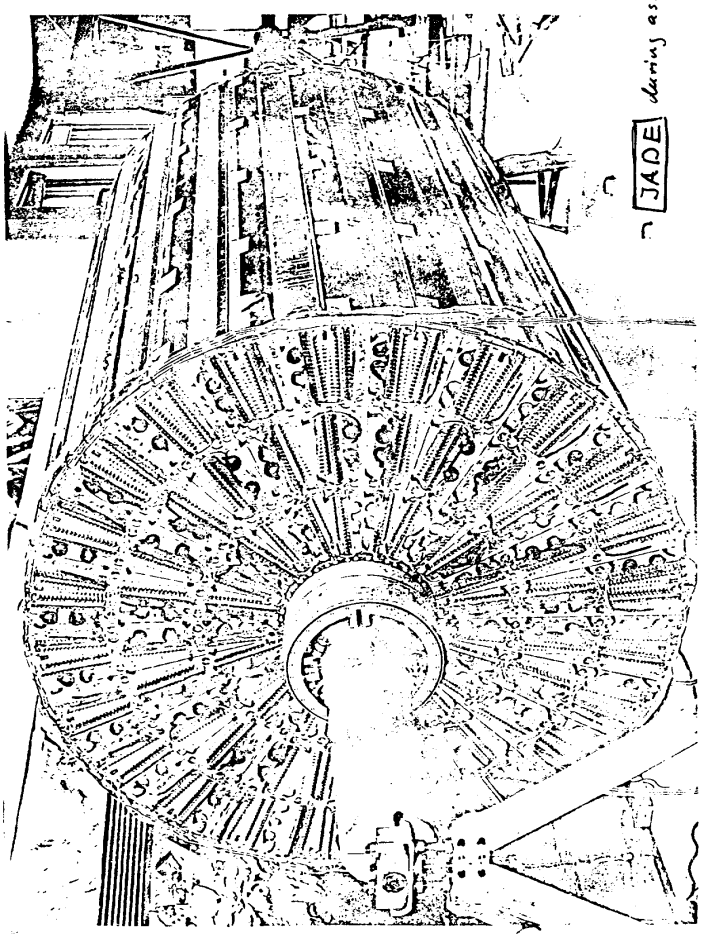

Particle Identification using dE/dx

Technical "details":

broad distribution : "Landau" distribution

results in considerable overlap

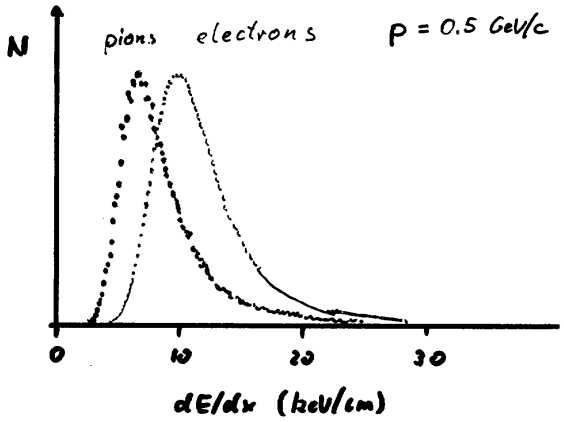

Oscilloscope signal of minimum ionizing particle. Longitudinal drift shows clusters.

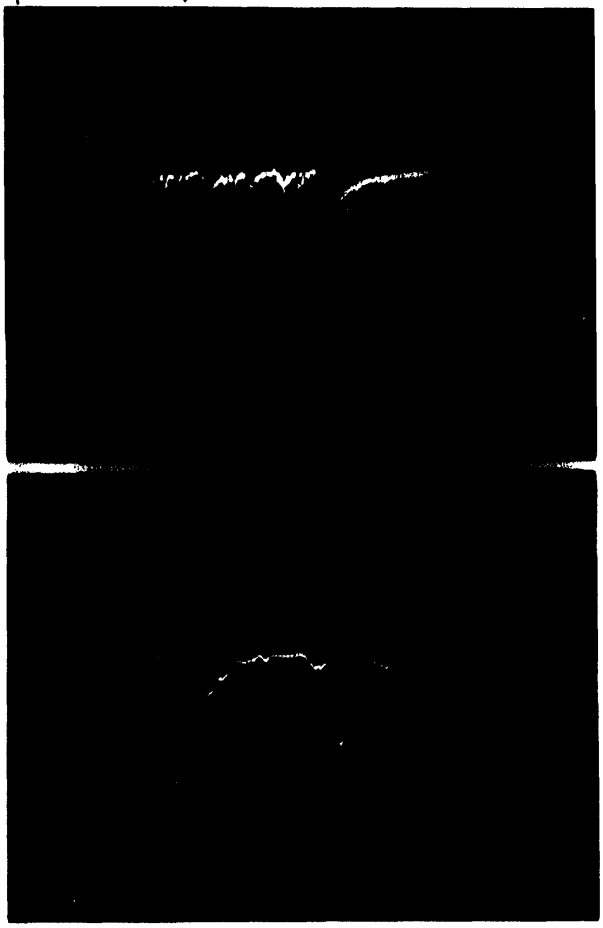

Cluster counting with longitudinal drift:

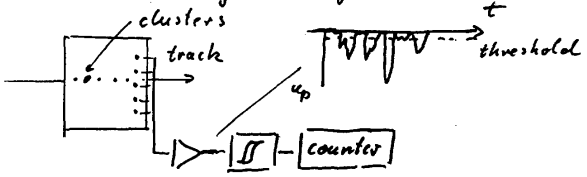

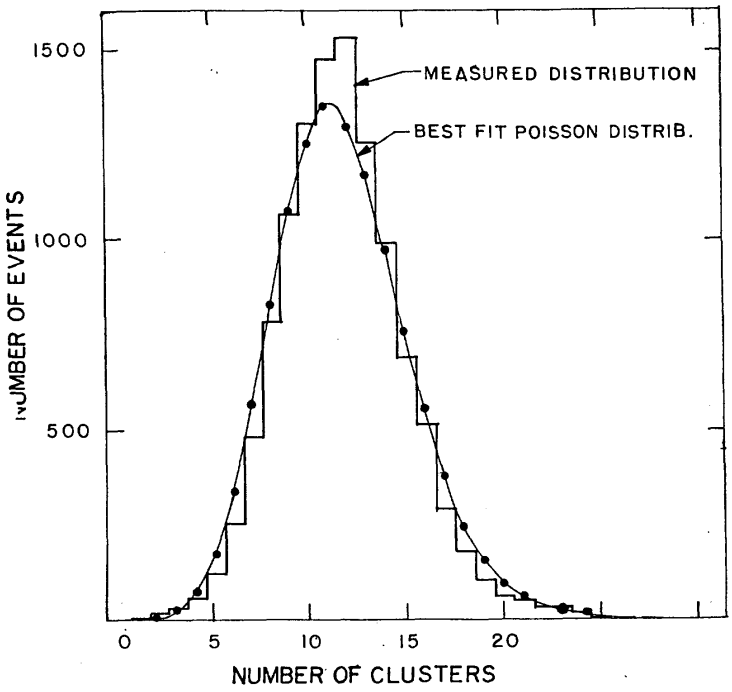

- Geiger / Streamer
- o Drift - chamber

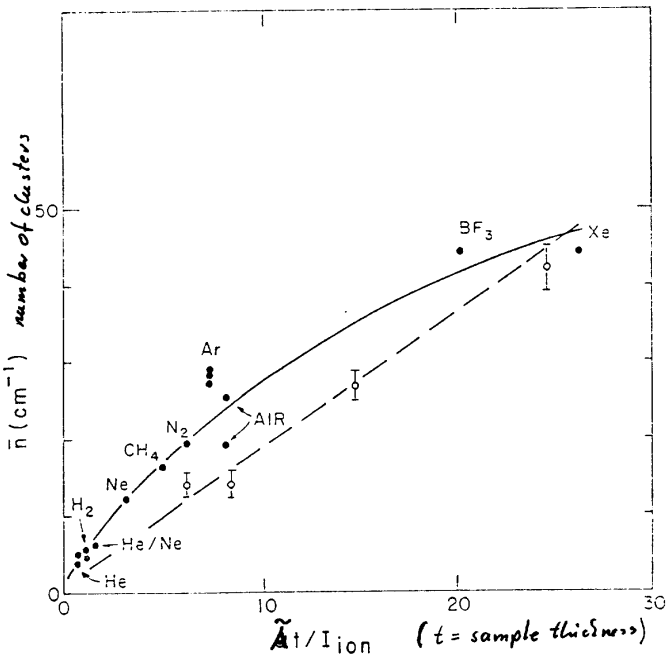

Fig. 26

Landau - Distribution

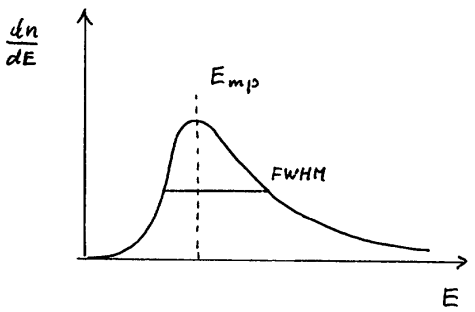

defined are: E_{mp}, FWHM, no $\left(\frac{\Delta E}{E}\right)_{rms}$! and no $\bar{E}$!

$\phi(\varepsilon)\,d\varepsilon$: Probability for encounter with ε

$\rightsquigarrow$ $E = \sum_{1}^{N} \varepsilon_i$ with N Poisson distributed

$\bar{E} = \int_{\varepsilon_{min}}^{\varepsilon_{max}} \phi(\varepsilon)\,\varepsilon\,d\varepsilon$ with $\phi(\varepsilon)\,d\varepsilon \approx \frac{Aqt}{\beta^2}\frac{d\varepsilon}{\varepsilon^2}$

$\Rightarrow$ $\boxed{\bar{E} = \frac{Aqt}{\beta^2} \ln \frac{\varepsilon_{max}}{\varepsilon_{min}}}$ depends on limits!

$\boxed{\left(\frac{\Delta E}{E}\right)_{rms} = \frac{1}{N}\int (\varepsilon - \bar{\varepsilon})^2 \phi(\varepsilon)\,d\varepsilon = \frac{1}{N}\,\frac{\varepsilon_{max}}{\varepsilon_{min}}\,\frac{1}{\ln \frac{\varepsilon_{max}}{\varepsilon_{min}}}}$

worse!

MONTE CARLO II (without density effect)

Cluster-size distribution:

$$N\phi(\varepsilon) = \frac{dn}{d\varepsilon} = \frac{\bar{A}\varrho t}{\beta^2}\left\{\frac{1}{\varepsilon} f(\varepsilon)\left(\ln\frac{2m_e c^2\beta^2\gamma^2}{\varepsilon} - \beta^2\right) + \frac{1}{\varepsilon^2}\int_0^{\varepsilon} f(\varepsilon)\,d\varepsilon\right\}$$

Resonant — Rutherford

$f(\varepsilon)$: Oszillatorstrength

Ansatz: $f(\varepsilon) \sim \sigma(\varepsilon)$ für Photoabsorption

$$\sigma(\varepsilon) \approx \frac{1}{\varepsilon^2}$$

$$f(\varepsilon) = \begin{cases} B/\varepsilon^2 & \text{für } \varepsilon \geq \varepsilon_i \\ = 0 & \text{für } \varepsilon < \varepsilon_i \end{cases}$$

Integration of Rutherford-part

$$\int f(\varepsilon)\,d\varepsilon = \int_{\varepsilon_i}^{\varepsilon} \frac{B}{\varepsilon^2}\,d\varepsilon = B\left(\frac{1}{\varepsilon_i} - \frac{1}{\varepsilon}\right) \quad \text{für } \varepsilon \geq \varepsilon_i$$

$\Rightarrow$

$$\frac{dn}{d\varepsilon} = \frac{\bar{A}\varrho t}{\beta^2}\left\{\frac{1}{\varepsilon} f(\varepsilon)\underbrace{\left(\ln\frac{2m_e c^2\beta^2\gamma^2}{\varepsilon} - \beta^2\right)}_{V(\varepsilon)} + B\left(\frac{1}{\varepsilon^2\varepsilon_i} - \frac{1}{\varepsilon^3}\right)\right\}$$

Normalized on number of clusters:

$$N_{tot} = \int_0^{\infty} \frac{dn}{d\varepsilon}\,d\varepsilon \quad , \quad \text{splitting in shell contributions}$$

$$N_{tot} = \frac{\bar{A}\varrho t}{\beta^2}\sum_i \left\{\int_0^{\infty} \frac{f_i(\varepsilon)}{\varepsilon} V(\varepsilon) + \frac{B_i}{\varepsilon_i}\int_{\varepsilon_i}^{\infty}\left(\frac{1}{\varepsilon^2} - \frac{\varepsilon_i}{\varepsilon^3}\right)d\varepsilon\right\}$$

$V(\varepsilon)$ weakly variabel, $V(\varepsilon) \approx V(\varepsilon_i) \approx$ const.

1. Integral

$$V(\varepsilon_i)\int_0^{\infty} \frac{f(\varepsilon)}{\varepsilon}\,d\varepsilon = B_i V(\varepsilon_i)\int_{\varepsilon_i}^{\infty} \frac{1}{\varepsilon^2}\,d\varepsilon = \frac{1}{2} B_i V(\varepsilon_i)\frac{1}{\varepsilon_i^2}$$

2. Integral

$$\frac{B_i}{\varepsilon_i}\int_{\varepsilon_i}^{\infty}\left(\frac{1}{\varepsilon^2} - \frac{\varepsilon_i}{\varepsilon^3}\right)d\varepsilon = \frac{1}{2}\frac{B_i}{\varepsilon_i^2}$$

With $B_i = \varepsilon_i \frac{n_i}{Z} = f_i \varepsilon_i$ $\quad n_i$: number of electrons

$\sum n_i = Z \quad f_i = \frac{n_i}{Z}$

$$N_{tot} = \frac{\bar{A}\varrho t}{\beta^2}\sum_i \frac{1}{2} f_i \frac{1}{\varepsilon_i}\left[V(\varepsilon_i) + 1\right]$$

$\Rightarrow$

$$\frac{dn}{d\varepsilon} = \frac{\bar{A}\varrho t}{\beta^2}\sum_i f_i\left\{\frac{\varepsilon_i}{\varepsilon^3}\left[V(\varepsilon_i) - 1\right] + \frac{1}{\varepsilon^2}\right\}$$

Bem. $\Delta E = \int \varepsilon \frac{dn}{d\varepsilon}\,d\varepsilon$

Photoabsorption cross section

from Chechin et al.
– hydrocarbon

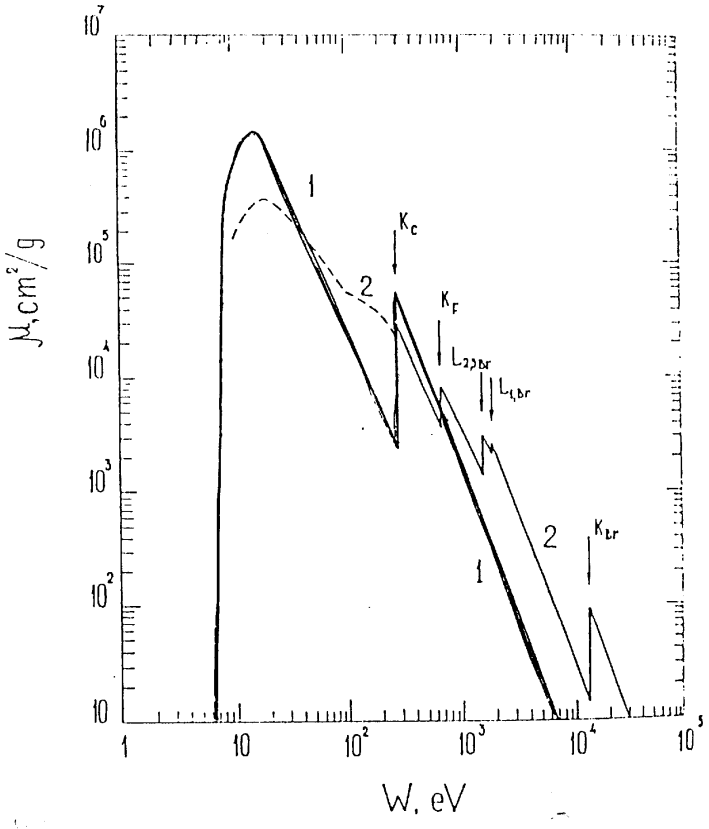

Application to Monte Carlo:

1) determination of contributions from shells

$$P_i = \frac{n_i/\varepsilon_i\,(V(\varepsilon_i)+1)}{\sum n_i/\varepsilon_i\,(V(\varepsilon_i)+1)}$$

2) Determination of resonant contribution

$$P_{i\,res} = \frac{V_i}{V_i+1} \qquad \left(P_{i\,Ruth} = \frac{1}{V_i+1} \right)$$

3) choice of N_{tot}

4) cutoff for low energies : Eion adjusted such that

$$W = \frac{E}{n_e} = \text{measured value}$$

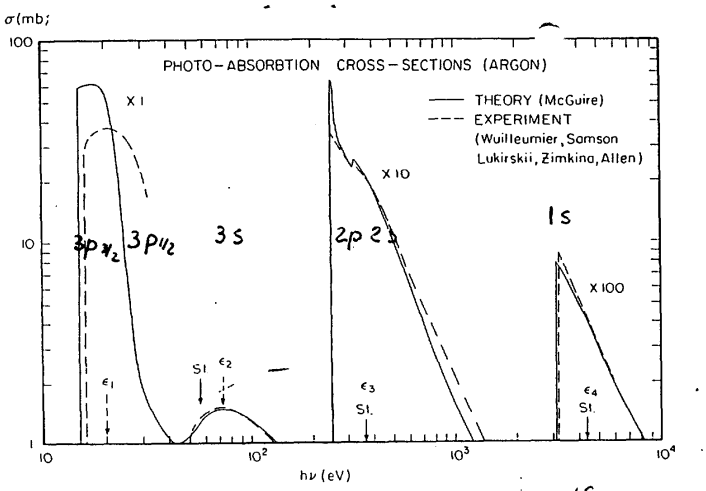

Fig. 1. Observed[13]) and calculated[12]) photo-absorption cross sections for photons incident on argon. the locations of equivalent δ-functions used in this paper. Arrows labelled St. are values of Sternhe

3p1/2 3p3/2 3s 2p 2s

Allison

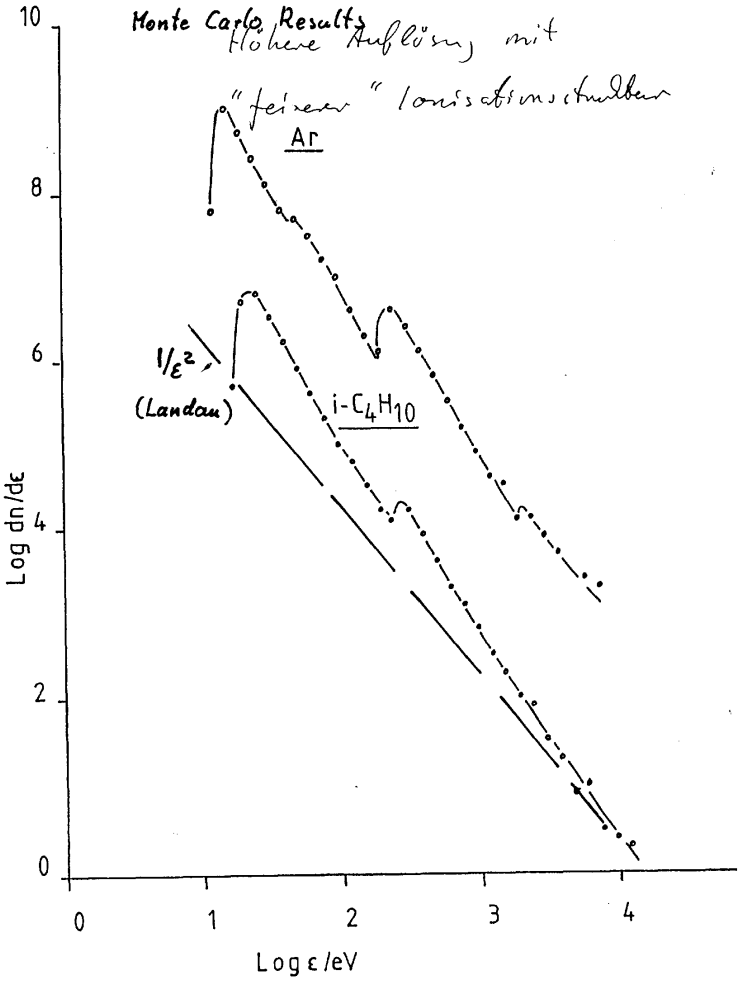

adjust Nref,

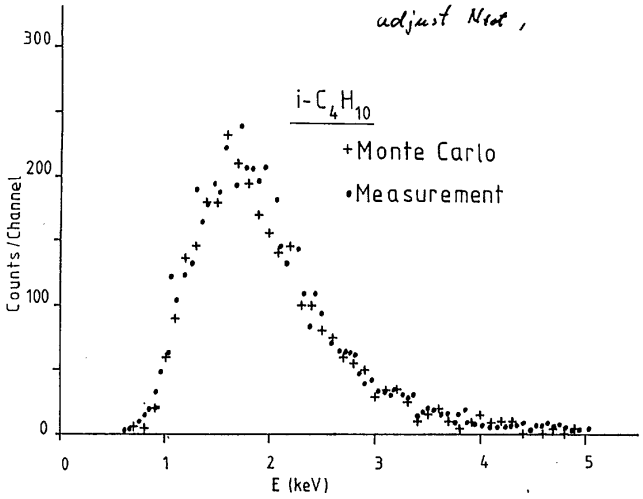

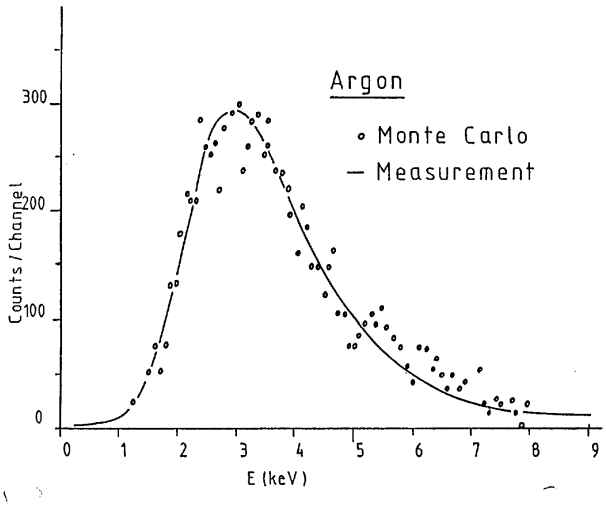

Effect of rel. rise Ermilova et al. 16j)

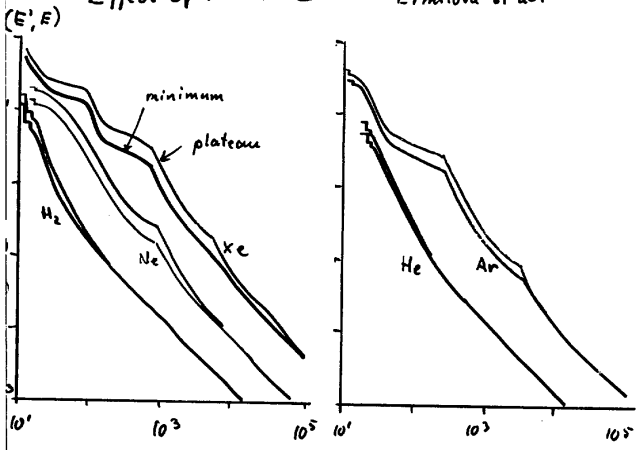

$$\left\langle \frac{dN}{dx} \right\rangle_{min} = \int_{E'_{min}}^{E'_{max}} \phi(E', E)\, dE'$$

Number of collisions/cm for $E'_{min} = 0$ (ionisation + exitation)

gas	minimum	plateau
He	5.3	8.0
Ne	12.8	19.3
Ar	29.3	40.7
Kr	35.4	50.0
Xe	48.1	65.3

Energy Loss in 1cm Material

for minimum ionising particles

($\beta\gamma \approx 3.5$)

material	a_x(keV)	ΔE(keV) mean	ΔE(keV) most probable
H_2	0.0147		
CH_4	0.0716	1.54	0.862
C_3H_8	0.188	4.30	2.16
CO_2	0.157	3.20	1.77
P-10	0.122	2.30	1.17
X-10	0.352	5.99	3.05
plastic Sc.	$1.06 \cdot 10^2$	$2.43 \cdot 10^3$	$1.8 \cdot 10^3$

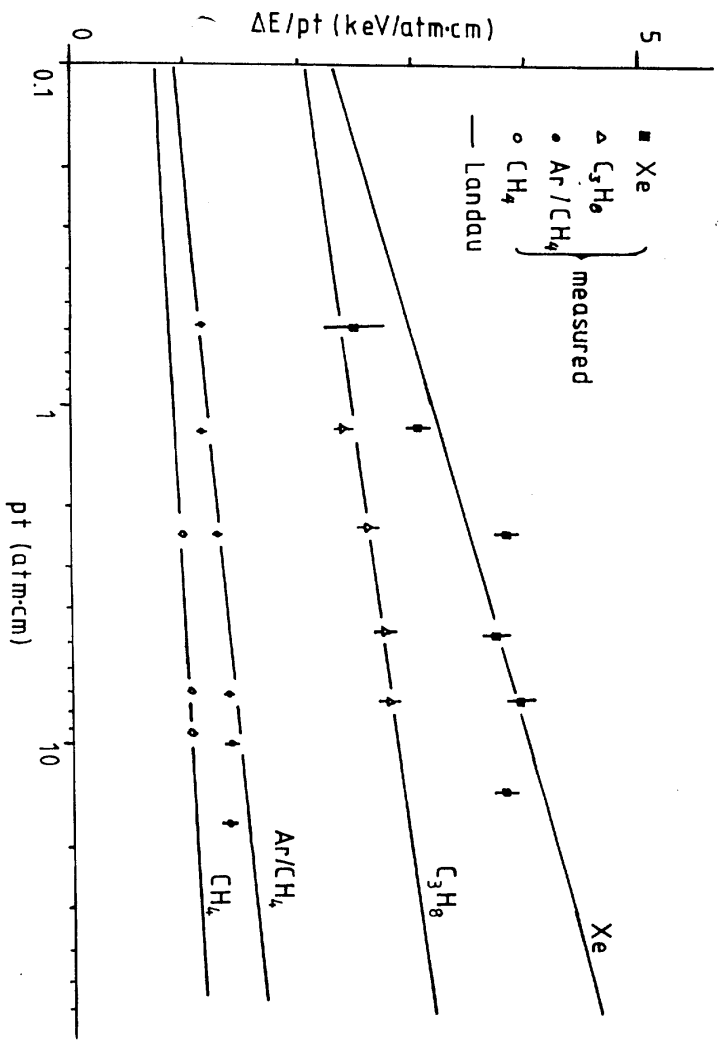

Energy loss distribution

W: FWHM E: most probable energy loss

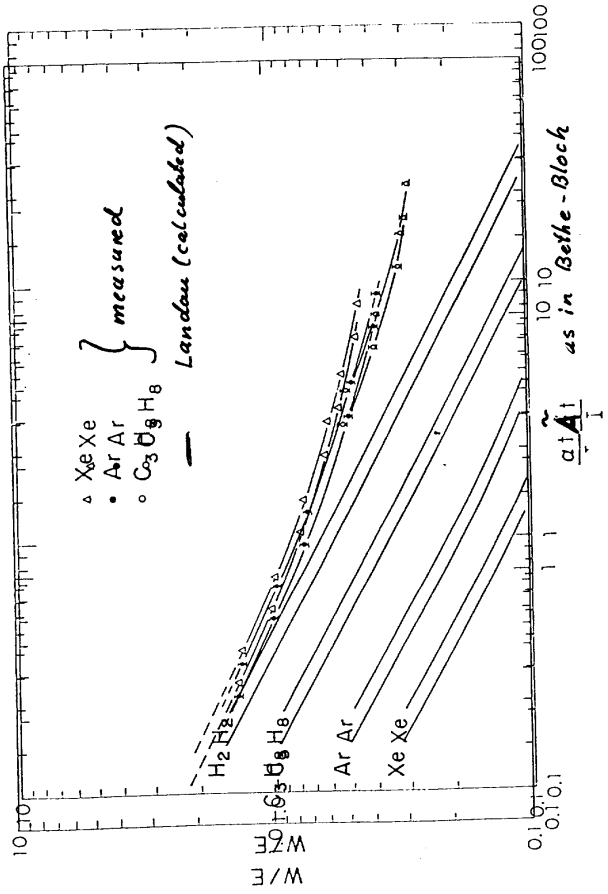

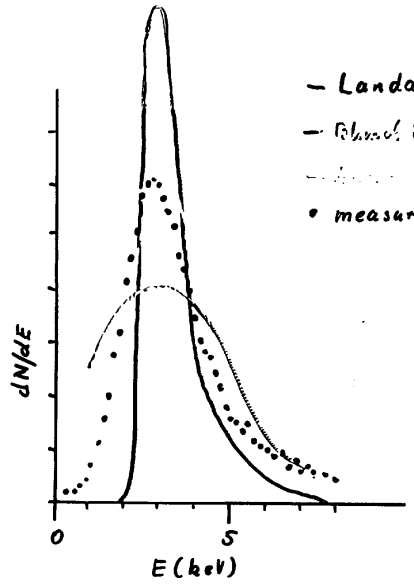

Historical remark:

- Landau has no resonant contribution
- Blunck & Leisegang have too much r.c.
- Monte Carlo method (Chechin, Allison...) is right but needs detailed atomic information

Application

Particle identification

In region of rel. rise differences are small
($K-\pi$: 16 %)

⇒ measurement of energy loss $\frac{\Delta E}{E} \leq 5\%$

Best resolution in prop. gas counter

Landau limit $H_L/E \approx 0.2$

Therefore sampling and statistical treatment

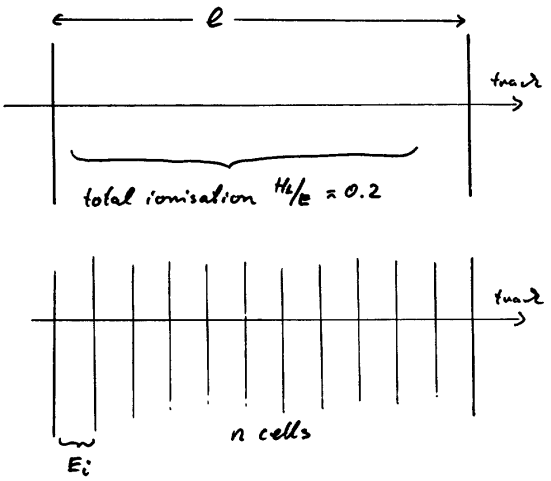

$$\frac{H_L^{(n)}}{E_i^{(n)}} = \frac{1}{g(n)} \frac{H_L^{(1)}}{E^{(1)}}$$ for n independent measurements

$\frac{1}{g(n)} = \frac{1}{\sqrt{n}}$ for Gaussian distributions

Landau distributions are <u>not</u> Gaussian

therefore :

- truncated mean
- max. likelyhood

improvement factor

$g(n) = n^{0.428}$

Cluster counting

$\frac{\Delta N}{N} = \frac{1}{\sqrt{N}}$ independent of sampling

$N = 20\ cm^{-1}$ ⇒ $\frac{\Delta N}{N} = 2.2\%$ for 1m track length

rel. rise limited

measurements not always in agreement with calculations.

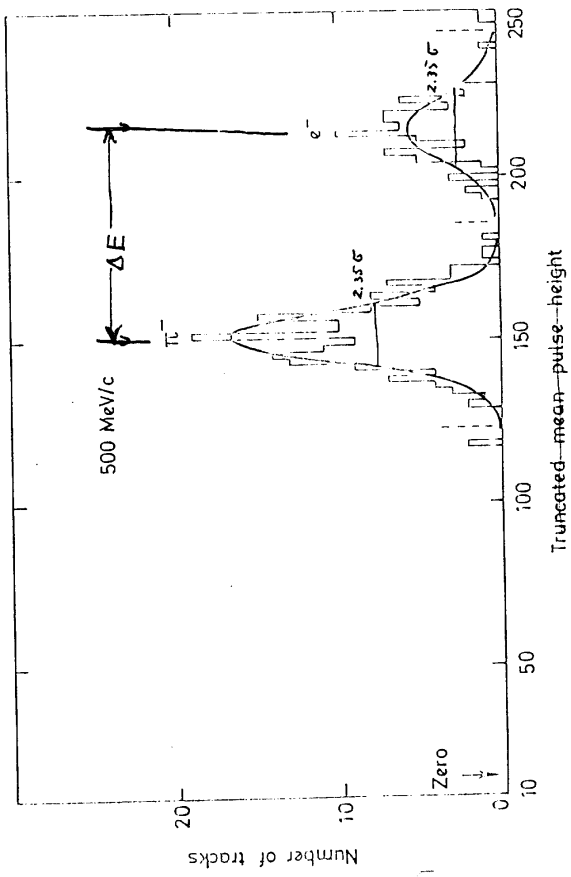

Fig. 5 — Tehrani et al.

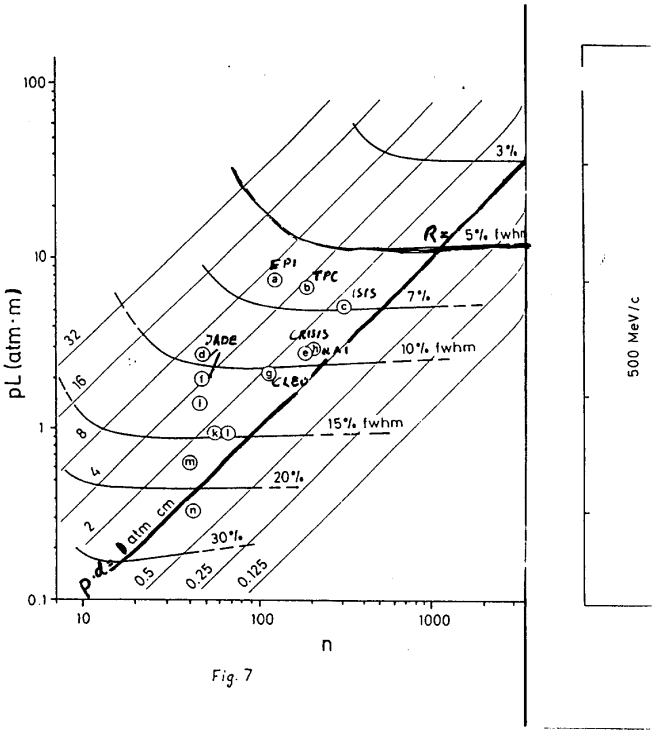

Fig. 7

Performance plot of dE/dx detectors

pL : pressure x length (total detector)

n : number of samples

p·d : pressure x width of one cell (parameter)

R : curves for constant resolution

Experimental Results

Device	particles	p (GeV/c)	exp. $\Delta E/\sigma$	theor. $\Delta E/\sigma$	Ratio
ISIS II[T]	π/e	0.5	8.0	8.1	1.01
CRISIS[T]	p/π	40	2.16	3.2	1.48
EPI	p/π	50	5.1	6.1	1.20
TPC[T]	π/e	0.8	11.8	15.0	1.36
JADE	π/e	0.45	4.2*	7.8	1.86
"	"	"	5.0	7.8	1.56
HRS[T]	π/e	4	3.2	4.1	1.32
Cleo	π/e	0.45	8.25	11.1	1.36

* analysis in jet

Response of detectors to x- and γ-rays

- o applications in industry
  non destructive testing (NDT)
- o performance defined by
  - interaction of photons in detector
  - mechanism of gas amplification

first example: precision

Fig. 11. Projection radiograph with Hatwell E.12 microfocal X-ray unit of integrated circuit showing extensive variability in the chip bonding interface which can affect heat dissipation. A × 1 radiograph for comparison is shown in the inset circle. Parish and Kear (1977).

Quality control of chip electronics
- o thermal contact
- o bonding

Composite material here: glass fiber-epoxi inspect for delamination

Fig. 11.

linear precision ~ single photon counting

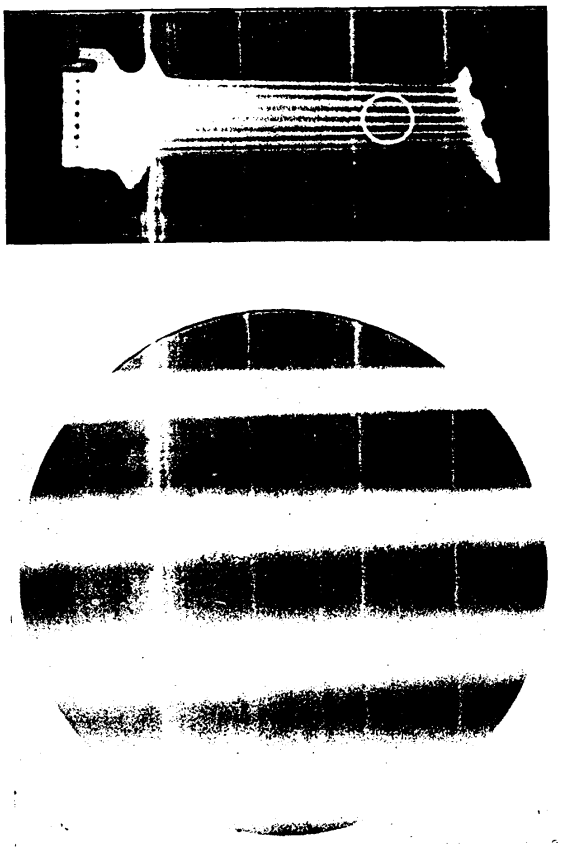

Fig. 10. Microporosity in a precision cast turbine blade as revealed in an enlarged image by microfocal radiography (compared with a conventional ×1 radiograph). Parish and Cason (1977).

Micro Focus Radiography

H.J. Bosch, H.W. Schenk, A.H. Walenta

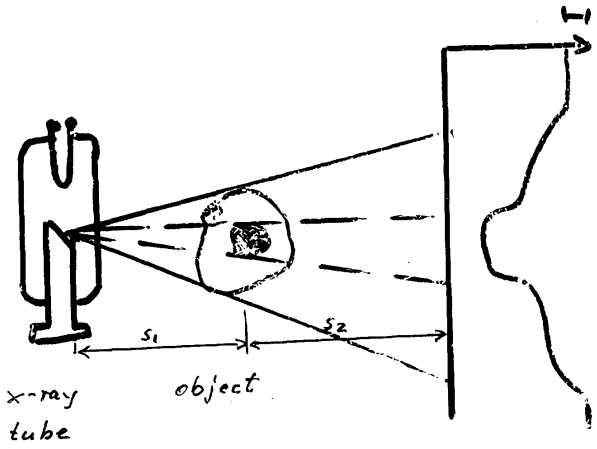

Magnification: $A = \frac{s_1 + s_2}{s_1}$

Problem for film: "low rate" $\approx 10^2 s^{-1} cm^2$

ideal for fast photon counter

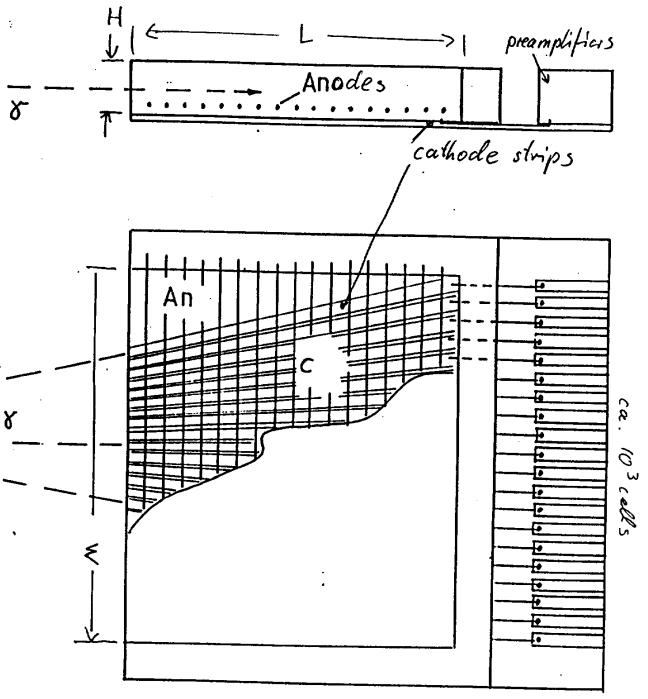

Fig. 2

gas proportional wire chamber with cathode read out

Sensitive : 30 keV ... 100 keV !

Interaction of Photons with Matter

1) Thomson scattering

incoming EM-wave :

$$\vec{E}(t) = \vec{\varepsilon}\, E_0 \sin\omega t \qquad \vec{k} \perp \vec{\varepsilon}$$

$\vec{\varepsilon}$: polarisation

acceleration of atomic electron :

$$\vec{a} = \frac{e\,E}{m} = \vec{\varepsilon}\,\frac{e}{m} E_0 \sin\omega t$$

$$\langle a^2 \rangle = \tfrac{1}{2}\frac{e^2}{m^2} E_0^2$$

Larmor's formula of radiation by accelerated charge :

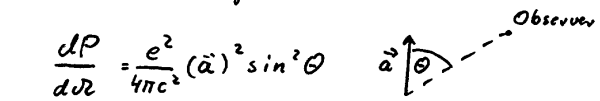

$$\frac{dP}{d\Omega} = \frac{e^2}{4\pi c^3}(\ddot{a})^2 \sin^2\Theta$$

$$\Rightarrow \frac{dP}{d\Omega} = \frac{c}{8\pi}\left(\frac{e^2}{mc^2}\right)^2 E_0^2 \sin^2\Theta = \frac{c}{8\pi} r_0^2 E_0^2 \sin^2\Theta$$

Energy flow/time/area : Poynting Vector S

$$\langle S \rangle = \frac{c}{8\pi}\langle \vec{E} \times \vec{H} \rangle = \frac{c}{8\pi} E_0^2$$

$$\frac{d\sigma}{d\Omega} = \frac{dP}{d\Omega}\,\frac{1}{\langle S \rangle} = r_0^2 \sin^2\Theta$$

Mean over polarization in x-y-plane

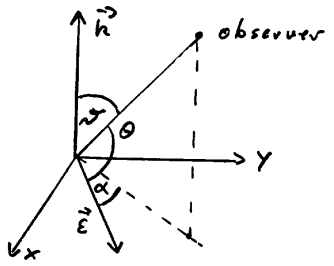

$$\left\langle \frac{d\sigma}{d\Omega} \right\rangle_{pol} = r_0^2 \frac{1}{2\pi} \int_0^{2\pi} (1 - \sin^2\vartheta \cos^2\alpha)\, d\alpha$$

$$\left\langle \frac{d\sigma}{d\Omega} \right\rangle_{pol} = r_0^2 \frac{1}{2} (1 + \cos^2\vartheta)$$

total cross section:

$$\sigma_{tot} = \int_{\Omega} d\sigma = \int_{\Omega} \frac{r_0^2}{2} (1 + \cos^2\vartheta)\, d\Omega$$

$$\sigma_{tot}^{TH} = r_0^2 \frac{8}{3} \pi \quad \text{per electron}$$

Dense material: N electrons/volume

$$dn = -n N \sigma\, dx = -n \mu\, dx \qquad \mu = N\sigma$$

$$n(x) = n(0)\, e^{-\mu x} \qquad \mu: \text{absorption coefficient}$$

Thomson cross section, absorption

Numerical exercise:

$$\mu = N\sigma = 6.025 \cdot 10^{23} \cdot 6.651 \cdot 10^{-25} \rho \frac{Z}{A} \ (cm^{-1})$$

ρ in g/cm^3

$$\mu = 0.40\, \rho \frac{Z}{A}$$

$\rho = 1\ g/cm^3$ (water), $Z/A \approx 0.5$

$$\mu = 0.2\ cm^{-1}$$

$$\lambda = \frac{1}{\mu} = 5\ cm$$ (sets scale, for gases)

Resonant absorption (photo-effect)

Absorption by bound electrons:

- energy conservation: $h\nu \geq \varepsilon_i$
- momentum c.. : falls off with $h\nu$

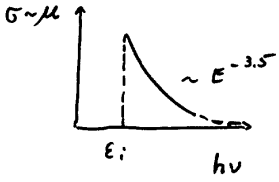

$$\sigma_K = \sigma^{TH} 4\sqrt{2} \frac{Z^5}{137^4} \left(\frac{mc^2}{h\nu} \right)^{3.5}$$

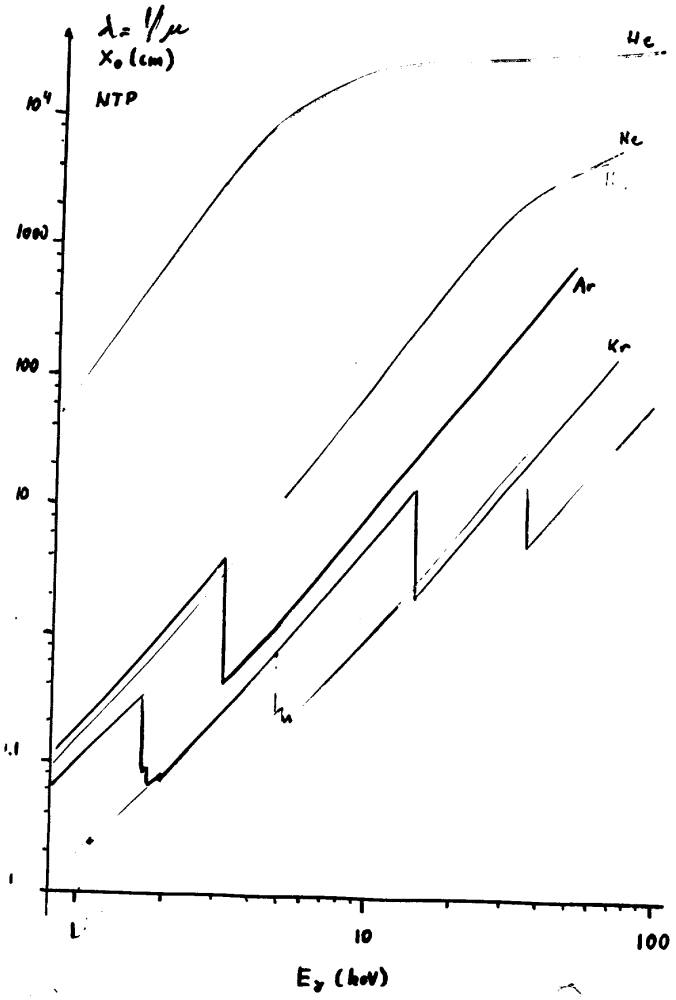

absorption : Kr or Xe , 30...50 bar , 5cm

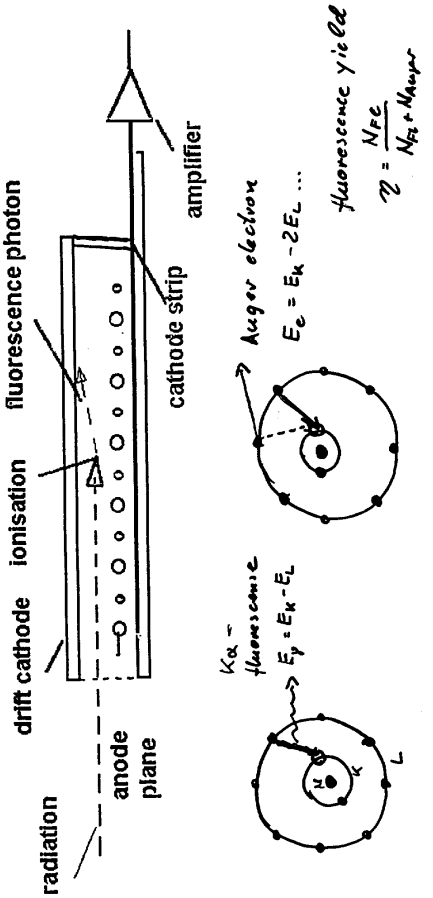

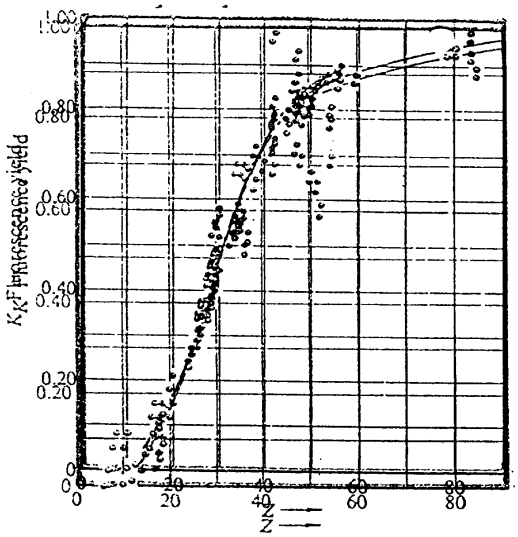

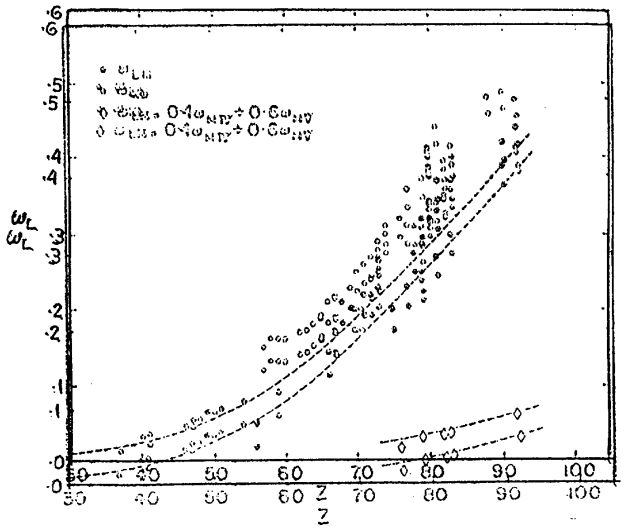

Position resolution

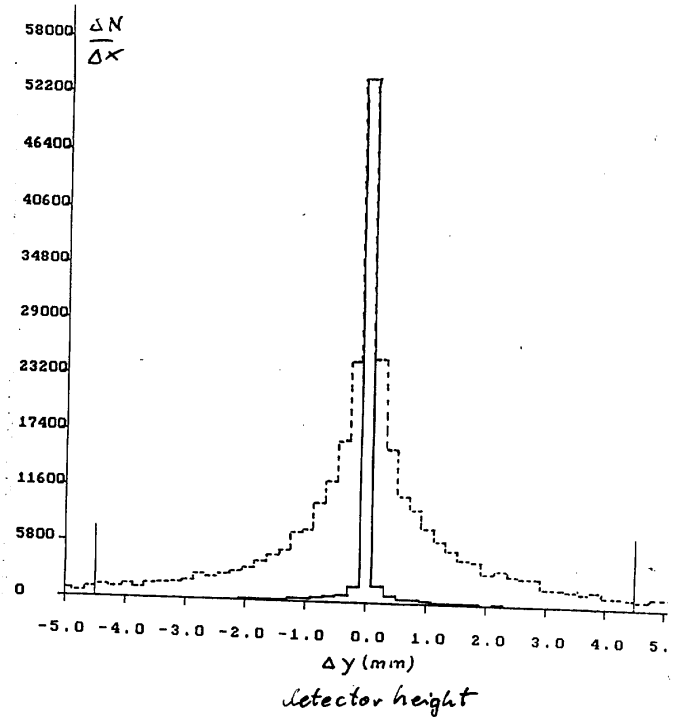

detector height

influence of fluorescens radiation (x_e)

Position resolution:

incident beam

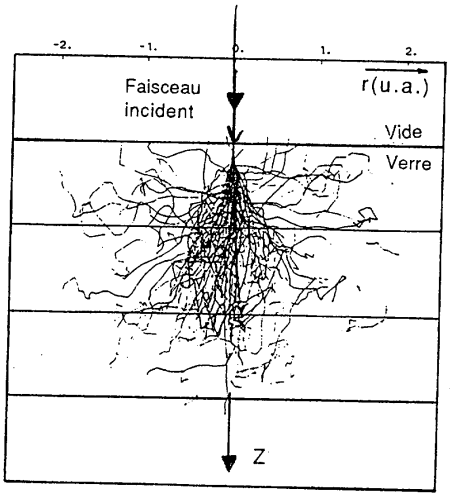

photo electron range $\rightsquigarrow E_{\gamma\,max}$

Electron range and resolution

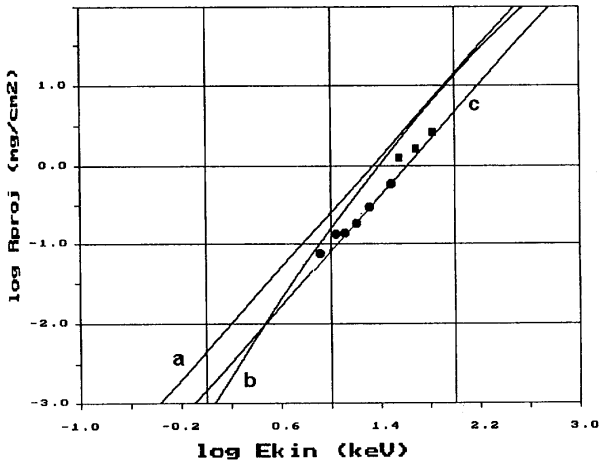

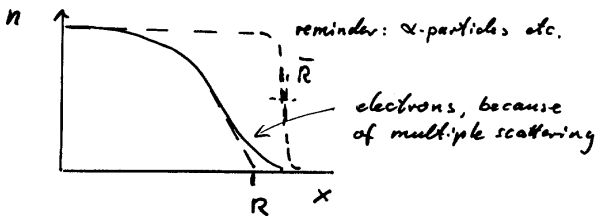

b) Katz-Penfold: $R(g/cm^2) = 0.412\,(E/MeV)^n$
$n = 1.265 - 0.0954\,\ln E/MeV$

a) Grün : $R(g/cm^2) = 0.665\,(E/MeV)^{1.75}$

c) effective resolution including photo-absorption
$\Delta X\,(fwhm) = 3.4\ mg/cm^2\,(E/keV)^{1.75}$

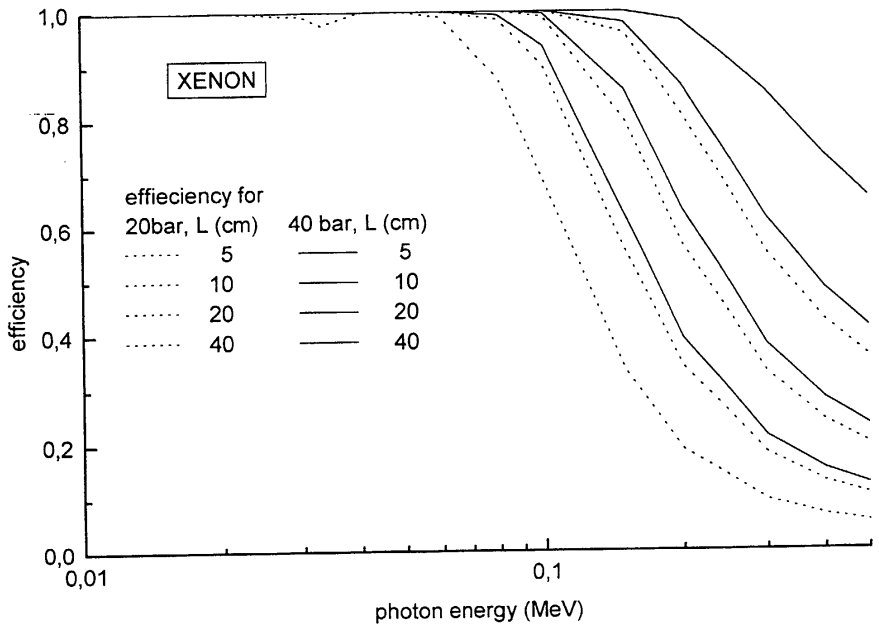
XENON
effieciency for
20bar, L (cm)
5
10
20
40
40 bar, L (cm)
5
10
20
40
efficiency
1,0
0,8
0,6
0,4
0,2
0,0
0,01
0,1
photon energy (MeV)

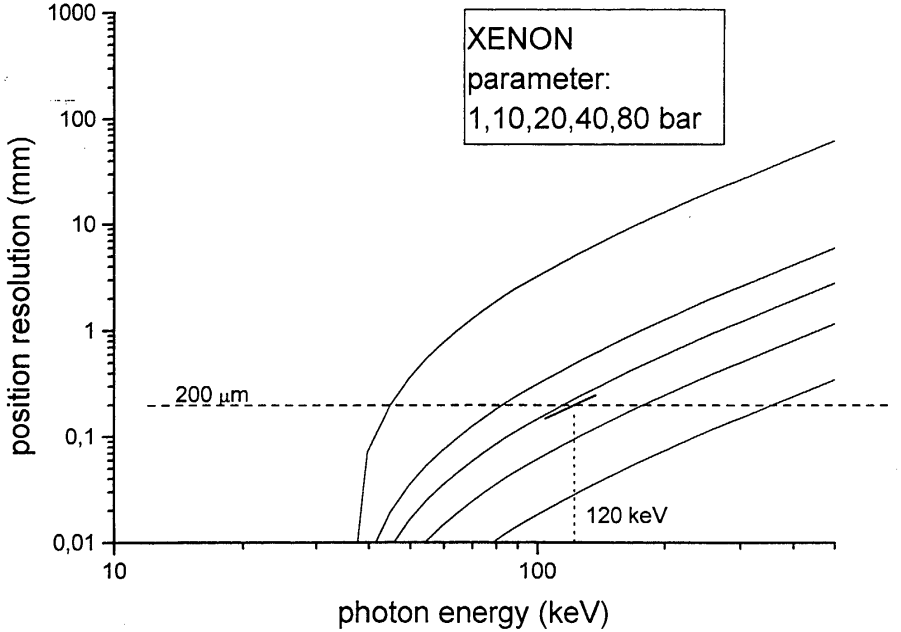
XENON
parameter:
1,10,20,40,80 bar
position resolution (mm)
1000
100
10
1
0,1
0,01
200 µm
120 keV
10
100
photon energy (keV)

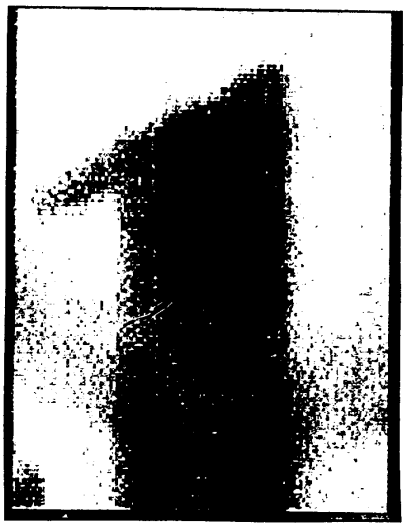

1000 counts/ pixel

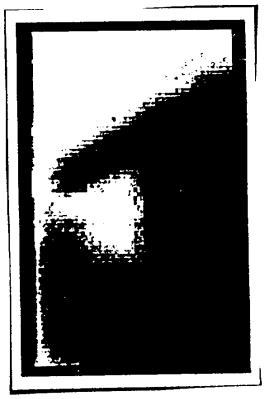

12.000 counts/ pixel

56 µm

COIN

x-ray inspection of welding seam

Figure 3. continued

no cracks but:

- additional information
  - x-ray picture of a material composition ?
  - welding seam.
    - inclusions ?
    - structure ?

No cracks

Plate I continued

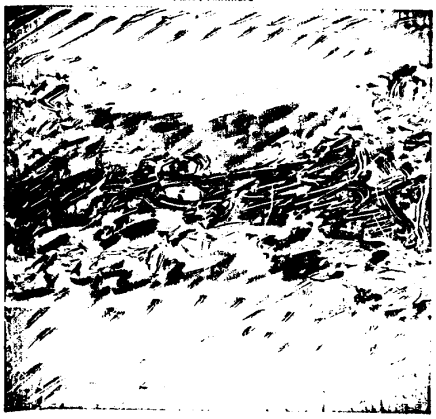

Figure 3. continued

A!

→ phase separation

measurement done with electron microscope and fluorescence analysis.

Non destructive method needed!

Dual Energy Methode

measurement at two energies:

$$S_1 = \ln I_1 / I_0 = (\mu_{1,1} x_1 + \mu_{1,2} x_2)$$

$$S_2 = \ln I_2 / I_0 = (\mu_{2,1} x_1 + \mu_{2,2} x_2)$$

or

$$\vec{S} = \begin{pmatrix} \mu_{1,1} & \mu_{1,2} \\ \mu_{2,1} & \mu_{2,2} \end{pmatrix} \circ \vec{x}$$

Solutions for rows and columns linear independent.

↳ Compton effect

Mehode of measurement:

- two monoenergetic radiation sources
- detector with energy resolution

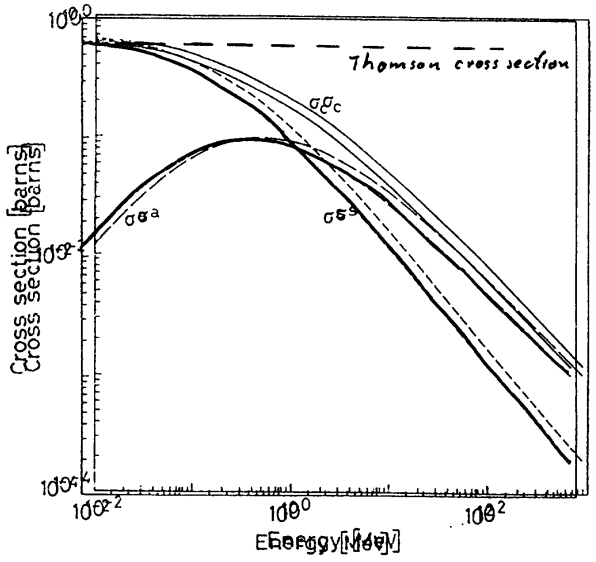

σ_c : total Compton cross section

$$\left.\begin{aligned} \sigma_a &= \frac{T_e}{h\nu}\,\sigma_c \\ \sigma^s &= \frac{h\nu'}{h\nu}\,\sigma_c \end{aligned}\right\} \quad \sigma_a + \sigma^s = \sigma_c$$

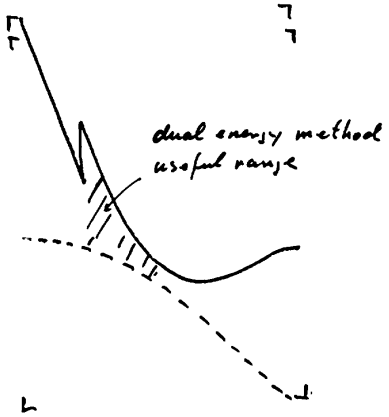

7. Annexe

LETI, Grenoble

monte carlo simulation of composite materials

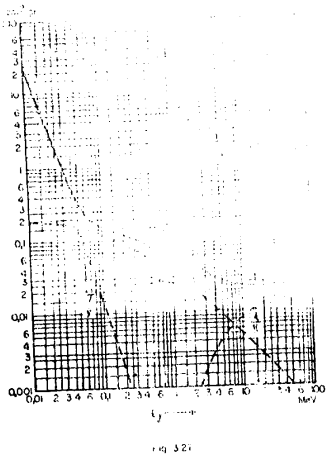

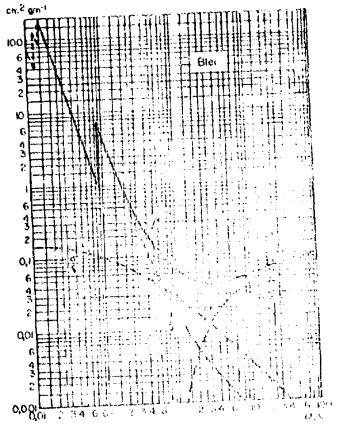

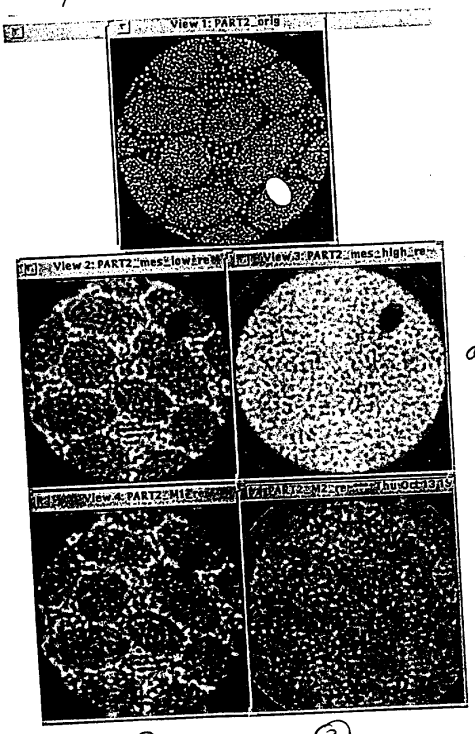

density

material

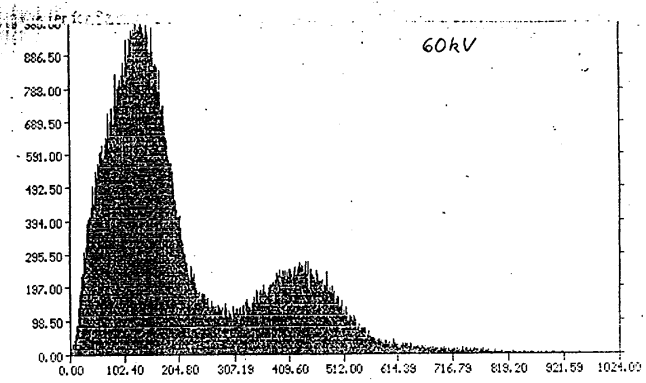

Fig.7

problem: simultaneously good position resolution $\Delta x \leq 0.25$ mm

Implemented in BRITE/EURAM Project:

CTS, ISO-Test, LETI, SIEGEN

+ industrial partners

Energy response (K_E)

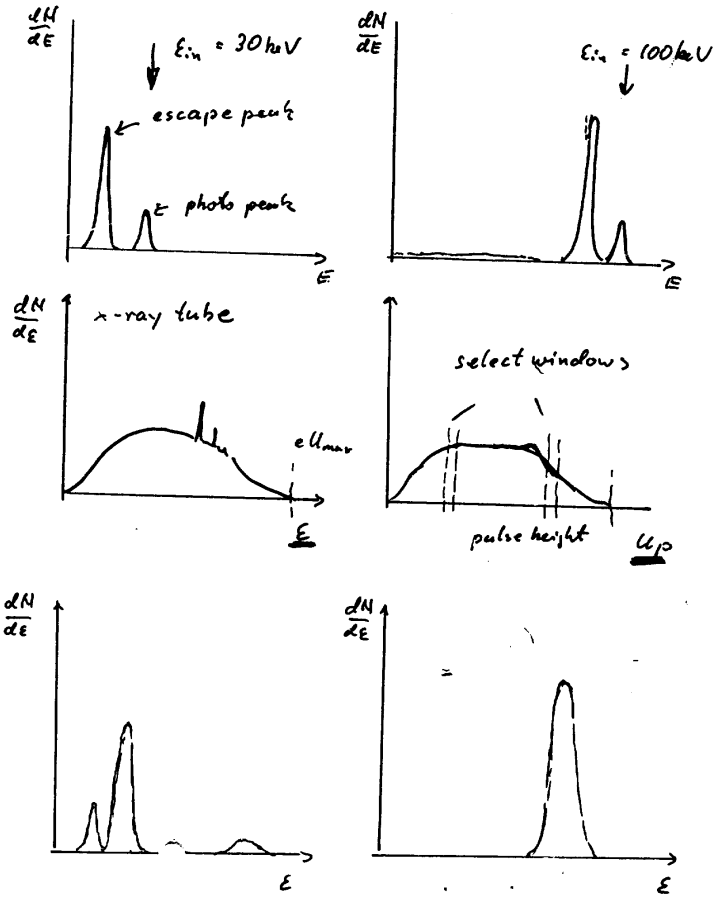

Gas Amplification in Proportional Counter

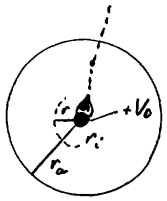

$$E(r) = \frac{V_0}{r} \frac{1}{\ln r_a/r_i} \qquad V(r) = \frac{V_0}{\ln r_a/r_i} \ln \frac{r_a}{r}$$

avalanche:

$$dn = n(r)\,\alpha\,dr \qquad \alpha : \text{1. Townsend coeff.}$$

$$n = n_0 \exp\left(\int_{r_a}^{r_s} \alpha(r)\,dr \right)$$

From definition: $\alpha = \sigma N$ σ: crossection for ionisation by electron impact

$N = N_0 p$ density of atoms

$$\alpha = \sigma N_0 p$$

$$\Rightarrow$$

$$\frac{\alpha}{p} = N_0\,\sigma\left(\frac{E}{p}\right)$$

Since σ denpends on energy distribution of electrons in gas at reduced field E/p: "physics" scales with mean free path

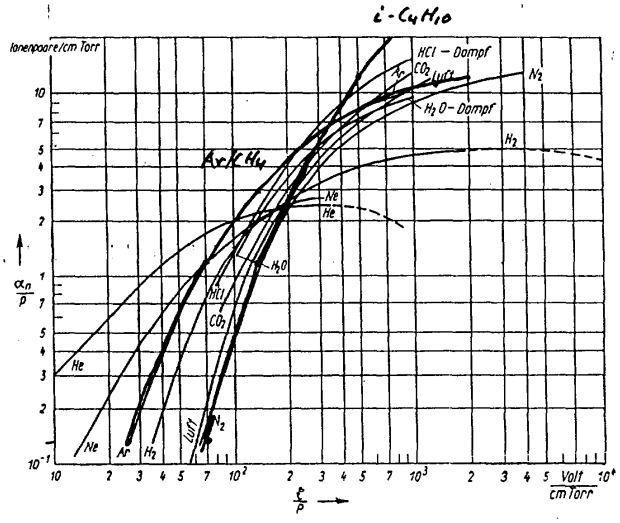

Parametrisation:

$$\frac{\alpha}{p} = A \cdot \exp\left\{ -B \cdot \frac{1}{(E/p)^k} \right\}$$

best: $k = 0.65$

Townsend: $k = 1$

Ward: $k = 1/2$

Problem: in counters mixtures are used.

$\rightsquigarrow$ measurement

Ar/CH_4 (90/10)

$i\text{-}C_4H_{10}$

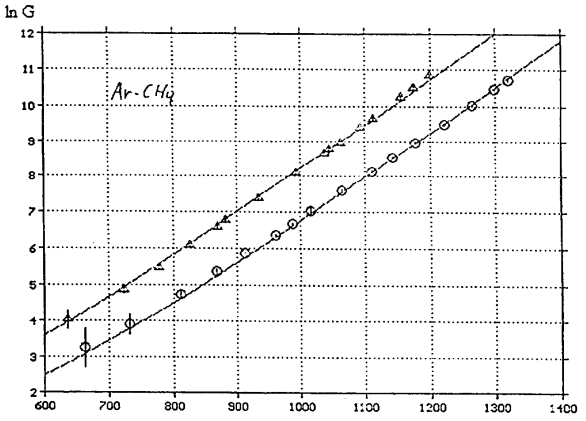

Δ r_{anode} = 10 μ

○ " = 15 μ

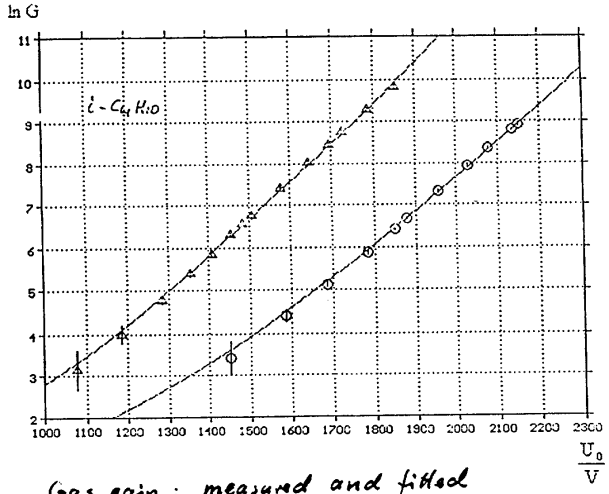

Gas gain : measured and fitted to $\frac{\alpha}{p} = A \exp\{-B(\frac{\alpha}{p})^{-0.6}\}$

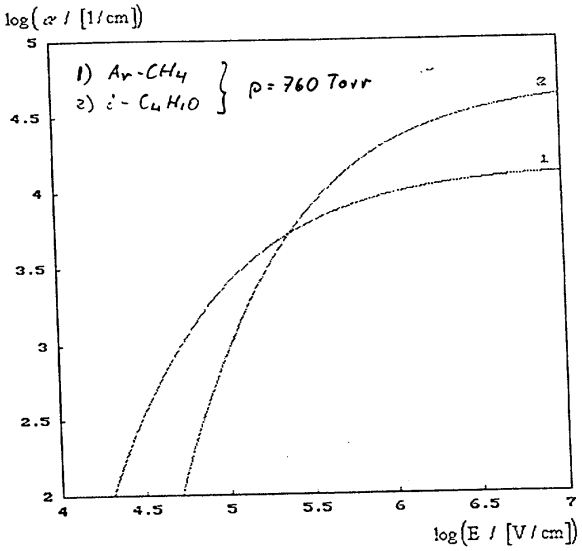

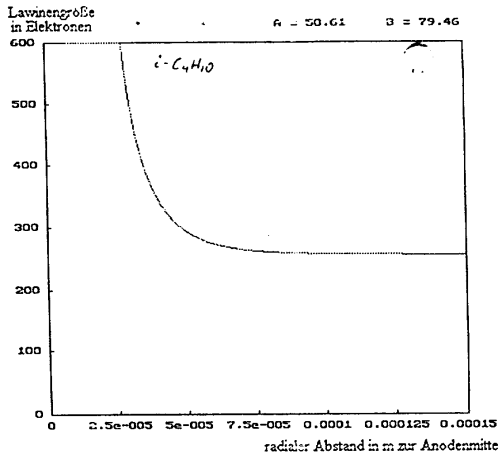

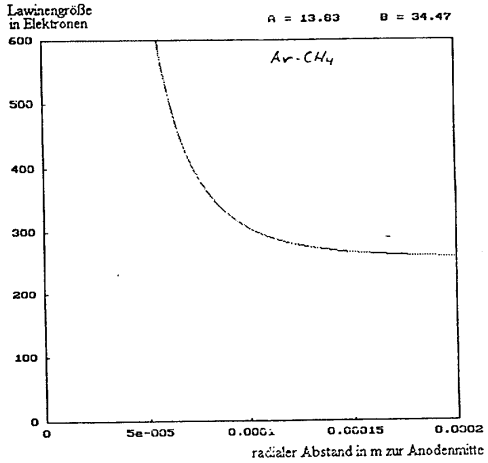

calculated avalanch development
$n(r)$

Statistical Fluctuation and Energy Resolution

1) Primary ionisation:

$\bar{N}_0 = \frac{E_0}{W}$ W: mean energy/ion pair, measured

$(\Delta N_0)^2 = F \bar{N}_0$ $F < 1$: Fano factor

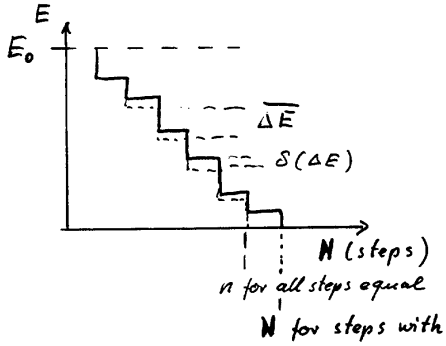

- for equal steps error is independent of n and given by $\Delta E/\sqrt{12}$
- for fluctuation in energy deposition it becomes dependent on number of steps:

$(\Delta N_0)^2 \sim \bar{N}_0$ $F \approx 0.2$

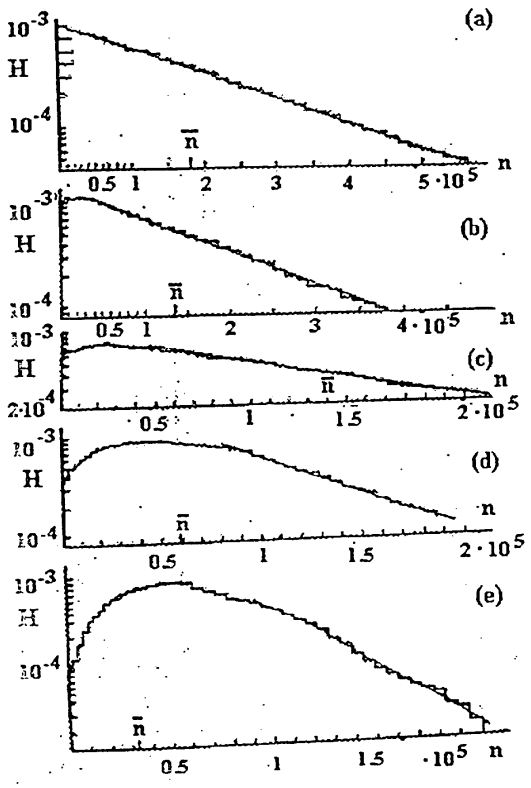

2) gas amplification

avalanche $\bar{n} = n_0 e^{\int_{r_1}^{r_2} \alpha \, dr}$ $n_0 = 1$ electron

$\rightarrow$

$P(n) = \frac{1}{\bar{n}} \left(1 - \frac{1}{\bar{n}}\right)^{n-1}$ (Furry)

$(\Delta n)^2_{rms} = \bar{n}^2 \left(1 - \frac{1}{\bar{n}}\right) = f \bar{n}^2$

$\bar{n} \gg 1 \rightsquigarrow P(n) \approx \frac{1}{\bar{n}} e^{-\frac{n}{\bar{n}}}$, $f = 1$

observe for larger gain deviation (s. fig.)

Physics background:

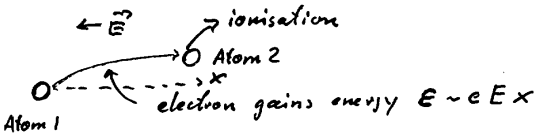

cross section for ionisation:

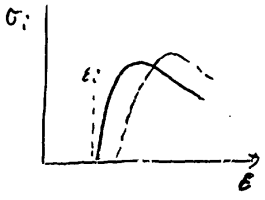

$\rightsquigarrow$ mean free path becomes meaningless
electron ionises in well defined intervals
$\rightsquigarrow$ less fluctuation

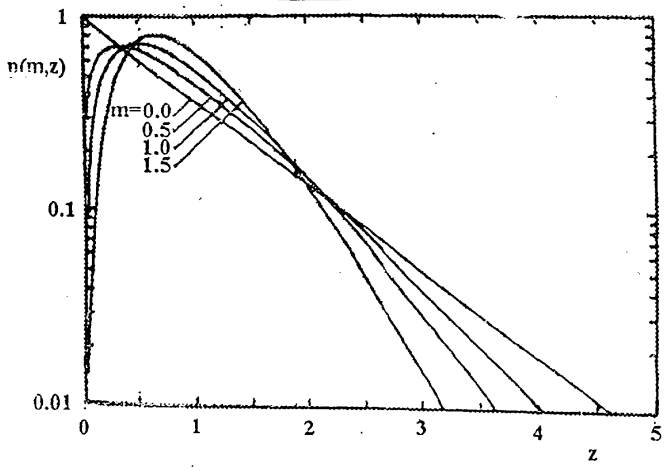

Polya - distribution:

$$P(m,z) = \frac{1}{\bar{n}} \frac{m^m}{\Gamma(m)} z^{m-1} e^{-mz}$$

$f = \frac{1}{m+1}$ m: width param., $z = \frac{n}{\bar{n}}$.

Detailed calculations by Alkhazov:

$m \approx 1 \Rightarrow f \approx 0.5$

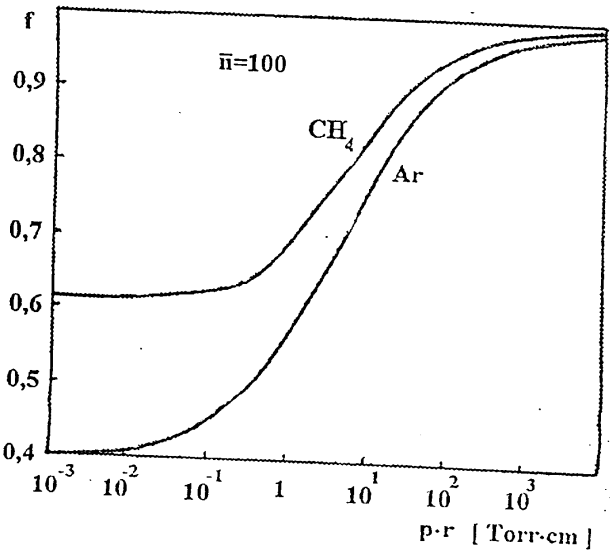

detailed calculation (Alkhazov)

Signal fluctuations:

$$(\Delta S_{tot})^2 = (\bar{n})^2 F \bar{N}_0 + (\bar{n})^2 f \bar{N}_0$$

$$\left(\frac{\Delta S_{tot}}{\bar{n}\bar{N}_0}\right)^2 = \left(\frac{\Delta S}{S}\right)^2 = \frac{F+f}{\bar{N}_0} = \frac{(F+f)W}{E}$$

examples: $W = 26\,eV$ $E = 1\,keV$ $F = 0.2$ $f = 0.6$

$f = 0.6$ ($p \approx 5\,bar$) $\frac{\Delta S}{S} = \frac{0.34}{\sqrt{E/keV}}$ (fwhm)

$f = 0.8$ ($p = 30\,bar$) $\frac{\Delta S}{S} = \frac{0.38}{\sqrt{E/keV}}$ (fwhm)

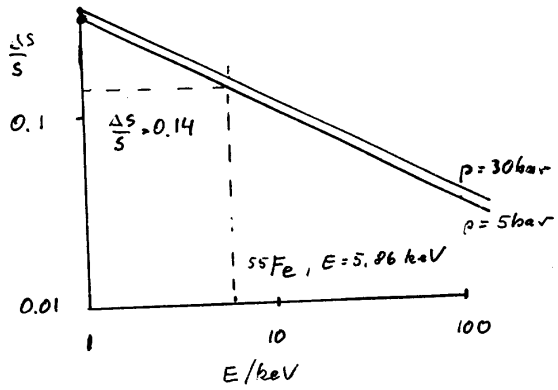

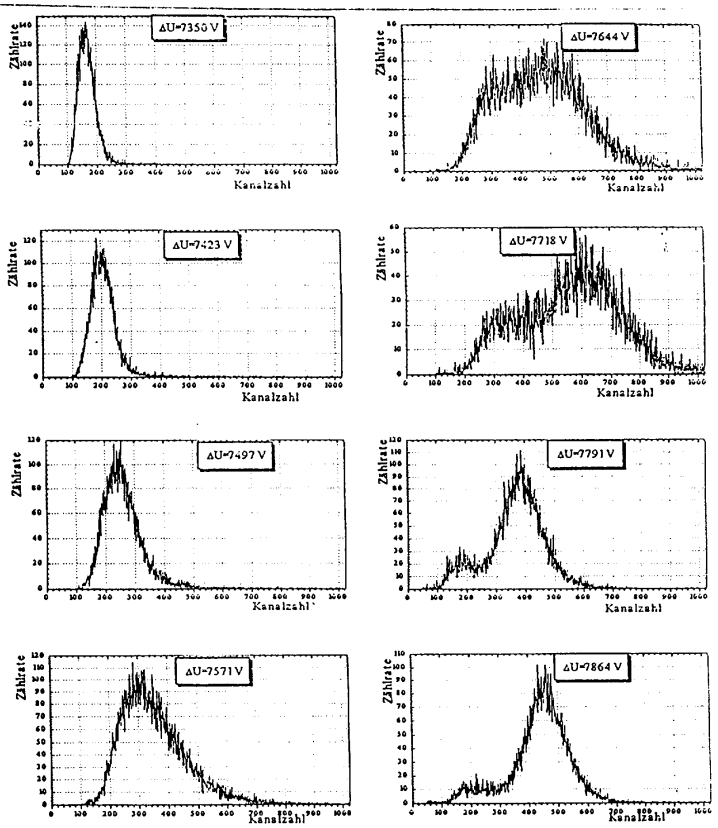

measurements at 50 bar

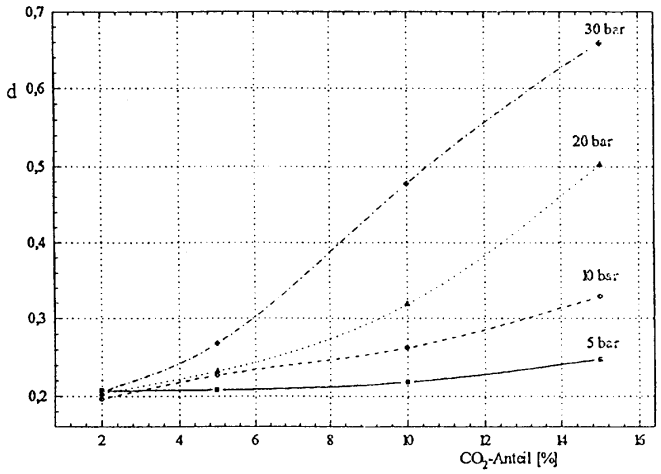

CO_2 fraction

influence of quencher

~> limited streamer mode

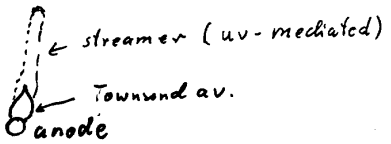

Energy resolution at 50 bar

1) pressure, recombination, attachment

~> clean gas, etc.

2) limited streamer mode

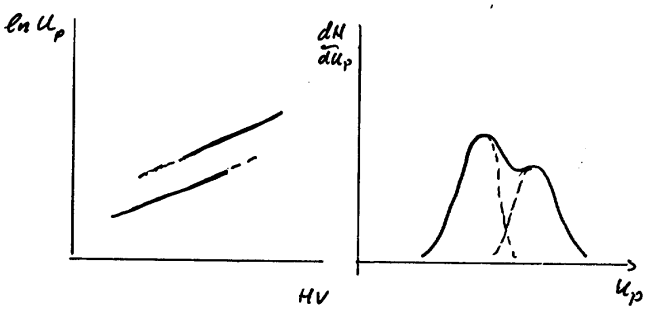

~> gas mixture, geometry

(Ar/CH_4, 95:5 -> 98:2)

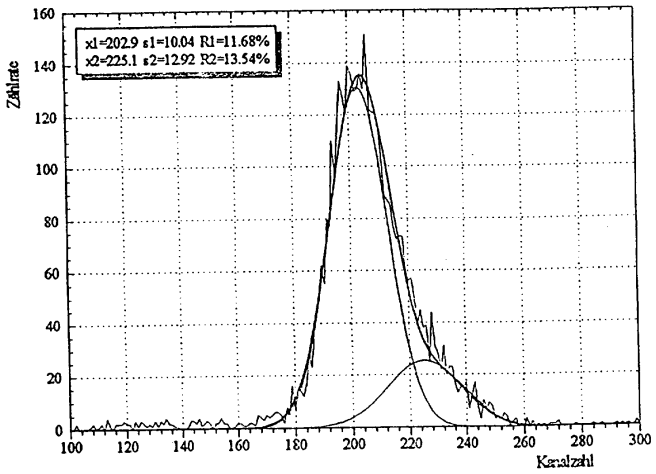

^{109}Cd (Ag K_α, K_β lines)

Detectors for Position Resolution

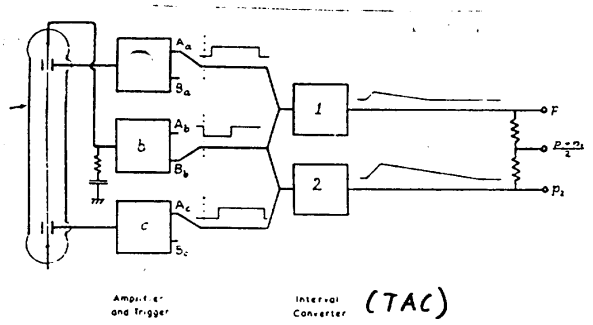

Fig. 2.

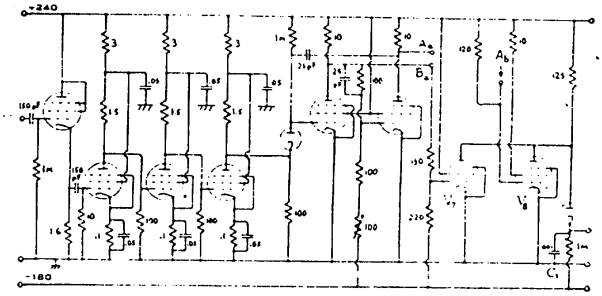

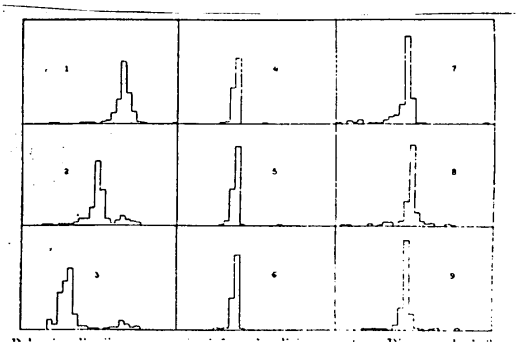

Frank, Cambridge 1951

Principles of Position Resolution

1) Charge Division (Lauterjung, 1959)

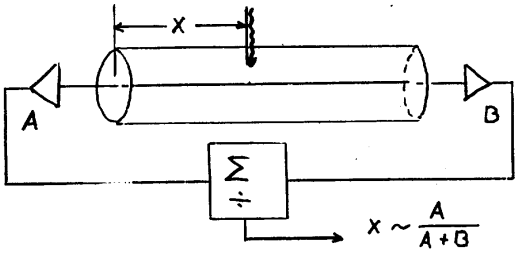

$\Delta e/e = N/S \approx 10^{-3}$

2) Delay Line

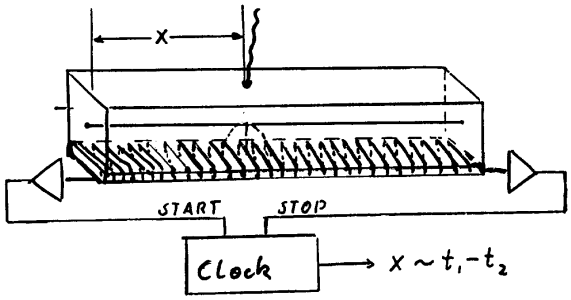

Multiwire - Proportional - Chamber (PWC)

G. Charpak

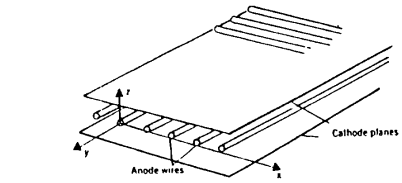

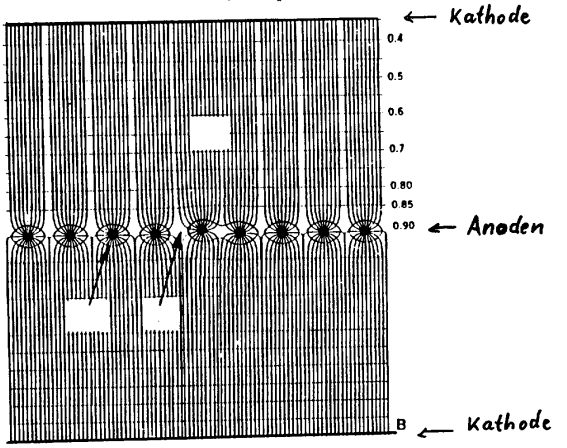

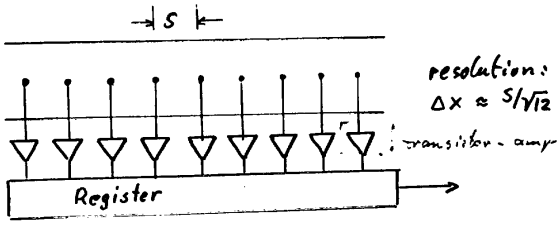

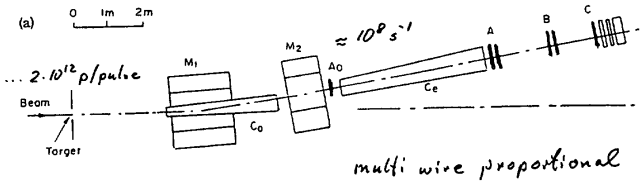

multi wire proportional chambers

J. J. Aubert et al. Phys Rev. Lett. 33(74) 1404

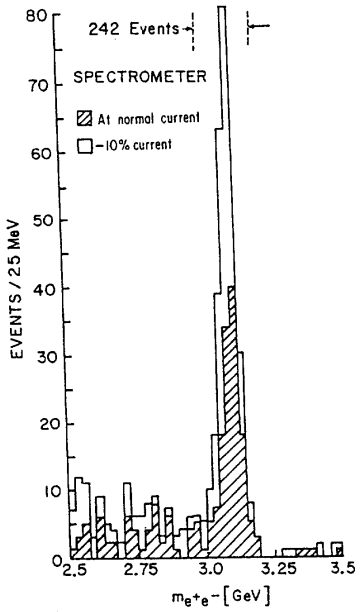

FIG. 2. Mass spectrum showing the existence of J. Results from two spectrometer settings are plotted showing that the peak is independent of spectrometer currents. The run at reduced current was taken two months later than the normal run.

Signal Formation

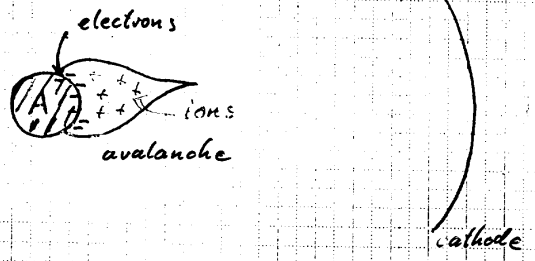

useful approximation:

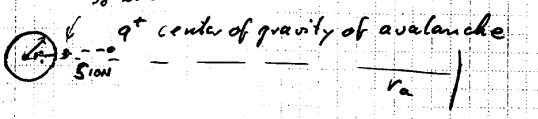

1) calculate

$$V_{dr} = \frac{ds_{ion}}{dt} = \mu^+ E(s_{ion}) \qquad \mu^+ : \text{mobility of ions}$$

$$E(s_{ion}) = \frac{V_0}{s_{ion}} \frac{1}{\ln r_a/r_i}$$

$$\int_{s_0}^{s_{ion}} ds_{ion} = \mu^+ V_0 \frac{1}{\ln r_a/r_i} dt$$

$$s_{ion}^2 = \frac{2\mu^+ V_0}{\ln r_a/r_i} t + s_0^2$$

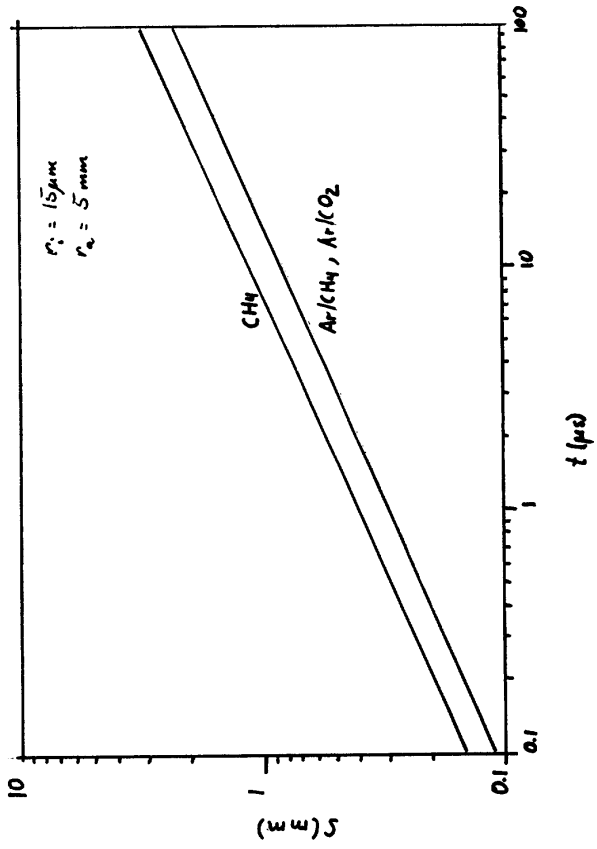

Fig. 6

Induction:

$$Q^+ = -\frac{|q^+|}{\ln r_a/r_i} \ln \frac{r_a}{s_{ion}} \qquad |q^+| = |q^-| = q$$

$$Q^- = \frac{|q^-|}{\ln r_a/r_i} \ln \frac{r_a}{s_{el}}$$

$$Q_{tot} = Q^+ + Q^- = \frac{|q|}{\ln r_a/r_i} \left(\ln \frac{r_a}{s_{el}} - \ln \frac{r_a}{s_{ion}} \right)$$

$$Q_{tot} = \frac{|q|}{\ln r_a/r_i} \ln \frac{s_{ion}}{s_{el}}$$

Electrons fast ($< 1\,ns$) on wire: $s_{el} \approx r_i$

$$\Rightarrow \quad Q_{tot} = \frac{|q|}{\ln r_a/r_i} \ln \sqrt{\frac{2\mu^+ V_0}{C r_i^2} t + \left(\frac{s_0}{r_i}\right)^2}$$

$$\boxed{Q_{tot} = \frac{|q|}{\ln r_a/r_i} \ln \left[t/\hat{t} + \left(\frac{s_0}{r_i}\right)^2 \right] \qquad \hat{t} = \frac{\ln r_a/r_i \cdot r_i^2}{2\mu^+ V_0}}$$

Example:

$r_i = 10^{-3}\,cm \quad r_a = 0.5\,cm \quad \ln r_a/r_i = 6.2$

$\mu^+ V_0 = 3\,cm^2/ms \quad (Ar/CH_4)$

$\Rightarrow \hat{t} = 1\,ns$

$s_0 - r_i \approx 2\lambda_0 \qquad \lambda_0 = 1/\alpha = \frac{1}{p}\frac{1}{\alpha/p}$

$\alpha/p = 7.6 \cdot 10^3\,cm^{-1}\,atm^{-1}$

$$\Rightarrow \quad s_0 - r_0 = 2\,\frac{1.3}{p(atm)}\,(\mu m) = \frac{2.6\,\mu m}{p/atm}$$

Current / charge

$$\frac{1}{q}\frac{dQ}{dt} = \frac{1}{\ln r_a/r_i}\,\frac{1/\xi}{t/\xi + (s_0/r_i)^2} = \boxed{\frac{1/t_0}{2\ln r_a/r_i}\,\frac{1}{1+t/t_0}}$$

$$t_0 = \frac{s_{ion}^2 \ln r_a/r_i}{2\mu^+ V_0} \qquad s_0 \approx r_i \text{ for } r_i \geq 10\,\mu m$$

Electron component

$$Q_{tot} = Q^{(+)} + Q^{(-)} = \frac{|q|}{\ln r_a/r_i}\ln s_{ion}/s_{el}$$

$$R_e = \frac{Q_{tot}(s_{ion}=s_0) - Q_{tot}(s_{ion}=r_i)}{Q_{tot}[s_{av}(t)]}$$

with $s_{av} = \sqrt{\frac{2\mu^+ V_0}{\ln r_a/r_i} + s_0^2} = s_0\sqrt{t/t_0 - 1}$

$$\boxed{R_e = \frac{\ln \frac{s_0}{r_i}}{\ln \frac{s_0}{r_i} + \frac{1}{2}\ln(t/t_0+1)}}$$

⇝ very small structure or low pressure

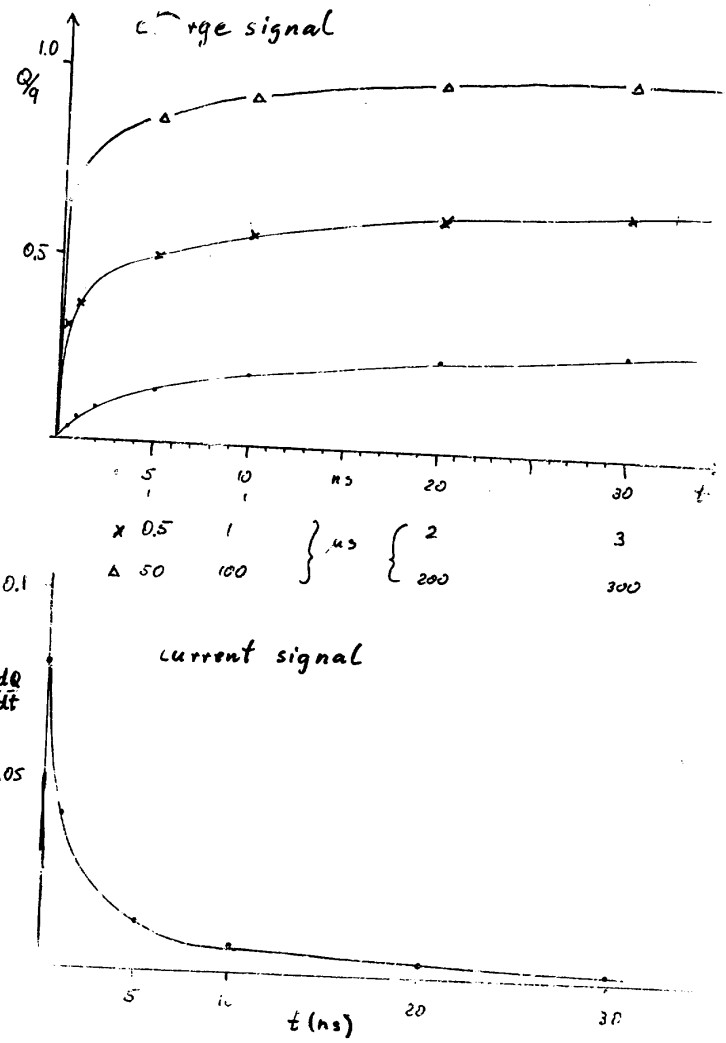

t_0 and electron component vs. r_{anode}

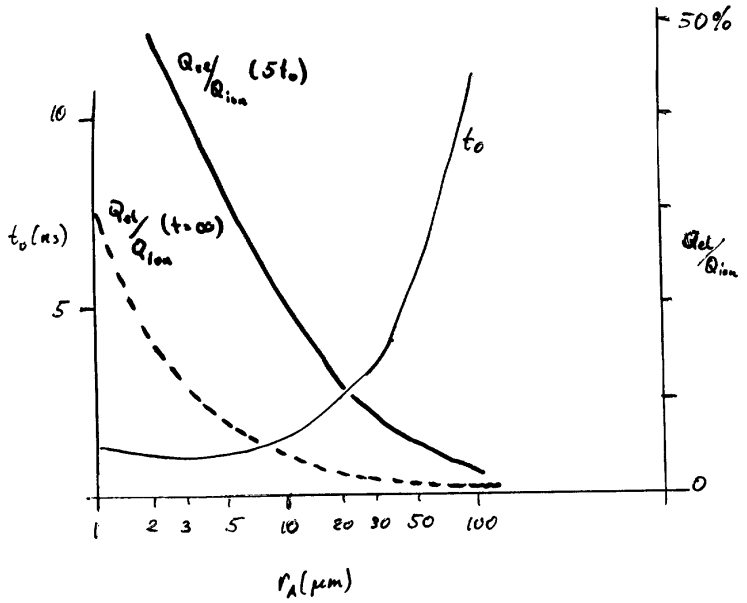

1967 Heidelberg, Boor, Heinlse & Walenta

spark chamber

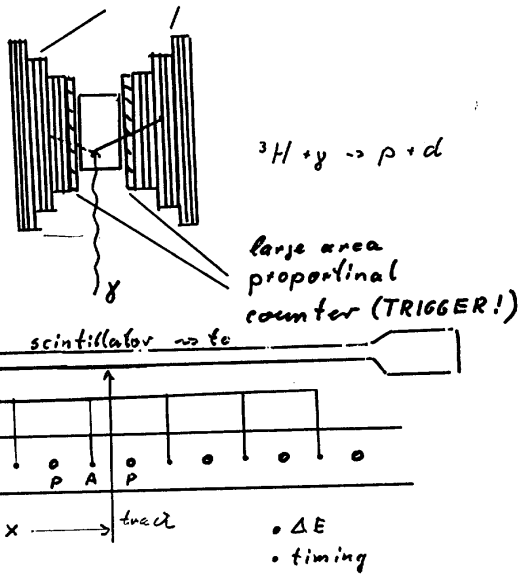

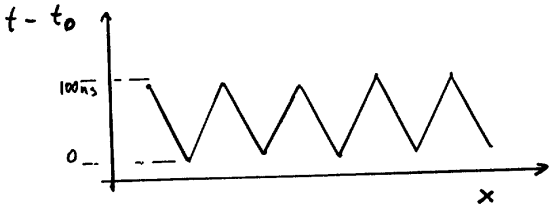

→ to be used as position detector

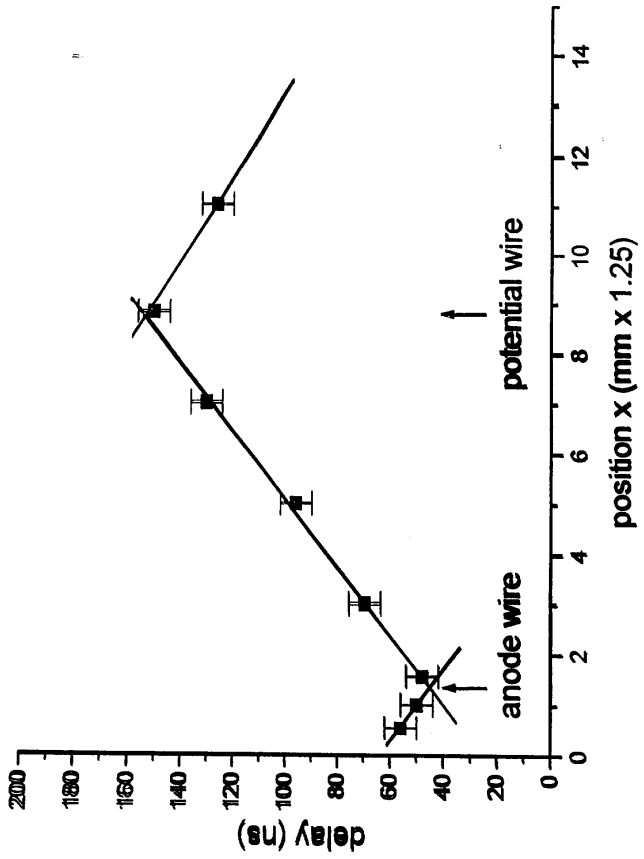

Right - Left Problem

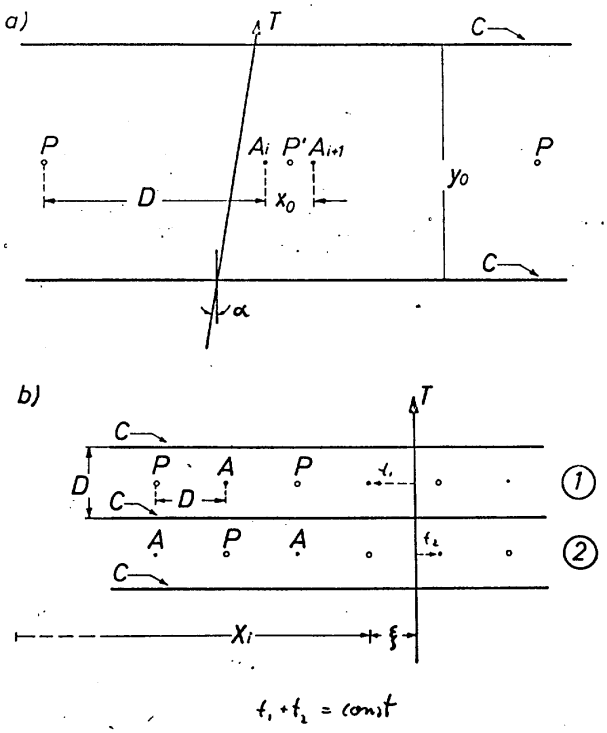

a) CERN

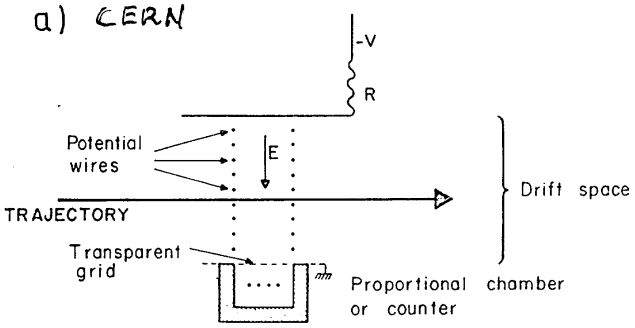

b) Saclay

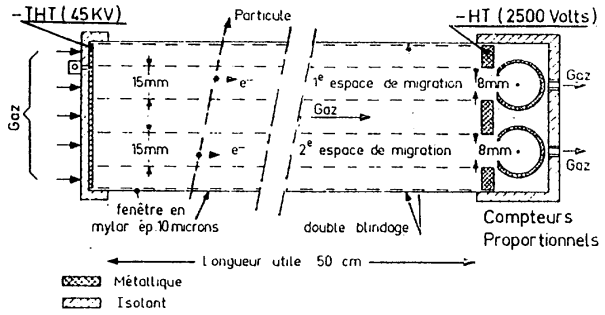

single cell drift chamber

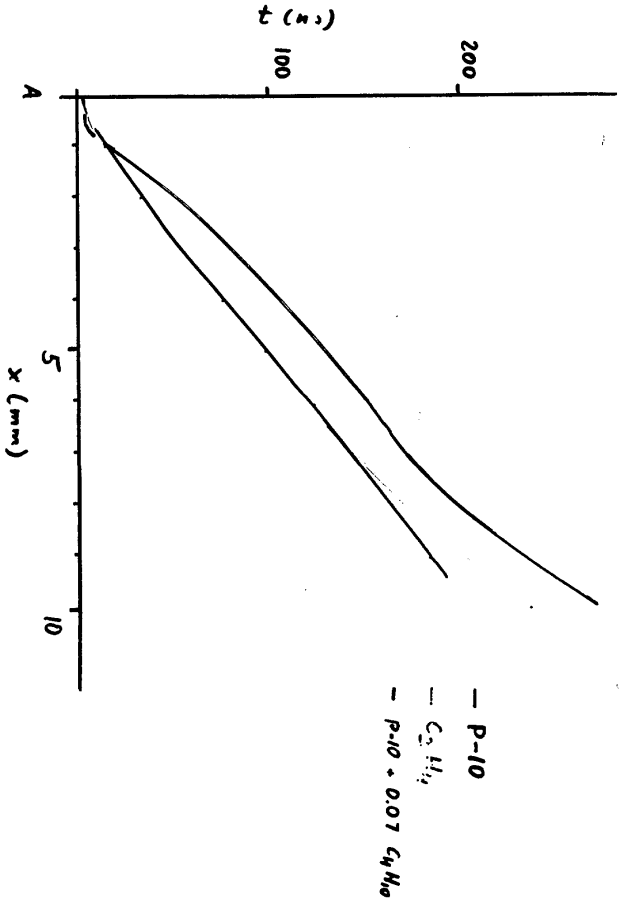

Drift and Diffusion I

A. H. Walenta

Free charges in electric field in gas

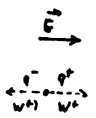

$\vec{F} = q\vec{E}$

collisions with atoms

stationary

$\varepsilon = \frac{3}{2} kT$ random energy (= Maxwell distribution)

$\vec{w} = \mu \vec{E}$ directed motion "drift"

total current: superposition of directed motion + random motion

1) $\vec{\Gamma} = n\vec{w} - D \operatorname{grad} n$ $D = D(\varepsilon)$ n: density

continuity equation

2) $\frac{\partial n}{\partial t} + \operatorname{div} \vec{\Gamma} = 0$

interest in detectors: $n(x, y, z, t)$

1) and 2) with $\vec{w} = \begin{pmatrix} 0 \\ 0 \\ w_z \end{pmatrix}$, $\vec{E} = \begin{pmatrix} 0 \\ 0 \\ E_z \end{pmatrix}$

$$\frac{\partial n}{\partial t} = -\frac{\partial z}{\partial t}\frac{\partial n}{\partial z} + D \operatorname{div} \operatorname{grad} n$$

solution

$$n(x,y,z,t) = \frac{1}{2(\pi D t)^{3/2}} \int_0^\infty n(x',y',z') \, e^{-\frac{(x-x')^2 + (y-y')^2 + (z - w_z t - z')^2}{4Dt}} \, dx'dy'dz'$$

$n(x', y', z') = n(t=0)$ $\sigma^2 = 2Dt$ (Einstein formula)

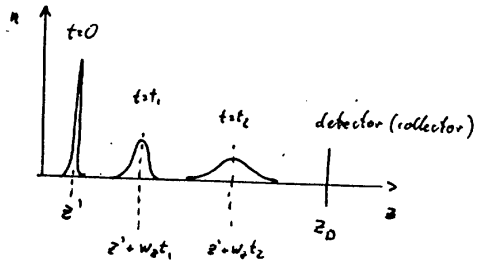

at detector $n(z_D, t)$ distortion

$z_D - w_z t_m = \frac{1}{2} \frac{\sigma^2}{z_D}$ for max. of $n(z_D, t)$ signal on detector

$= 0$ for max. of $n(z, t)$ centroid

The mean-electron-modell

1) Momentum conservation

$$m\vec{w} = \left\{ \int_0^{t_s} e\vec{E}\,dt \right\} \qquad \vec{w} = \vec{v}_{Drift}$$

t_s : time between encounters

$\overline{t_s} \approx \tau$ mean collision time

$\vec{q}$: statistical factor $= 0.85$

$$\Rightarrow \quad m\vec{w} = \vec{q} \int_0^{\tau} e\vec{E}\,dt$$

$$= \vec{q} e \vec{E} \tau$$

$$\Rightarrow \quad \vec{w} = \vec{q} \frac{e}{m} \tau E \qquad \text{for } \tau = \frac{\lambda}{\bar{c}} = \frac{1}{N\sigma\bar{c}}$$

$$\boxed{\vec{w} = \vec{q} \frac{e}{m} \frac{\vec{E}}{N} \frac{1}{\sigma\bar{c}}}$$

2) Energy conservation

$d\varepsilon$: energy from E / time intervall

$$d\varepsilon = eE\frac{dx}{dt}$$

$$= eEw$$

$d\varepsilon'$: energy absorbed / mean collision time

$d\varepsilon' = \eta\varepsilon/\tau$ η: mean energy loss / impact

$$\Rightarrow$$

$$eEw = \eta\varepsilon/\tau$$

$$\Rightarrow$$

$$w^2 = \vec{q}\,\eta\,\varepsilon$$

$$w = \vec{q}\sqrt{\eta}\,\bar{c} \qquad \vec{q} \approx 0.65$$

3) From transport equation

$$e\frac{D}{\mu} = \frac{2}{3}\varepsilon$$

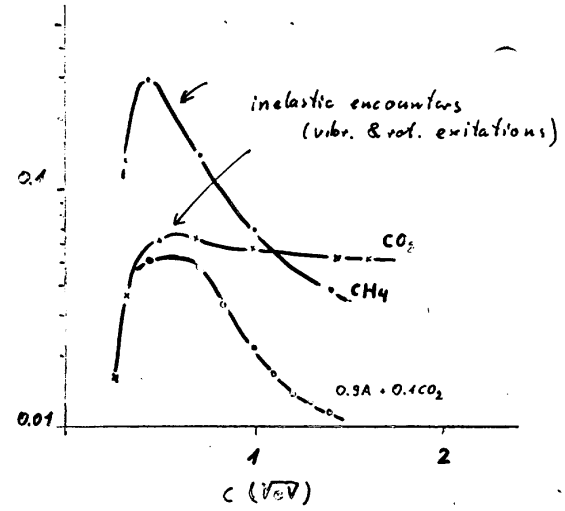

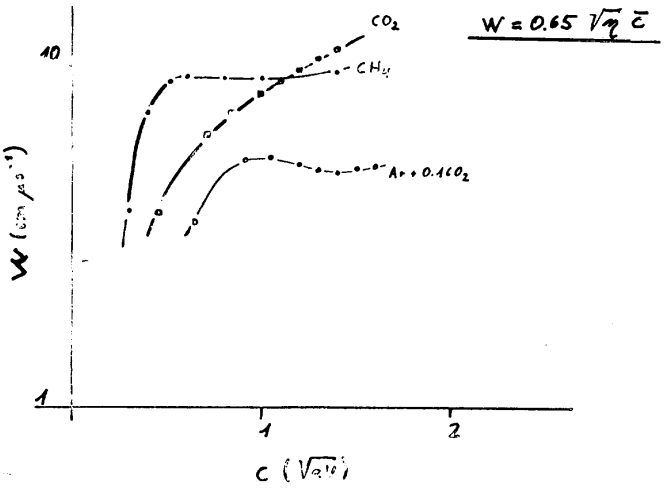

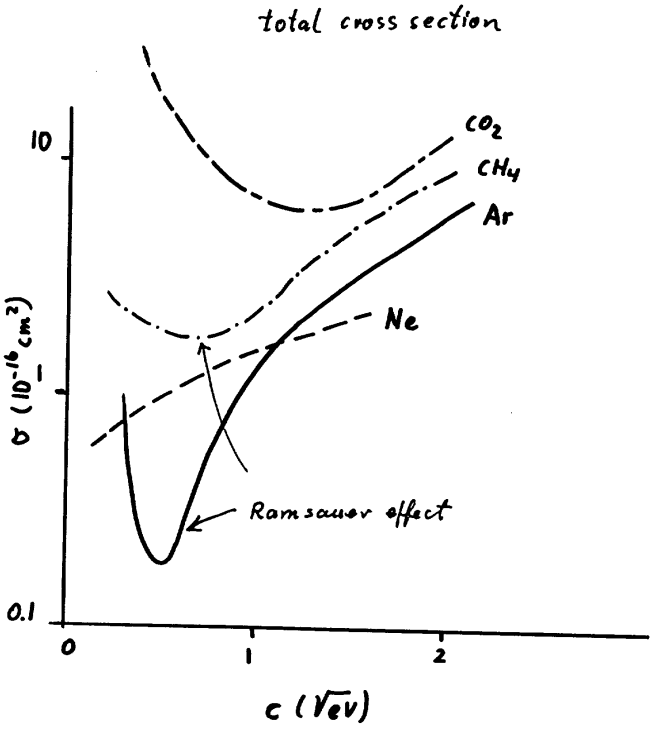

$V_{Dr} \sim \frac{E/N}{\sigma \bar{c}}$ $\quad \bar{c}$: thermal

σ : large

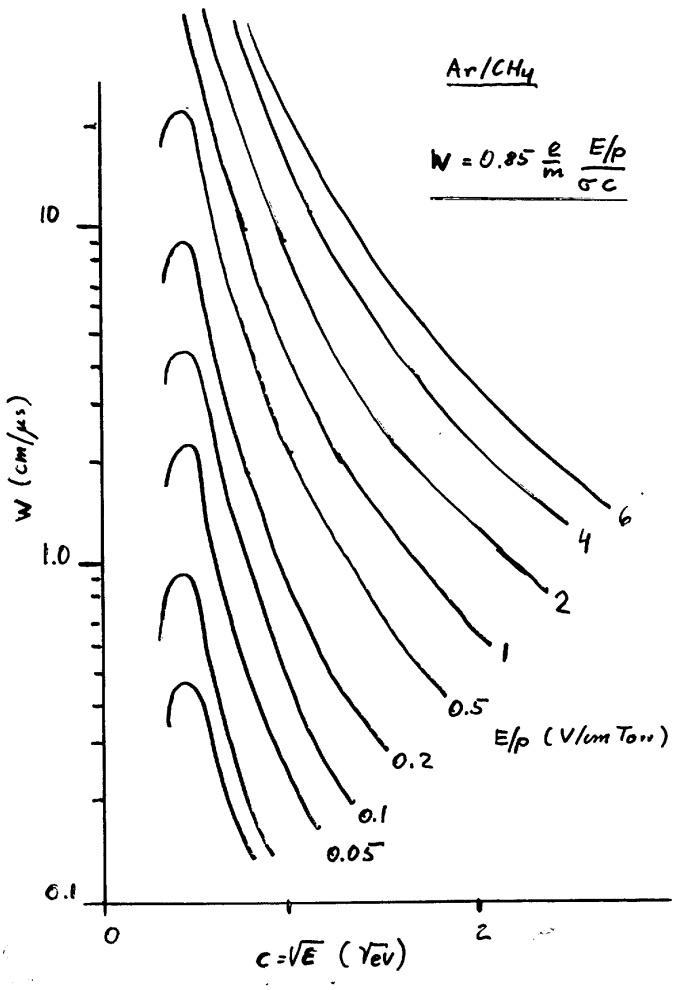

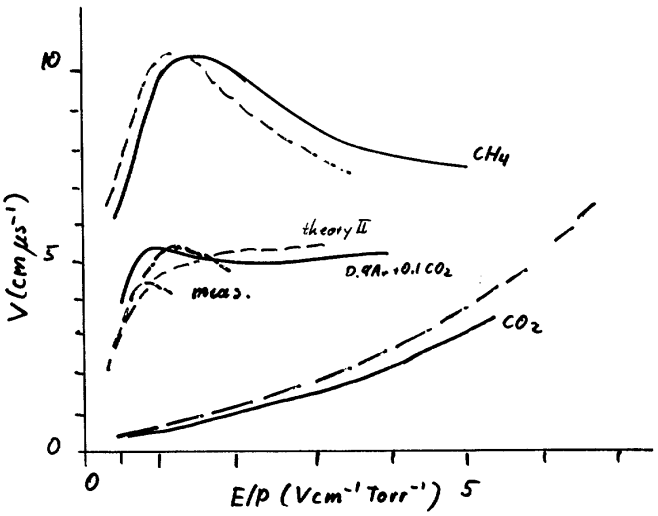

CH_4: Cottrel & Walker

Ar/CO_2: Nagy & Dési
Hakeem & Mathieson

CO_2: Hake & Phelps

Diffusion

$\sigma^2 = 2Dt \qquad x = \mu E t$

rel. resolution: $\frac{\sigma}{x} = \sqrt{\frac{\sigma^2}{x^2}} = \sqrt{\frac{\sigma^2}{x}} \cdot \frac{1}{\sqrt{x}}$

$$\frac{\sigma^2}{x} = \frac{2Dt}{\mu E t} = 2\frac{D/\mu}{E} = \frac{2\varepsilon_k}{E}$$

ε_k: characteristic energy

$\varepsilon_k = kT$ for $E = 0$ or no heating by electric field

Small diffusion:

$$\frac{\sigma^2}{x} = \frac{2D}{V} = \frac{2D}{\tilde{q}\sqrt{\eta}\,\bar{c}} = \frac{2 \cdot \frac{2}{3}\varepsilon}{\tilde{q}\sqrt{\eta}\, m N \sigma \bar{c}^2}$$

$$\boxed{\frac{\sigma^2}{x} = \tilde{q}\frac{2}{\sqrt{\eta} N \sigma}}$$

no explicit field or v_{or}-dependence!

$\hat{q}, \tilde{q}$ statistical factors ≈ 1

$\rightsquigarrow$ N large (pressure) density, σ large, $\sqrt{\eta}$ large

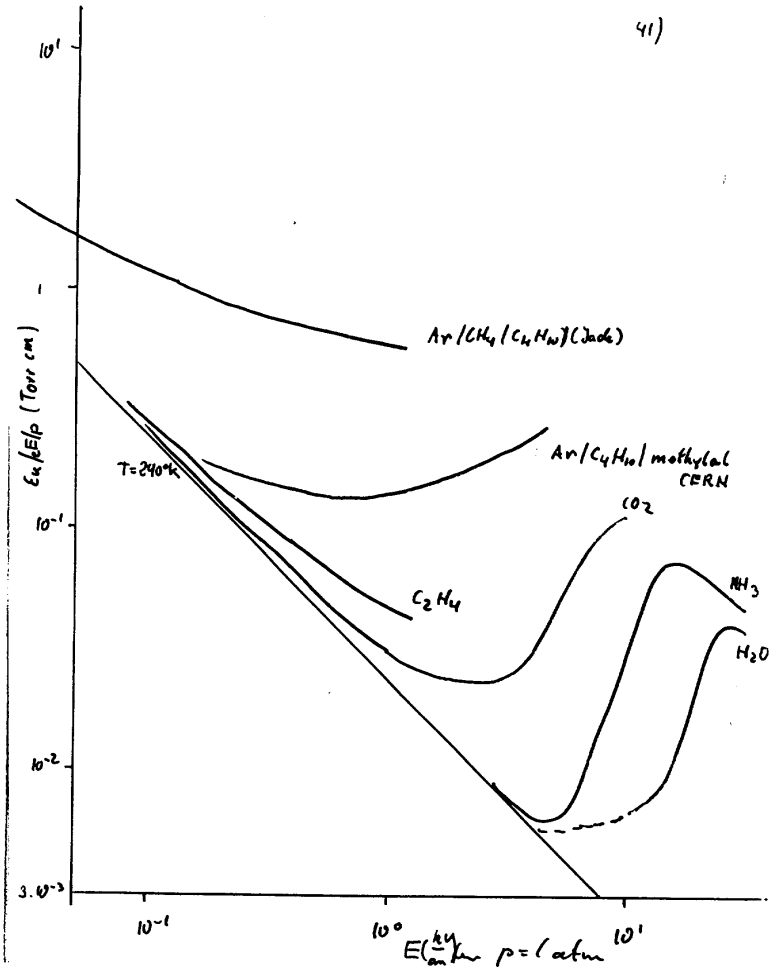

Diffusion with respect to drift direction

Experimentally discovered $D_L < D_0$
(Wagner, Davis, Hurst)

Reason for $D_L \neq D_0$:

$$\frac{\partial nf}{\partial t} + \operatorname{div}_r \vec{c} nf + \operatorname{div}_c (a + \omega_0 \vec{c}) nf = \frac{\partial f}{\partial t}\Big|_{coll}$$

this term had been neglected!

Formal solution by Parker & Lowke

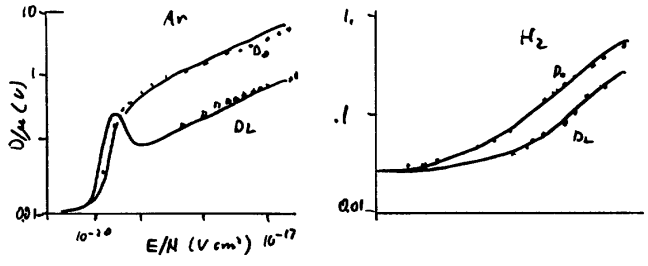

Simple calculation of D_L/D_0

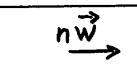

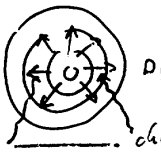

if $w_{Dr}(\varepsilon)$ decreases with incr. ε :

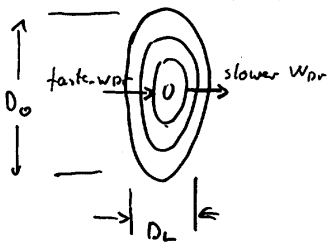

$$W = \frac{neE}{m}\frac{1}{\nu} \qquad \underline{\nu = nc\sigma}$$

Approx. $\nu = \nu_0 + \frac{\partial \nu}{\partial \varepsilon}\Delta\varepsilon$

$\varepsilon = \varepsilon_0 + \Delta\varepsilon$

Energy conservation:

$$\eta \frac{2m}{M} \varepsilon \nu = \frac{eE}{n}\Gamma \qquad \Gamma = \text{total current}$$

$\vec{\Gamma}_{tot} = n\vec{w} - D \operatorname{grad} n \qquad \vec{w} = \begin{pmatrix} 0 \\ 0 \\ w_z \end{pmatrix}$

$\Rightarrow$

$\Gamma_{tot}/n = \frac{eE}{m}\frac{1}{\nu} - \frac{2}{3}\frac{\varepsilon}{m\nu}\frac{1}{n}\frac{\partial n}{\partial z}$

$= \eta \frac{2m}{n} \varepsilon \nu$

solve for $\Delta\varepsilon$

$\Delta\varepsilon = -\frac{2}{3}\frac{\varepsilon_0}{eE}\frac{1}{1+2\gamma}\frac{1}{n}\frac{\partial n}{\partial z}$ $\qquad \boxed{\gamma = \frac{\partial \nu}{\partial \varepsilon}\frac{\varepsilon_0}{\nu_0}}$

influence on current:

$\Gamma_{tot} = \frac{1}{\nu}\left(\frac{neE}{m} - \frac{2}{3}\frac{\varepsilon}{m}\frac{\partial n}{\partial z}\right)$

$\approx \frac{1}{\nu_0}\left(1 - \frac{\partial \nu}{\partial \varepsilon}\frac{1}{\nu_0}\Delta\varepsilon\right)\left(\frac{neE}{m} - \frac{2}{3}\frac{\varepsilon_0}{m}\frac{\partial n}{\partial z}\right)$

$\approx \underbrace{\frac{neE}{m}\frac{1}{\nu_0}}_{\text{old drift-current}} + \underbrace{\frac{\gamma}{1+2\gamma}\frac{\partial n}{\partial z}}_{\text{new term}} - \underbrace{\frac{2}{3}\frac{\varepsilon_0}{m}\frac{1}{\nu_0}\frac{\partial n}{\partial z}}_{\text{old diffusion current } D_0} + \text{negl.}$

$= n w_0 - D_0\left(1 - \frac{\gamma}{1+2\gamma}\right)\frac{\partial n}{\partial z}$

$= n w_0 - D_L \frac{\partial n}{\partial z}$

$D_L/D_0 = \frac{1+\gamma}{1+2\gamma}$

Application to gases:

$\sigma = \sigma_0 \left(\frac{\varepsilon}{\varepsilon_0}\right)^{\ell/2}$

$\Rightarrow$

$\nu = \nu_0 \left(\frac{\varepsilon}{\varepsilon_0}\right)^{\frac{\ell+1}{2}}$

$\Rightarrow$

$D_L/D_0 = \frac{1}{2}\frac{3+\ell}{2+\ell}$ better formula (Robson): $D_L/D_0 = \frac{1}{\ell+2}$

examples

		simple	Robson
$\ell = -1$	(ν = const)	$D_L/D = 1$	1
$\ell = 0$	(σ = const)	$D_L/D = 3/4$	1/2
$\ell = 1$	($\sigma = (\frac{\varepsilon}{\varepsilon_0})^{1/2}$)	$D_L/D = 2/3$	1/3
limit for ℓ large		$D_L/D = 1/2$	0

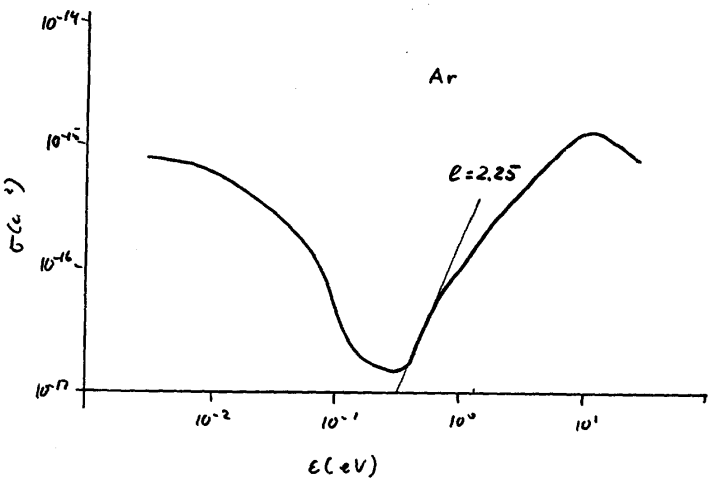

D_L/D_0 = 0.24 observed (Jade) D_L/D_0 = 0.285

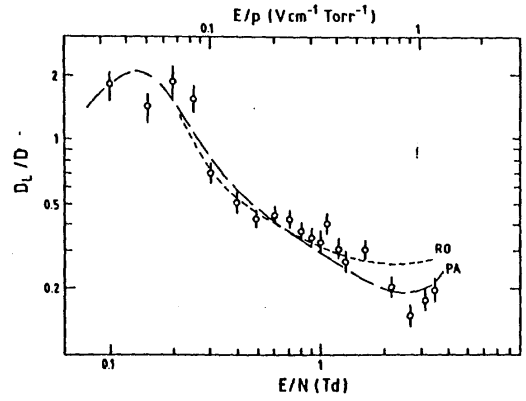

Fig.1.12: Anisotropie der Diffusionskoeffizienten parallel (D_L) und senkrecht (D) zum elektrischen Feld als Funktion des reduzierten elektrischen Feldes E/p (Einheit V cm^{-1} $Torr^{-1}$) bzw. E/N (Einheit Td = 10^{-17} Vcm^2). Meßpunkte nach [SC 80], berechnete Kurven nach [PA 68] und [RO 72].

position resolution in drift chamber
x: position in cell. "0" = pos. of anode

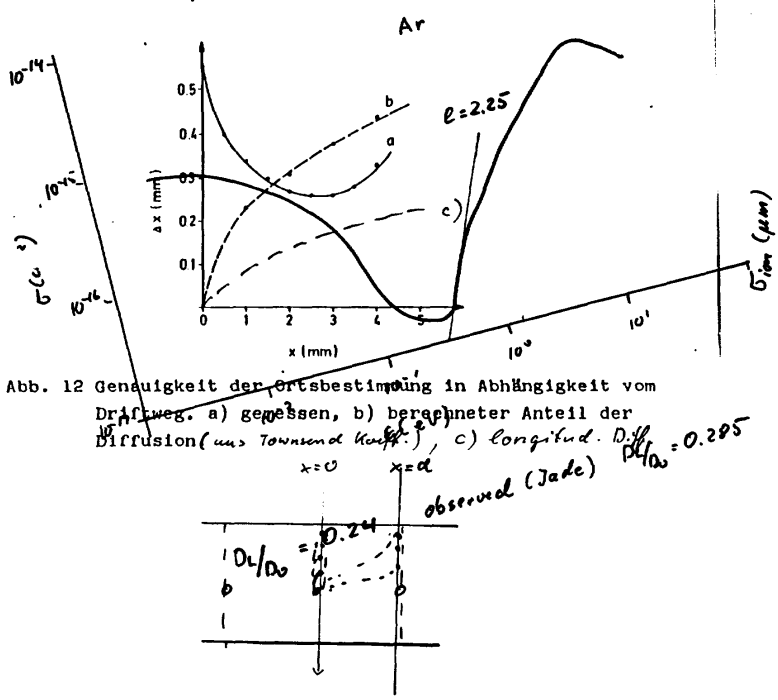

Abb. 12 Genauigkeit der Ortsbestimmung in Abhängigkeit vom Driftweg. a) gemessen, b) berechneter Anteil der Diffusion (aus Townsend Koeff.), c) longitud. Diff. $D_L/D_0 = 0.285$

Effect of clusters

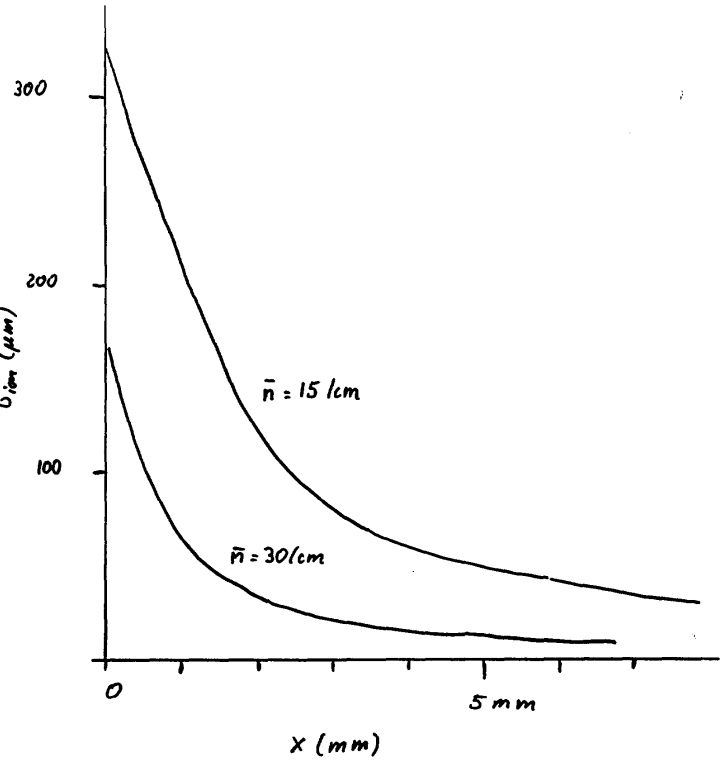

Center of Gravity

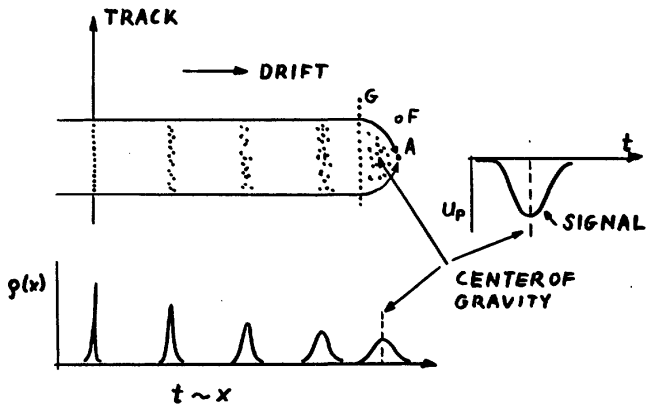

2') IN TEC SIGNAL FOLLOWS IONISATION STRUCTURE

3') MEASUREMENT OF CENTER OF GRAVITY OF n_e ELECTRONS

$$\rightsquigarrow \quad \boxed{\sigma = \frac{1}{\sqrt{n_e}}\,\sigma_0}$$

Leading Edge
(Standard Drift Chamber)

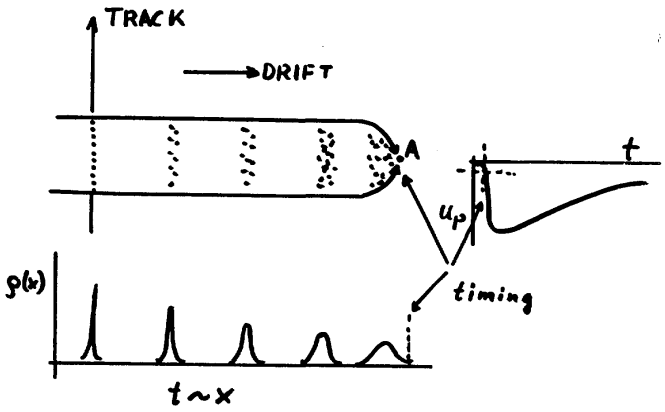

timing for drift distance determination is given by first electron arriving at the anode

$$\sigma_{1,t} = \frac{\pi}{2\sqrt{3\ln n}}\,\sigma_0$$

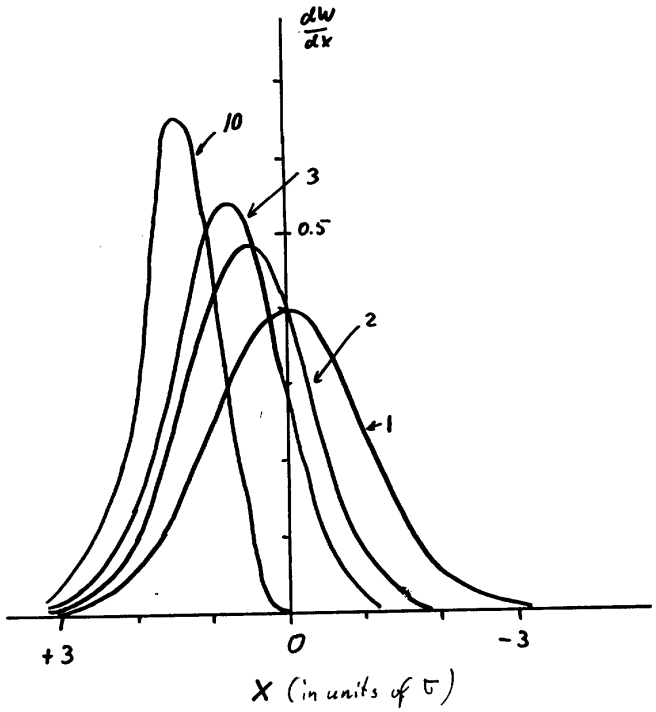

n	fwhm/2.4
1	1
2	0.79
3	0.68
10	0.40

$$\frac{dW}{dx} = n\,g\,e^{n-1}$$

g : Gauss-function

e : error - "

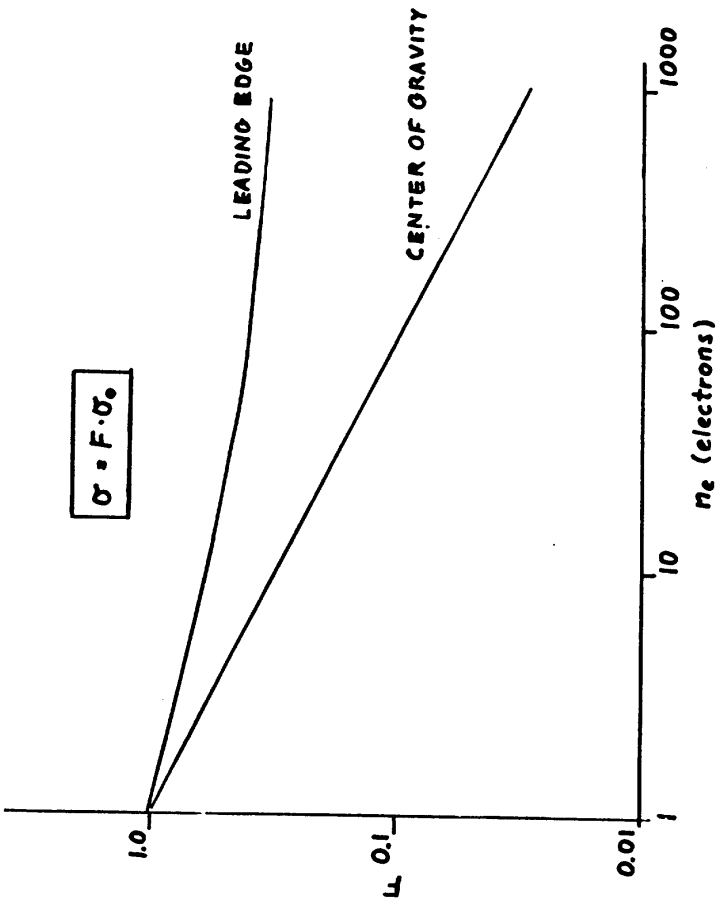

Drift Chamber Adaption

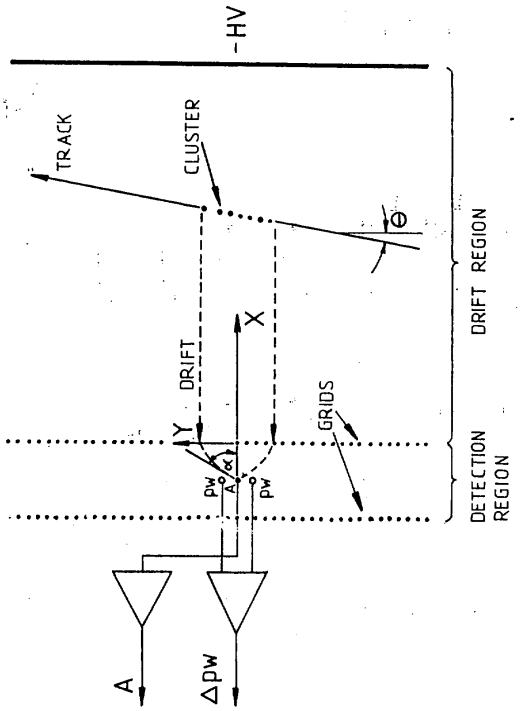

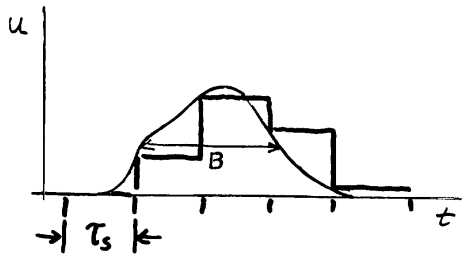

$B \geq 200\mu m$, $\tau_s = 10ns$ $\Big\}$ $v_{Dr} \leq \frac{B}{3\tau_s} = \frac{200\mu m}{30ns} = 7\mu m/ns$

$\Rightarrow$ 1) slow $v_{Dr.}$

2) band width of "gas-amplifier" $\geq 50MHz$

Charge Distribution | Signal | Signal after Shaper

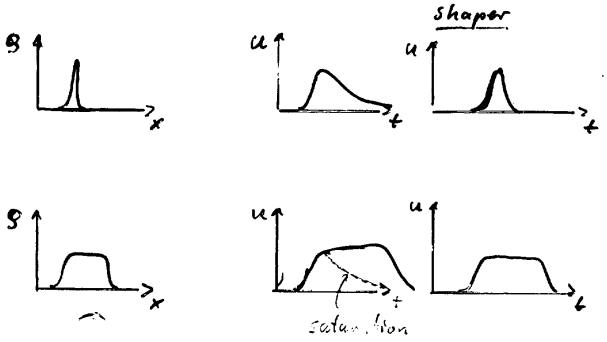

Diffusion for TEC

Einstein relation : $\sigma^2 = 2Dt$

$$\sigma^2 = 2\frac{D}{\mu E}x$$

using : $\frac{D}{\mu} = \frac{2}{3e}\varepsilon \Rightarrow$

$$\frac{\sigma^2}{x} = \frac{4}{3e}\frac{\varepsilon}{E}$$

Drift - Velocity for TEC

$$w = \frac{e}{m}\frac{E}{N}\frac{1}{\sigma c} \Rightarrow$$

$$w\frac{\sigma^2}{x} = \frac{e}{m}\frac{E}{N}\frac{1}{\sigma c}\frac{4}{3e}\frac{1}{E}\frac{1}{2}mc^2$$

$$\approx \frac{2}{3}\frac{c}{N\sigma}$$

$\rightsquigarrow$ c small (thermal)
N large (density)
σ large (molecules)

} small w and small $\frac{\sigma^2}{x}$

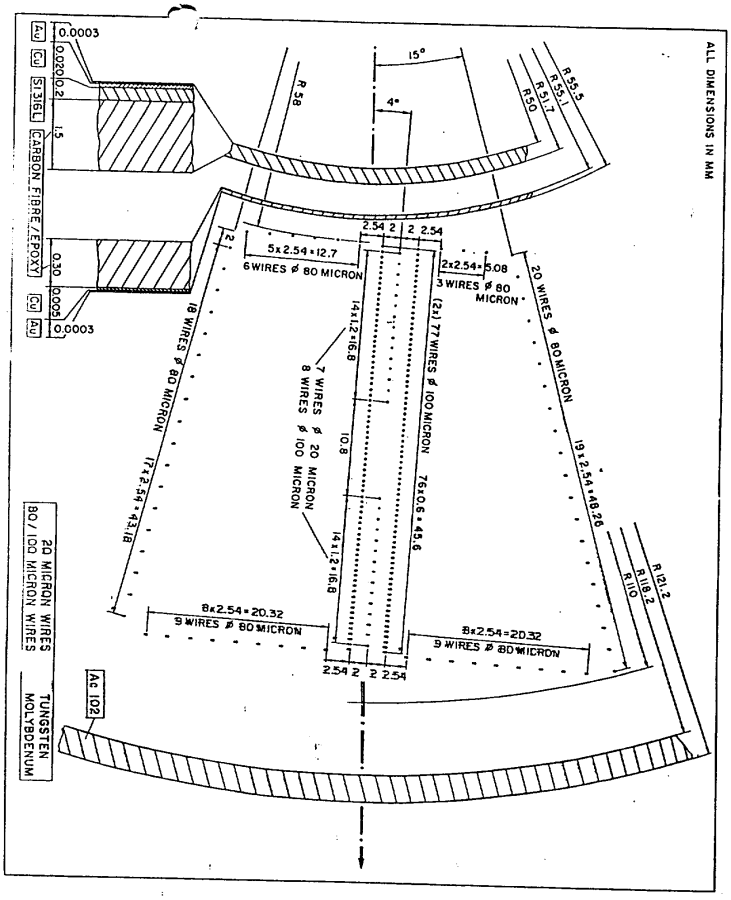

Mark J → L3

TEC

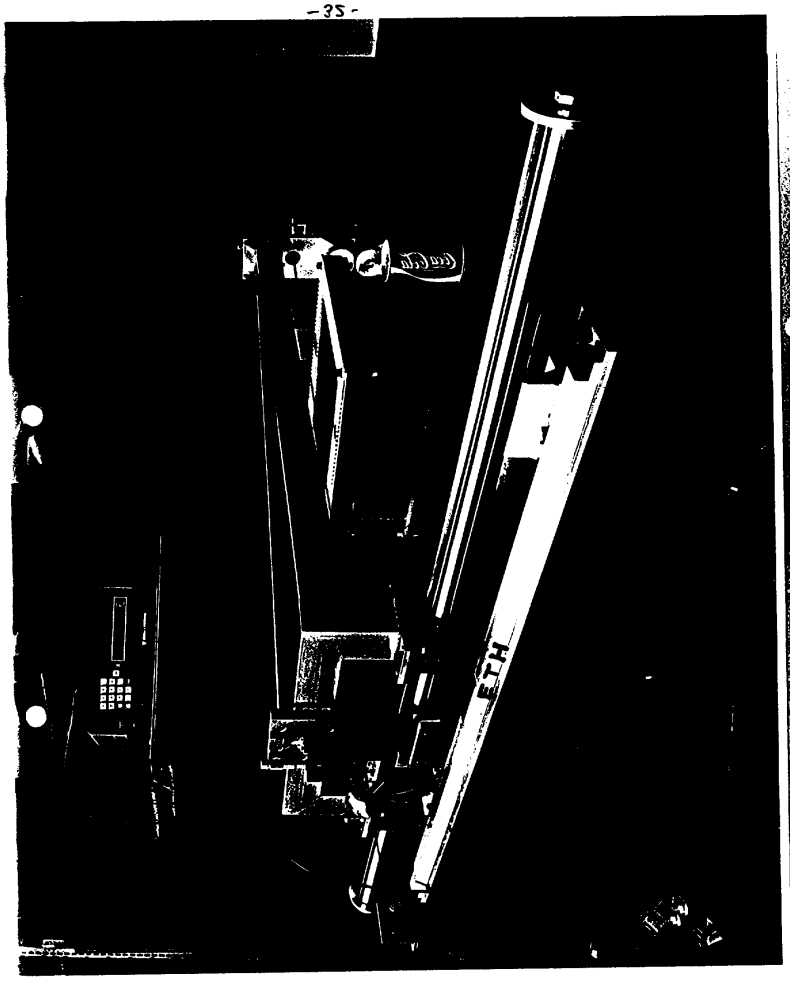

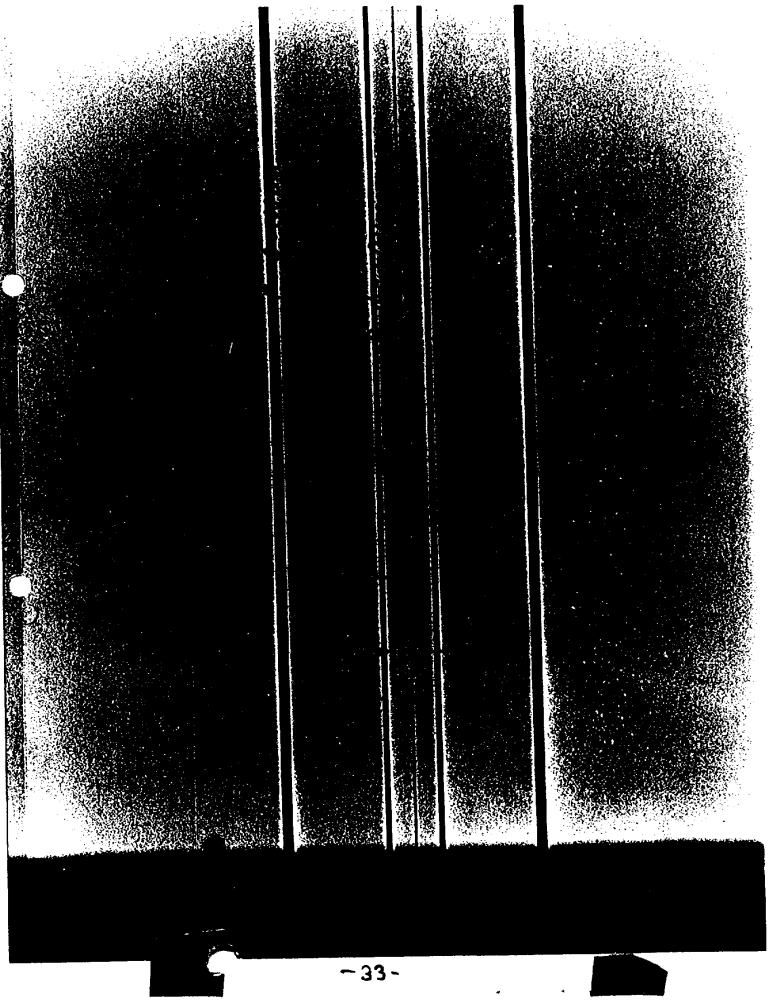

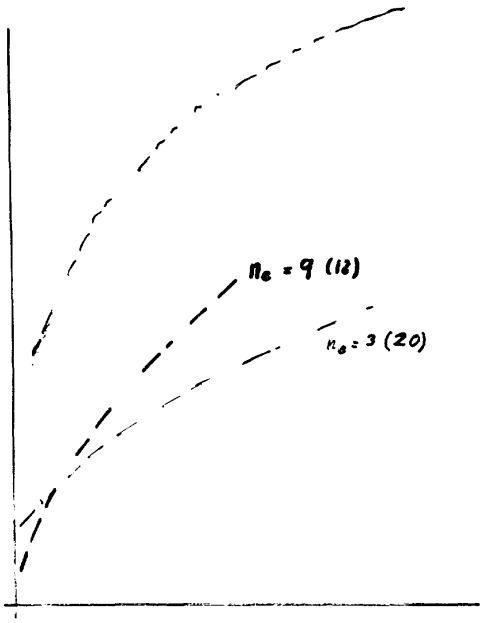

COMPARISION BETWEEN TWO
ANALYSIS METHODES:
<< LEADING EDGE >> : ●[0.8°] ○[3.2°]
<< CENTER OF GRAVITY >> : ■[0.8°] □[3.2°]
([ ] BEAM ANGLE)
RUN: 28-32 ETH/Siegen

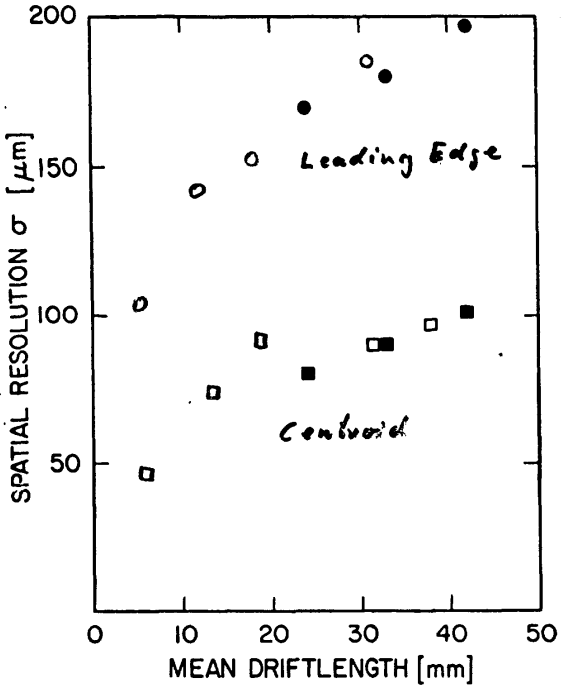

CERN DATA : Ar-C_2H_6 + methylal

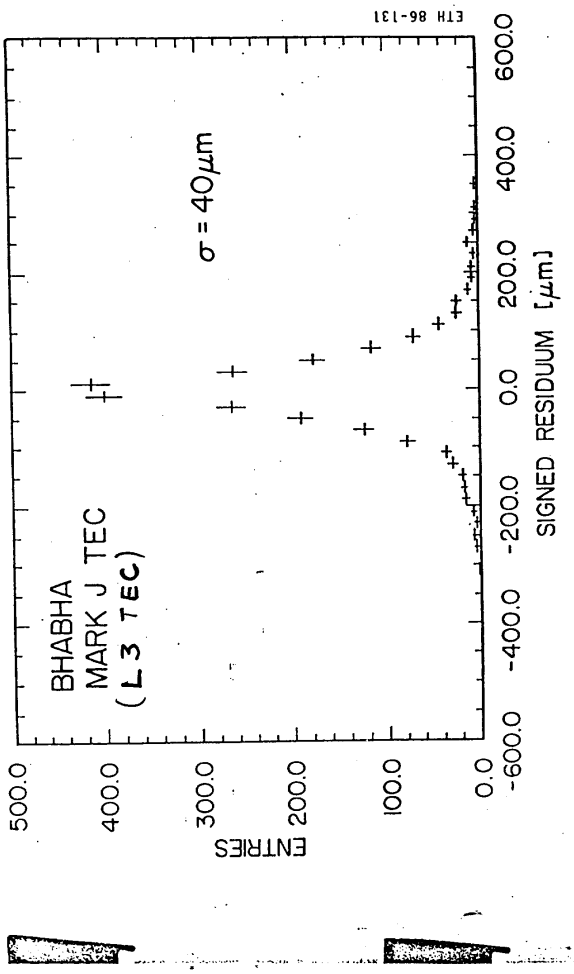

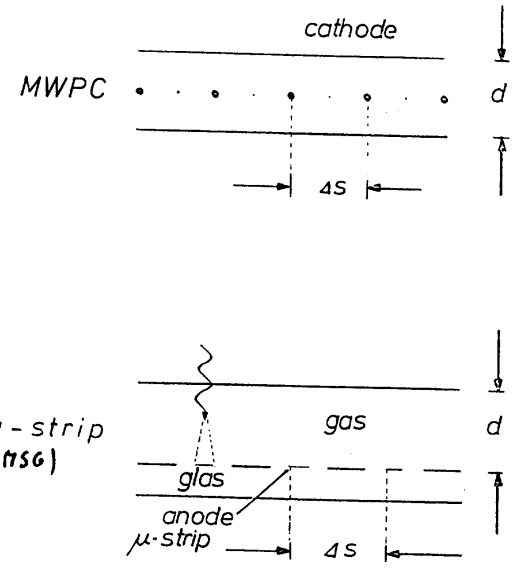

MPWC : $\Delta s \approx 0.5\,mm \ldots 2\,mm$

MSG : $\Delta s \approx 0.25\,mm$

SMALL CELLS

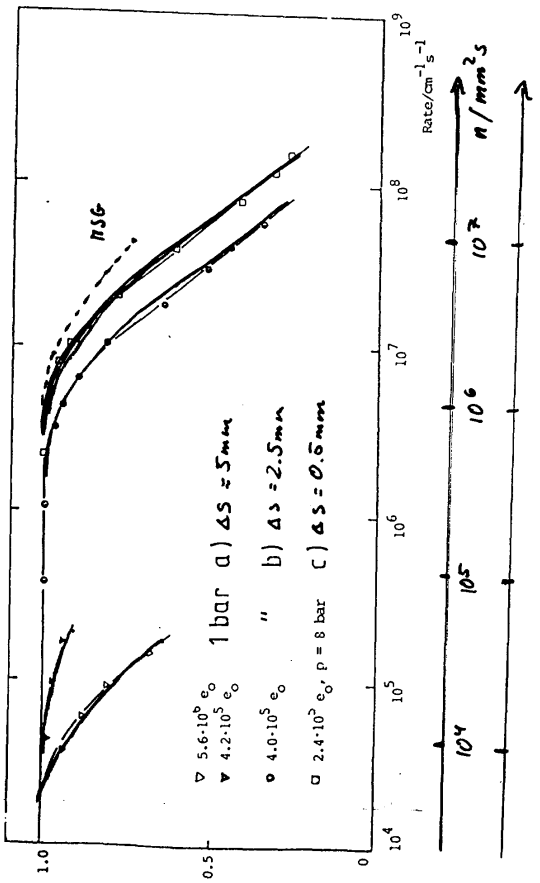

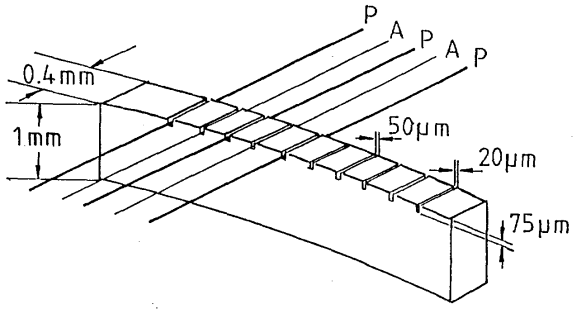

Fig.11

Support of wires to prevent electrostatic instabilities

MSGC (A. Oed)

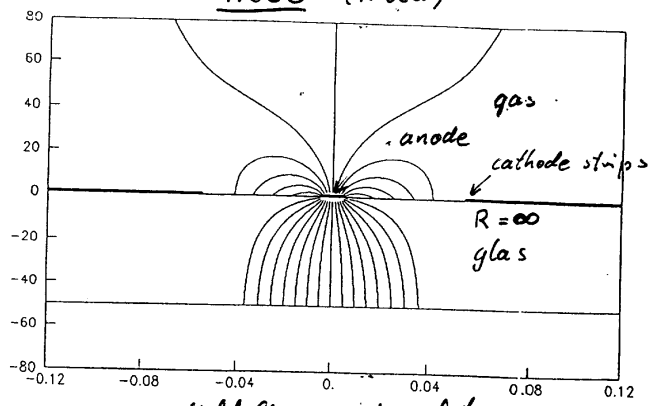

field lines on insulator ⇝ space charge

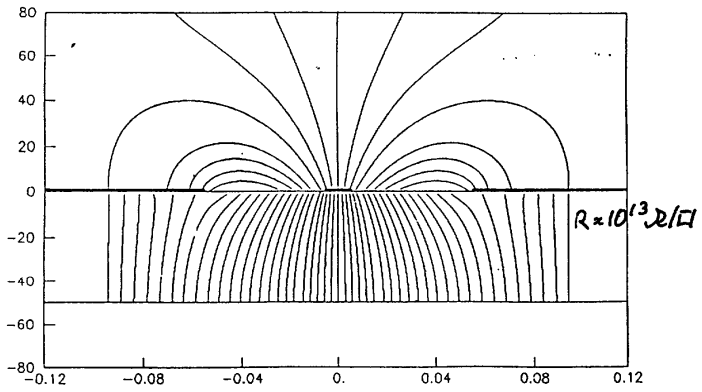

field lines on conductors ⇝
no charging of insulator
⇝ stable operation

b) Glass : D263

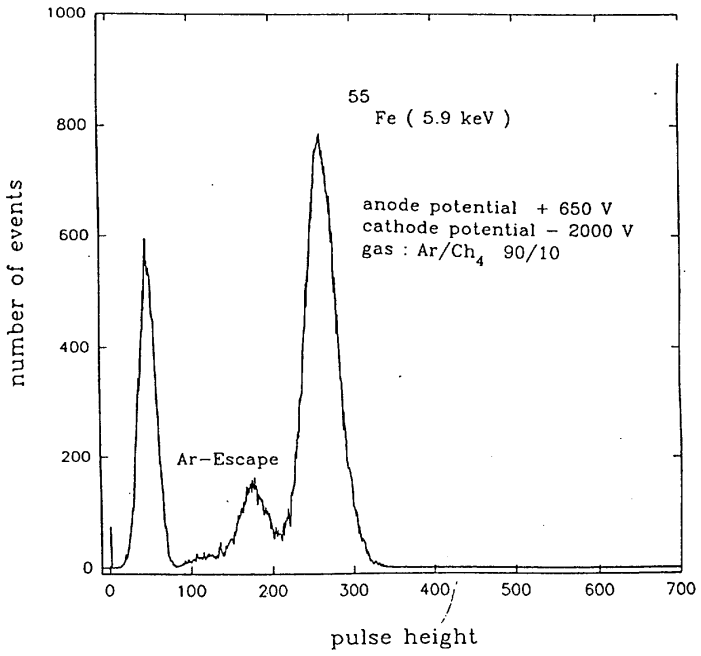

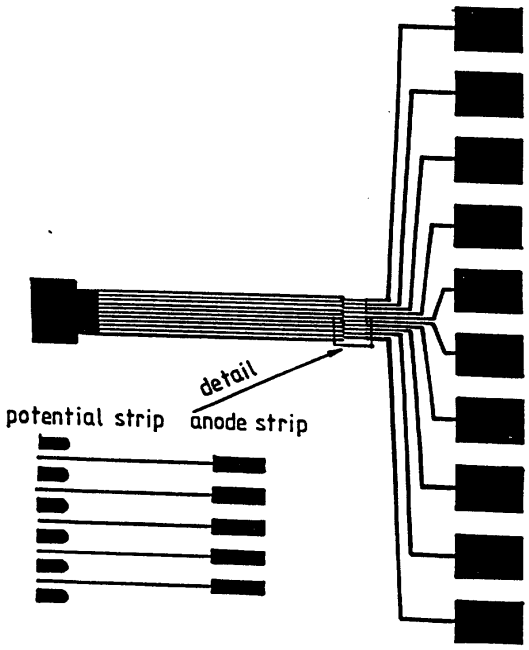

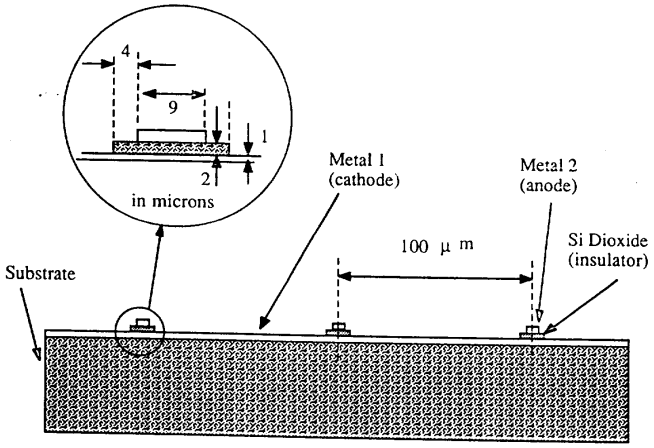

Fig.1) A cross section of the detector internal structure

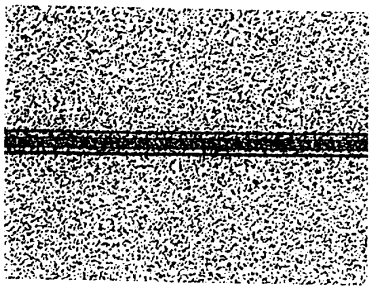

Fig.2) A photograph of one anode-cathode micro-gap

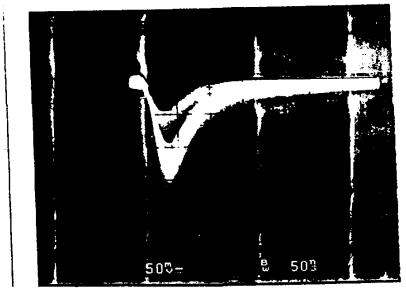

Fig.9) The 5.4 keV signal from the OR of several anode strips at a flux of 2 x 10^6 p/mm^2 s

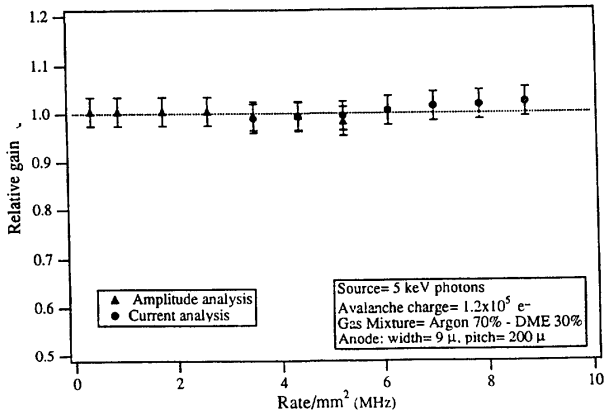

Fig.10) The normalized gain as a function of rate

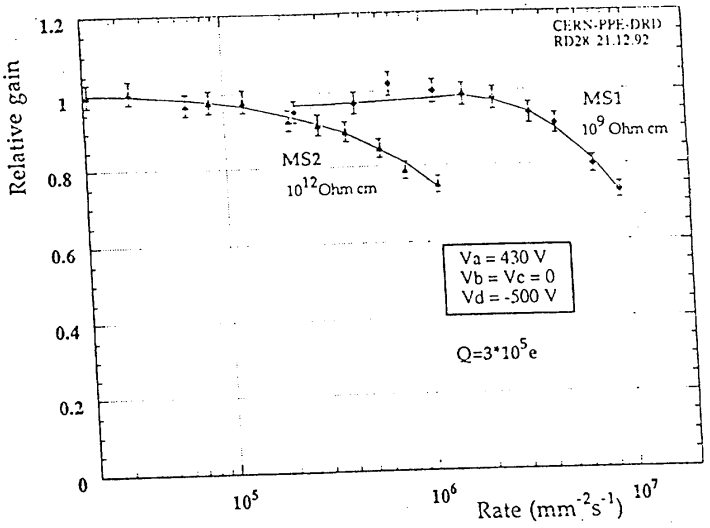

Fig. 8. Gain as a function of rate measured with MS1 and MS2 at an avalanche size of $3 \cdot 10^5$ electrons.

conductive glass

latest achievment:
conductive coating with C, N, Si